SAFETY RISK MANAGEMENT FOR RAILROAD HUMAN FACTORS: CASE STUDIES ON RESTRICTED-SPEED ACCIDENT AND TRESPASSING

By

ZHIPENG ZHANG

A dissertation submitted to the

School of Graduate Studies

Rutgers, The State University of New Jersey

In partial fulfillment of the requirements

For the degree of

Doctor of Philosophy

Graduate Program in Civil and Environmental Engineering

Written under the direction of

Dr. Xiang Liu

And approved by

_____

_____

_____

_____

New Brunswick, New Jersey

May 2020

ABSTRACT OF THE DISSERTATION

SAFETY RISK MANAGEMENT FOR RAILROAD HUMAN FACTORS:

CASE STUDIES ON RESTRICTED-SPEED ACCIDENT AND TRESPASSING

By ZHIPENG ZHANG

Dissertation Director:

Dr. Xiang Liu

Railroads play a key role in the transportation infrastructure and economic development of the United States, and safety is of the utmost importance. Railroad safety is mainly affected by infrastructure, rolling stock, and human factors. Over the past decade, relatively less research has been undertaken to mitigate the human-factor-caused railroad incident risk despite considerable efforts and improvements in the infrastructure and rolling stock. The human errors in railroads may result in injuries or fatalities, infrastructure and rolling stock damages, and environmental impacts. This dissertation presents a methodological framework for railroad human-factor-caused safety risk management that encompasses risk assessment and mitigation. First, accident/incident data and information should be collected and used to identify safety risks, undesired human factor-related events, and risk management objectives. Second, risk assessment should be conducted to evaluate safety risks and contributing factors. The third step is to develop and evaluate effective risk mitigation strategies based on the risk analysis results. The proposed safety risk management framework is applied to two human-factor-caused risk scenarios: restricted-

speed train accidents and trespassing events, both of which collectively constitute over 95% of all rail-related fatalities.

First, in terms of restricted-speed safety research, the dissertation consists of a collection of historical restricted-speed train accidents, quantitative and qualitative safety risk analysis, PTC-based accident risk mitigation with a proposed Concept of Operations, and a Monte Carlo simulation-based quantitative assessment of mitigation strategies. Second, in terms of trespassing research, the dissertation focuses on Artificial-Intelligence-aided trespassing data detection and location-specific trespassing data analysis, as well as specific trespassing safety strategies and proactive risk management.

ACKNOWLEDGMENTS

There are many people who have earned my sincere appreciation for their continuous contributions to my graduate school studies. More specifically, I would like to thank my advisor, my thesis committee members, funding agencies and industrial collaborators, my friends and lab mates, and my family, without whom my thesis would not have been possible.

First and foremost, I would like to thank Dr. Xiang Liu for his endless encouragement, teaching, and advice throughout my graduate studies at Rutgers. From an academic perspective, Dr. Xiang Liu taught me the fundamentals of scientific research in transportation engineering. Over 2,100 emails (beginning in 2017) serve as evidence of his extreme dedication. On a personal level, Dr. Liu inspired me with his hardworking and passionate attitude. It has been an honor and great fortune for me to have the opportunity to work with him over the years and have him as my advisor.

In addition, I would especially like to thank Mr. Keith Holt, Dr. Jie Gong, and Dr. Peter J. Jin, who served on my doctoral committee. Their encouragement and invaluable support extend beyond the completion of this dissertation. I am extremely grateful to Mr. Keith Holt, a top expert in railroad communication & signal engineering, for sharing his tremendous experience and knowledge with me and for always kindly supporting me throughout my graduate studies. I also have immense gratitude for Dr. Jie Gong and Dr. Peter J. Jin, two distinguished professors in civil engineering, for their insightful comments and crucial remarks that shaped my final dissertation, and for supporting my future career.

Funding for this research was provided by the Federal Railroad Administration of the U.S. Department of Transportation. I would like to acknowledge Mr. Francesco Bedini Jacobini, Mr. Sam Alibrahim, Mr. Jared Withers, Dr. Mark Hartong, Mr. David Blackmore, Dr. David Thurston, Mr. Marco DaSilva, and Mr. Todd Hirt, all of whom provided insight and feedback. I also want to acknowledge the American Railway Engineering and Maintenance-of-Way Association (AREMA) for generously awarding me scholarships that supported my graduate studies.

I sincerely appreciate my colleagues and the staff at Rutgers University. This dissertation would not have been possible without contributions from Jinxuan Xu, Abigail Casazza, Asim Zaman, and Tejashree Turla. I am also grateful to Zhaojing Wang, Jihong Chen, and Zheyong Bian for their encouragement and support of my graduate studies and Gina Cullari for her continual help. Further, special thanks to Dr. Christopher P.L. Barkan and Dr. Rapik Saat for guiding and encouraging me in my early research stages.

Finally, I would like to express my deepest gratitude to my parents (Jing Zhang and Ye Shang), sister (Mimi Zhang), and my dear friends who always love and support me.

TABLE OF CONTENTS

LIST OF FIGURES

LIST OF TABLES

CHAPTER 1

INTRODUCTION

1.1 General Overview

Passenger and freight rail services play a crucial role in the economic prosperity of the United States. In the vast railroad network, safety is of the utmost importance and train accident may result in injuries or fatalities, infrastructure and rolling stock damages, and environmental impacts. Railroad safety is affected by infrastructure, rolling stock, and human factors. In particular, the great majority of train accidents resulted from either human factors or track related failures (FRA, 2007). Over the past decade, train safety has improved remarkably due to the considerable efforts and improvements in railroad infrastructure and rolling stock. Researchers, in cooperation with policymakers and railroads, constantly promote advanced technologies and operational enforcements to improve railroad safety. However, little work has been undertaken to mitigate the human-factor-caused railroad incident risk. Human errors in railroad operations may result in injuries or fatalities, infrastructure and rolling stock damages, and environmental impacts, and are one major target area for further improving railroad safety. This knowledge gap is the motivation for this dissertation, which develops a methodological framework for railroad human-factor-caused safety risk management.

As a safeguard against human error, Positive Train Control (PTC) is expected to prevent train accidents attributable to human error by slowing or stopping trains

automatically. PTC is designed to prevent train-to-train collisions, derailments caused by excessive speeds, unauthorized incursions into work zones, and movements of trains through misaligned railroad switches. However, even with fully implemented and functioning PTC systems, there are two types of high-consequence human-factor-related incident risks, which are restricted-speed train accidents and trespassing events. These events cannot be reduced due to regulation exemptions and lack of functionality in current PTC systems. As defined by current regulations (49 CFR 236 Subpart G), restricted speed is a speed that will permit stopping within one-half the range of vision, but not exceeding 20 miles per hour. In the United States, restricted speed operation is a common type of train operation that is found on virtually every mile of automatic blocks and extensively exists in terminals and yards. National Transportation Safety Board (NTSB) issued a report in 2012, highlighting five collisions due to restricted speed violations (NTSB, 2012). One of them led to two fatalities and more than $8 million damage cost. More recently, a Long Island Rail Road (LIRR) passenger train collided with the platform in the Atlantic Terminal, New York, on January 4, 2017 and led to 108 injuries and around $5.3 million in damage costs (NTSB, 2018a). However, current regulations do not require PTC to perform its functions when a train is traveling under restricted speeds. Besides, PTC would not prevent incidents due to trespassing on right-of-way or highway-rail crossing, where the vast majority of rail-related fatalities occur.

This dissertation demonstrates human-factor-related railroad safety risk managements in two major human-factor-caused accident scenarios, restricted-speed train operations and trespassing events. These events constitute over 95% of all rail-related fatalities. These two also represent two different aspects of human errors, of which

restricted-speed train accidents are mostly attributed to disengaged or inattentive train engineers and trespassing events predominantly pertain to noncompliant behaviors and poor judgment from pedestrians and highway users. Both are highlighted in the recent reports from the Federal Railroad Administration (FRA) and Congress. Based upon the 2015 Fixing Americas Surface Transportation (FAST) Act, the Federal Railroad Administration (FRA, 2016a) issued the Safety Advisory 2016-03 that aims at the mitigation and investigation of human-factor-related accidents, of which train operating with stub-end tracks are one focus. Congressional Research Service (CRS) remarked that trespassing risk occurrence has not been reduced because most rail-related fatalities are caused by trespassing while PTC systems cannot prevent these accidents/incidents.

In summary, this dissertation presents a methodological framework for human-factor-caused safety risk management. The dissertation specifically studies two major human-factor-caused train accident scenarios: restricted-speed train accidents and trespassing events. Two state-of-the-art technologies, PTC and Artificial Intelligence (AI) with computer vision, are implemented to contribute to the development of research innovations and technology solutions. Ultimately, this dissertation aims to promote railroad safety and achieve better-informed rail safety practices.

1.2 Research Background

Railroads are a safe and reliable mode of transportation. Train accident rates have declined considerably over the past decade. However, a train accident may result in injuries or fatalities, infrastructure and rolling stock damages, and environmental impacts. The US freight rail network consists of nearly 140,000 miles with 1.74 trillion ton-miles of traffic

annually (FRA, 2015; AAR, 2017a). This vast railroad network is crucial to the American economy, and consequently its safety is of great importance. Based on previous train accident analyses, derailments and collisions are common accident types (Barkan et al., 2003; Liu et al., 2011, 2012, 2013, 2016a; Li et al., 2018). Previous studies have analyzed the overall safety trends of derailments and collisions. Furthermore, infrastructure or equipment failures as derailment causes have been studied (Liu, 2011; 2012) but there is no study specific to analyzing human-factor-caused accident risks and this research aims to fill this knowledge gap.

Human factors are major causes of freight-train accidents (derailments and collisions) on mainlines resulting in a total of 1,510 accidents with 551 casualties and 9,214 derailed cars in the period of 2000 to 2016 (FRA, 2007; Madigan, et. al., 2016; Zhang et al., 2019a). Human factor accidents occur due to a number of factors that degrade the operators' performance. Studies of factors influencing human performance can be found in prior literature (Kyriakidis et al., 2015; Zhang et al., 2014). Similar analyses have been performed in other industries, such as oil and gas (Theophilus, 2017), maritime transportation (Chen et al., 2013; Yildirum et al., 2017), aviation (Low and Yang, 2018), metro systems (Chen et al., 2018), etc. Human factors involving the physical and organizational characteristics of train operators have been studied in order to optimize and apply a human factor analysis and classification system (HFACS) to the railroad industry (Reinach, 2006; Madigan et al., 2016). The HFACS methodology has also been used to study the potential root causes of railroad accidents in Indonesia (Iridiastadi, 2012). However, there has been relatively limited prior work focusing on human-error-caused train safety risk management in the United States.

Nationwide implementation of Positive Train Control (PTC) is underway in the United States. As a safeguard against human error, PTC is expected to prevent train accidents attributable to human error, by slowing or stopping trains automatically. PTC is designed to prevent:

- Train-to-train collisions;
- Derailments caused by excessive speeds;
- Unauthorized incursions into work zones; and
- Movements of trains through misaligned railroad switches.

Complying with the requirements of Subpart I in the Code of Federal Regulations (CFR, 2011), the territory of PTC implementation and operation includes Class I railroads, main lines servicing over 5 million gross tons (MGT) annually and over which toxic- or poisonous-by-inhalation hazardous materials are transported, and main lines involving intercity and commuter passenger trains. The full implementation of PTC would involve around over 60,000 route miles (AAR, 2017; FRA, 2017b). The large-scale, network-level PTC implementation affects the U.S. rail industry in several aspects, in terms of implementation cost, operational impact, and safety effectiveness (FRA, 2009; Van Dyke and Case, 2010; Peters and Frittelli, 2012; Zhao and Ioannou, 2015: AAR, 2017). As a federal mandate, PTC technology has been studied in federal regulations and industry reports (RSAC, 1999; FRA, 2009; Van Dyke and Case, 2010; Peters and Frittelli, 2012; GAO, 2015; AAR, 2017).

PTC systems must meet the functionality requirements established by the Rail Safety Improvement Act (RSIA) of 2008 in terms of capability to prevent accidents resulting from the activity or inactivity of train operators. PTC is not a single technology.

Instead, it is a suite of performance standards. Railroads are allowed to install different PTC technologies in their respective systems once approved by the FRA. PTC integrates various components (Figure 1. 1), namely the locomotive computer, wayside device, communication network, and back office (APTA, 2015; AAR, 2017). The locomotive computer is an onboard piece of equipment that accepts speed restriction information and movement authority so that these data can be compared against the train's location to ensure compliance. The wayside device on the side of the track is capable of monitoring and reporting switch position and signal status to locomotive computers and the back office. The back office is a centralized office for the communication and coordination of train orders, speed restrictions, train information, track authorities, crew sign-in and sign-off, and bulletins, as well as specialized data to and from the wayside and train operational and safety data (GAO, 2015). Integrated with these components, PTC systems use a combination of communication networks, GPS (or transponders), and fixed wayside signal devices to send and receive data about the location, direction, and speed of trains. Back offices process these data in real time and provide movement authority and speed restriction information to locomotive computers. Then locomotive computers accept the information and compare it against the train’s condition to ensure safety compliance. Whenever a train crew fails to properly operate within specified safety parameters, PTC systems automatically apply the brakes and bring the train to a stop.

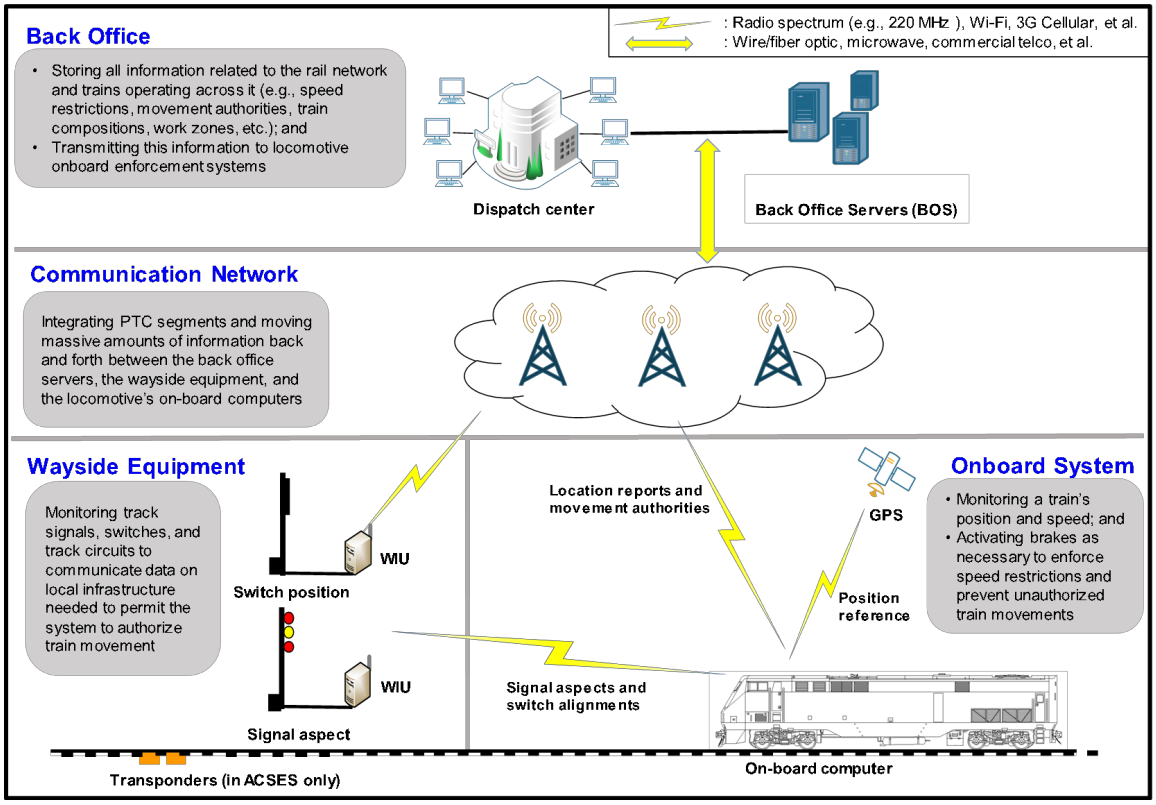

Figure 1. 1. Schematic Illustration of A General PTC System

The current regulation (49 CFR 236 Subpart I) does not require PTC to perform its functions when a train is traveling under restricted speeds. Transportation Economics & Management Systems, Inc. (TERMS) (2017) argued that the defined 20-mph restricted speed might be too fast and should be reduced to 10-mph since this would solve most of the problems related to PTC exemptions. Nonetheless, there has been little analysis yet showing the rationality of either the 20-mph or 10-mph restricted speed. To the authors' knowledge, no published studies pertain to the evaluation of PTC implementation below restricted speeds. It calls for research to better understand the safety benefits, cost, and operational impact of PTC enforcement at or below restricted speeds. Eventually, the regulators and railroad industry can use this type of analysis to evaluate whether PTC

implementation should be extended to restricted speeds (if so, what is the threshold for restricted speed), and whether there exist more cost-justified risk reduction alternatives. Furthermore, trespassing accidents/incidents account for the majority of rail-related fatalities. The U.S. railroad system is comprised of approximately 830 railroads, 134,000 miles of track, and 210,000 railroad crossings (FRA, 2018d). Trespassing accidents along rights-of-way (ROWs) and at highway-rail grade crossings constitute over 90% of rail-related deaths over the past ten years (FRA, 2018d). More specifically, there were 855 trespass-related fatalities in 2017, which demonstrates an increase of 18 percent from 2012 (FRA, 2018d). In addition to fatalities, these incidents resulted in other serious consequences, such as nonfatal injuries, train derailments, hazardous material spillage, train delays, and traffic congestion. From 2012 to 2016, trespassing accidents cost the United States approximately $43 billion (FRA, 2019a) that does not cover indirect costs (e.g., emotional distress or productivity losses).

1.3 Dissertation Organization and Research Objectives

The objective of this study is to develop a systematic methodological framework for railroad human-factor-caused safety risk management that encompasses both risk assessment and mitigation of human factor risks to mitigate train accidents caused by human factors and promote railroad safety. To achieve this primary objective, this dissertation analyzes the safety risk of these common, critical scenarios of rail-related human errors and proposed effective risk mitigation strategies based upon two emerging technologies, PTC systems and AI with computer vision.

This dissertation includes five chapters (Figure 1. 2).

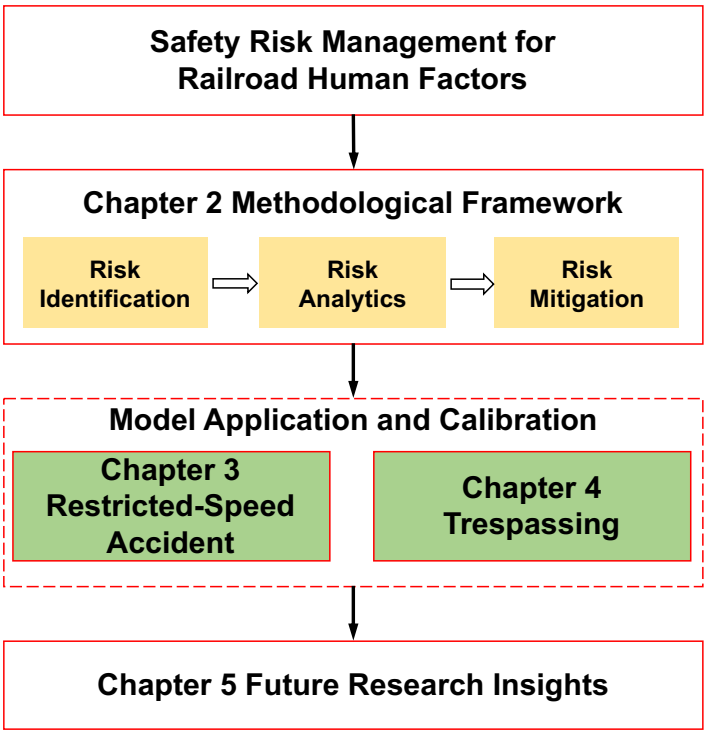

Figure 1. 2. Framework for This Dissertation

The specific objective of each chapter is as follows:

1. Introduction (Chapter 1)
    a. Introduce the background, motivations, objectives, and problems to address
    b. Briefly introduce the contents of each chapter and clarify the contributions to the field of railroad safety and human error risk management
2. Methodological Framework for Railroad Human Factor Risk Management (Chapter 2)
    a. Develop a systematic framework for human-factor-related safety risks in train operations

   b. Present methodologies and tools commonly used in railroad human-factor-related accident data collection, data analysis, and mitigation

3. Risk Management for Restricted-Speed Train Accidents (Chapter 3)
   a. Conduct empirical and statistical analyses of restricted-speed accidents in quantitative and qualitative ways
   b. Propose a Concept of Operations for the implementation of PTC systems to prevent restricted-speed accidents
   c. Develop a quantitative assessment of PTC-based risk mitigation in terms of incremental costs, safety benefits and operational impact assessment with Monte Carlo simulation
4. Risk Management for Trespassing Events (Chapter 4)
   a. Identify the trespassing risk and causal factors
   b. Develop effective AI-aided technology to collect trespassing events from both live stream and archive videos in fixed cameras
   c. Analyze the large volumes of collected trespassing data with developed technology in the case study
   d. Propose data-driven, effective prevention strategies
5. Future Research and Insights (Chapter 5)

1.4 Contribution Summary

The potential contributions of this dissertation are summarized below,

1. Contributions to academics and researchers

a. Propose a methodological framework for railroad human-factor-caused safety risk management
b. Provide a full-spectrum introductory view of restricted-speed train operations, as one of emerging critical issues in the age of PTC, and other PTC challenges
c. Develop both empirical analysis and statistical models to advance the understanding of restricted-speed accident probability, severity, and risk
d. Provide an AI-aided methodology to collect trespassing event from big data that overcome the limitations from data quality and uncertainty
e. Develop specific trespassing safety strategies and proactive risk management

2. Contributions to government, policymakers, and rail industry
    a. Propose a cost-effective, reliable end-of-track collision prevention strategy with PTC system
    b. Present collaboration opportunities to develop policies and practices that can optimize the use of PTC technology and advance rail safety
    c. Provide a risk-based approach with expected value and Conditional Value at Risk to evaluate rail transportation safety
    d. Provide a reference for the evaluation of cost-benefit analysis and operational impacts
    e. Present policymakers, railway practitioners, and academic researchers with valid references for safety options and future work directions, and ultimately enhance railroad safety

CHAPTER 2

METHODOLOGICAL FRAMEWORK FOR RAILROAD HUMAN FACTOR RISK MANAGEMENT

Partially adapted from
Zhang, Z., Turla, T., & Liu, X. (2019). Analysis of human-factor-caused freight train accidents in the United States. *Journal of Transportation Safety & Security*, 1-29.

Railroads play a key role in the transportation infrastructure and economic development of the United States, and safety is of the utmost importance. In the United States, train accident analysis has primarily focused on derailment, hazardous material releases, and highway-rail grade-crossing accidents (Anderson and Barkan, 2004; Liu et al., 2011; Chadwick et al., 2014; Liu, 2016a; Liu, 2016b). However, much less research has evaluated train risk and safety for human-factor-caused train accidents, in spite of the fact that human errors are the most common causes of accidents and rail-related fatalities on U.S. railroads and can result in extensive risks potentially.

This chapter aims to describe a methodological framework for railroad human factor risk management (Figure 2.1). In general, risk assessment is defined as the processes that identify hazards and risk factors, analyze and evaluate the risks associated with those hazards, and determine appropriate ways to control risk. Safety risk management models have also been developed in various fields, such as aviation (Lee, 2006), underground engineering (Qian and Lin, 2016), and construction site safety (Hallowell, 2008). The

benefits of systematic risk management include but are not limited to: improvement of operational effectiveness and efficiency, better understanding of the need to identify and treat risks, effective allocation of resources for risk mitigation, and a reliable basis for decision making and resource planning. Regarding railroad human factor safety risks, the proposed three-step methodological framework aims to assess the risks associated with identified hazards as well as risks from human factors, and to develop and implement effective and appropriate mitigations in train operations.

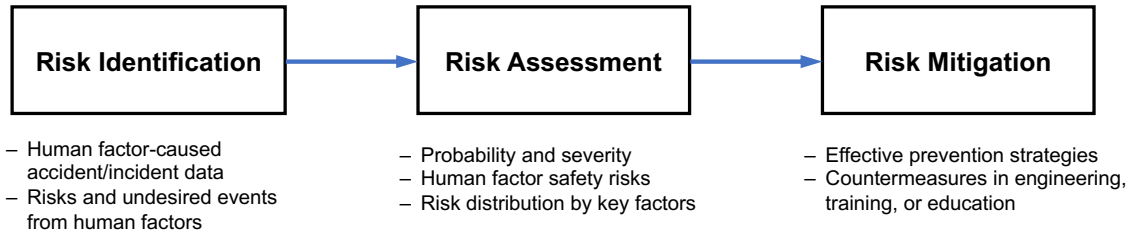

Figure 2. 1. Schematic Flow Chart in Railroad Human Factor Risk Management

2.1 Risk Identification and Data Collection

The first step in safety risk management includes problem definition and data preparation. Essential data and information are collected and assembled to identify the safety risk scope, risk characteristics, and risk management objective.

Data source preparation and data collection can contribute to the data-driven risk analysis and management. In the United States, railroad accident data is documented and also publicly accessible from the FRA's Rail Equipment Accident (REA) database. The FRA publishes train accident data based on reports submitted by railroads operating in the United States. Railroads are required to submit accident reports for all accidents that exceed a specific monetary threshold for damage and loss. The reporting threshold for the REA is

periodically adjusted for inflation and increased from $6,600 in 2001 to $10,500 in 2016 (FRA, 2017a). The REA database records comprehensive circumstances regarding the accidents under over 50 different fields, including operational factors, environmental factors, train characteristics, damage conditions, and other information necessary for accident analysis and prevention.

In addition to accident data, traffic volume is used to calculate derailment rate, which is defined as the number of derailments normalized by traffic volume (Anderson and Barkan, 2004; Liu, 2016b). Train-miles and car-miles are two common traffic metrics, each of which corresponds to certain types of accident causes. Schafer and Barkan (2008) found that some accident causes are more related to train-miles, including most human-error failures. On the other hand, the causes of most equipment failure and infrastructure failure are more closely related to car-miles. One publicly accessible traffic volume data source is the FRA Operational Safety Database.

In terms of lessons learned from literature, a review of relevant literature is able to support the identification of railroad human factor safety risks. Firstly, the scope of involved literature is clarified. This study mostly focuses on literature in English from 2000 to 2019 with qualitative and quantitative analysis in railroad human factors. It considers studies not only from the United States but also those of different countries all over the world. Secondly, major databases, such as those provided by major publishers including Science Direct, Emeralds, Scopus, and IEEE Xplore, to search for related articles were used in the literature collections. In addition to the journals, conference proceedings, and dissertations, the e-libraries from either federal governments or official railroad organizations (e.g., International Union of Railways) are another source of literature that

was utilized. In the third stage, railroad human factor-related keywords, such as “railroad accident”, “human factor”, and “human error”, are identified and used together to capture the synthesis of existing literature related to this study purpose. Fourthly, this literature review aims to discuss the definition, contributing factors, and existing countermeasures of railroad human factors. Per the contents of each literature, relevant full-text literature satisfying the eligibility are further studied and contribute to the risk identification.

2.2 Risk Assessment

2.2.1 Accident frequency and severity

Figure 2. 2 demonstrates the frequency distribution of accidents on mainlines from the FRA Rail Equipment Accident database. Although there is a declining trend for train accidents with all causes combined, human-factor-caused train accidents account for over one third of all FRA-reportable accidents.

There are several measures of train accident severity, such as the number of casualties (Lin et al., 2014), damage costs to rolling stock and infrastructure (Liu et al., 2010), and the number of cars derailed, a common metric in the studies of derailment (Barkan et al., 2003; Liu et al., 2012). In this study, two proxy variables are employed to measure the severity of human-factor-caused accidents, which are the number of casualties and the damage costs. Other proxies for accident consequence, such as business losses and environmental impacts, vary among accidents and this information is not reported to FRA, and was therefore excluded from the analysis herein. The number of casualties is the summation of injuries and fatalities. In terms of consequences measured by reportable damage costs (damages to track infrastructure, equipment and signals), inflation is taken

into consideration and the damage cost each year is also adjusted to the 2016 dollar-value using the GDP deflator (World Bank, 2017).

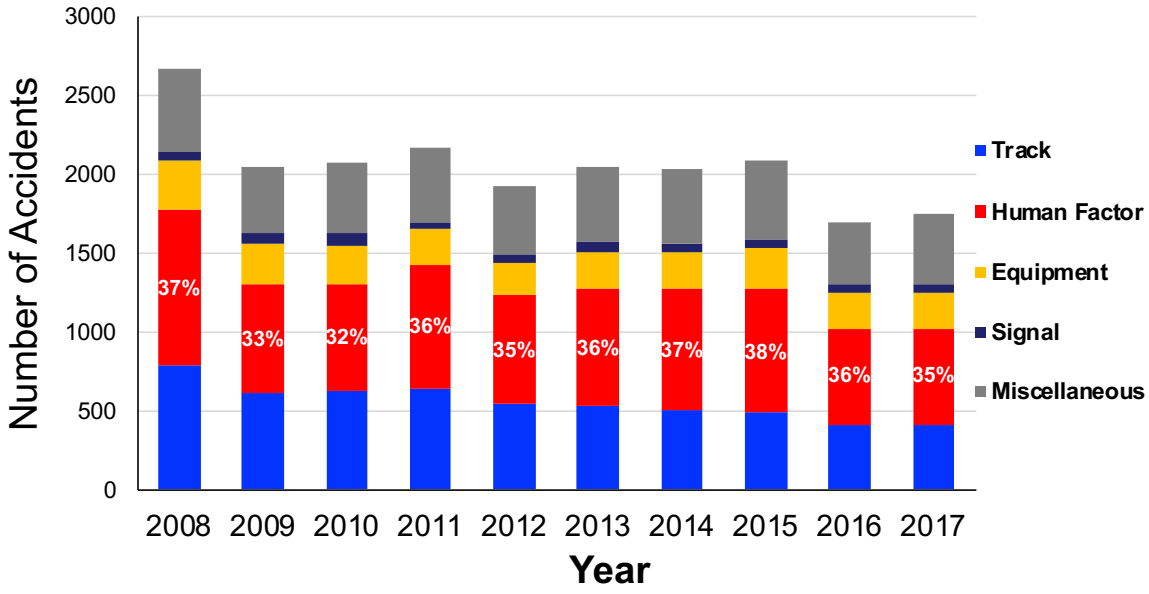

Figure 2. 2. Distribution of FRA-Reportable Accidents on Mainlines from 2008 to 2017

2.2.2 Accident risk

Several previous studies have defined risk as the combination of possible consequences and associated probabilities (Aven and Renn, 2009). In the field of railroad safety, accident risk is measured by the combination of expected accident frequency and expected accident consequences (Liu, 2016a). Using this risk measure, this research defines annual human-factor-caused accident risk as the expected number of casualties or damage costs during a year in total. As shown in the mathematical equation below (Equation 2-1), the risk is equivalent to the expected summations of either casualties or damage costs (accident severity, X_{ij}) for all restricted-speed accidents in one year (accident severity, N):

$$R_{1i} = E(\sum_{j=1}^{N} X_{ij}) \qquad (2-1)$$

Where

$$i = \begin{cases} 1, & \text{using number of casualties as accident severity metric} \\ 2, & \text{using damage costs as accident severity metric} \end{cases}$$

R_{1i}= annual accident risk (mean) based on the severity metric used;

N = number of accidents in one year; and

X_{ij} = accident severity, either in casualty or damage cost.

Both accident frequency (N) and severity (X_{ij}) are random variables. Using the Law of Total Expectation (Weiss, 2006), Equation (2-2) can be expanded as follows:

$$E(\sum_{j=1}^{N} X_{ij}) = E\left[E(\sum_{j=1}^{N} X_{ij}|N = n)\right] \qquad (2-2)$$

Then equation can be further written as:

$$E(\sum_{j=1}^{N} X_{ij}) = E\left[E(\sum_{j=1}^{N} X_{ij}|N = n)\right] = E\left[NE\left(X_{ij}\right)\right] = E(N)E\left(X_{ij}\right) \qquad (2-3)$$

The annual accident risk is numerically equal to the product of expected accident frequency and expected severity. E(N), as the expected value of accident frequency, can be calculated using a developed regression model, given traffic volume in each year. E(X_{ij}), as the expected value of accident severity, is equal to the mean value of empirical accident severity.

One limitation of using the expected consequence (mean value) to represent the risk is that it does not fully represent the low-probability-high-consequence characteristics of

train accidents. For example, most human-factor-caused accidents occurred with no casualties, yet some resulted in over 20 casualties. The mean value alone does not fully represent the potential of high-impact accidents. To account for the "heavy-tail" (long-tail) effect in risk analysis, alternative risk measures have been developed. They are referred to as "spectral risk measures" (SRM), particularly Value at Risk (VaR) or Conditional Value at Risk (CVaR), which have primarily been employed in financial engineering (Soleimani et al., 2014), social sciences (Cotter and Dowd, 2006), highway hazardous materials transportation (Toumazis and Kwon, 2016), and, recently, rail transport of hazardous materials (Hosseini and Verma, 2017). These prior studies have found that VaR and CVaR are useful alternative risk measures to capture the "worst-case-average" of accident consequences. To our knowledge, there has been no prior study applying alternative risk measures to the analysis of railroad accident risk.

The VaR is the α-quantile $\alpha \in (0,1)$ of a distribution. CVaR, also known as Expected Shortfall (ES), is basically the weighted average of all outcomes exceeding the confidence interval of a dataset sorted from worst to best. For example, $CVaR_{0.95}$ of the number of casualties is the mean (average) of all the numbers of casualties within the worst 5% of train accidents in terms of number of casualties. Overall, VaR gives a range of potential losses and CVaR gives an average expected loss within the most severe accidents. Equations 2-4 and 2-5 give the mathematical formulas for VaR and CVaR, respectively, and α is set as 95%.

$$VaR_{\alpha}(X) = \min\{x: P(X \leq x) \geq \alpha\} \qquad (2-4)$$

$$CVaR_{\alpha}(X) = \mathrm{E}[x | x \geq VaR_{\alpha}(X)] \qquad (2-5)$$

Previous studies stated that VaR does not account for the losses/consequences beyond the threshold amount indicated by the measure (Rockafellar and Uryasev, 2000). It also has undesirable mathematical characteristics, such as a lack of subadditivity and convexity. In addition, VaR is difficult to optimize when it is calculated from scenarios (Rockafellar and Uryasev, 2000). As an alternative measure of risk, CVaR displays superior properties in comparison to VaR, such as being positively homogeneous, convex, and monotonic (Rockafellar and Uryasev, 2000). Thus, the following analysis employs CVaR as an alternative risk measure. However, the analysis can be adapted to VaR or other spectral risk measures as well.

This chapter considers $CVaR_{95\%}$, which represents the mean of the 5% most severe (in terms of either damage costs or casualties) train accidents. The annual risk is defined as follows:

$$R_{2i} = CVaR_{95\%}\left(\sum_{j=1}^{N} X_{ij}\right) \qquad (2-6)$$

Where

$$i = \begin{cases} 1, & \text{using number of casualties as accident severity metric} \\ 2, & \text{using damage cost as accident severity metric} \end{cases}$$

R_{2i} = annual accident risk (spectral risk measure) based on severity metric used;

N = number of accidents in a specific year; and

X_{ij} = accident severity (e.g., casualty or damage cost).

2.3 Risk Mitigation and Countermeasures

Risk mitigation strategies and countermeasures can be developed based on risk assessment. For example, in the fault tree analysis, the bottom leaves are basic events and

represent the lowest-level events which may contribute to the occurrence of the top event. The identification of human factors behind a specific accident can contribute to the development of prevention strategies.

2.3.1 Near miss analysis

FRA initiated a partnership with National Aeronautics and Space Administration (NASA) and is working on a research project called Confidential Close Call Reporting System (C3RS), to better understand the events called “close calls”, which could have resulted in accidents but fortunately did not yet. This program facilitates anonymous reporting of unsafe railroad conditions. With this closed participation system, railroad employees will be able to report human-factor-related safety issues voluntarily and confidentially, which may have been ignored before. These reports involve incremental unsafe conditions and descriptions of human errors in railroad industry and then be analyzed by a Peer Review Team (PRT) comprising labor, management, and FRA representatives. The system can provide understanding of the impacts of aforementioned company-level factors in human error accidents, such as periodic train operation education, working schedule, and engineer fatigue monitoring program, and could also promote the enhancement of these factors. Similarly, Rail Safety and Standards Board (RSSB) also maintains the “Close Calls” reported by railroad personnel in the accident database that is used in the analysis with Safety Risk Model (Van Gulijk et al., 2015). To achieve convenient user interfaces, the workers in Great Britain (GB) railroads can use mobile applications to make a close call report, which is freeform text report. Van Gulijk et al. (2015) disclosed that over a period of two years, approximately 150,000 entries were collected and saved into the GB’s Close

Call Database. The big data can be extracted and contribute to added value for safety and risk domain.

2.3.2 Appropriate medical program for safety-sensitive personnel

Among the NTSB railroad accident reports that investigated human-factor-caused accidents in the last five years, the violation of operating rules due to crewmembers' human error is one primary cause. In particular, human error due to physical condition (e.g., vision problems and sleep disorders) is identified as one root cause behind restricted-speed accidents. For example, in the investigation of a head-on collision of two Union Pacific Railroad freight trains in 2012, NTSB (2013) concluded this human-factor-caused accident resulted from the engineer's inability to see and correctly interpret the restricting signals. In both the NJT train accident at Hoboken Terminal in 2016 and the Long Island Rail Road (LIRR) train accident at Atlantic Terminal in 2017, the investigation results indicated that both engineers in both human-factor-caused accidents were operating trains despite their fatigue due to untreated obstructive sleep apnea (OSA). Consequently, NTSB has suggested an appropriate, comprehensive medical program to ensure that employees in safety-sensitive positions should follow medical standards to be fit for duty. Accounting for vision issues in medical tests, NTSB (2013) suggested the implementation of a validated, reliable, and comparable color vision field test. Railroads should establish an acceptable medical program involving this vision test and ensure that personnel in safety-sensitive positions have sufficient color discrimination to perform safely. As for crewmembers who fail the color vision test, it would be advisable to restrict such crewmembers from working in yard assignments or unsignaled territory (NTSB, 2013).

2.3.3 Implementation of alerters

Inattentive behaviors from crew members are one common causal factor behind human-factor-caused accidents. Such accident risk can be mitigated through an alerter, which can be implemented in the locomotive cab to promote the engineer's attentiveness through both audible alarms and visual alarms. With this safety device in the locomotive cab, if the system detects no control activity from the engineer in a predetermined time, both kinds of alarms are activated to prompt a response. Ultimately, the engineer's inattentiveness may be mitigated to some degree.

2.3.4 Train engineer education and training

A variety of strategies and practices are being implemented in the railroads. For example, Rowe (2012) presented the development of train driver training simulator that has the ability to train multiple drivers simultaneously and to review performance in detail. In this effective simulator, essential tasks (e.g., being able to look around while driving, taking power/applying brakes) are included. Both normal and abnormal driving were documented in a full task list and analyzed with the task assessment observations. To mitigate train engineer fatigue risk, a real-time online prototype driver-fatigue monitor was proposed by Ji et al. (2004). In this non-intrusive monitoring, it uses prototype computer vision system for real-time video images of the driver and monitors driver's vigilance.

2.4 Evaluations of Risk Mitigation

An ex-ante evaluation of proposed risk mitigation strategies and countermeasures provides a comprehensive assessment. These follow-up assessment results can help railroads and policy makers evaluate trade-offs among proposed risk mitigation actions and

also support the comparisons with alternative transportation investments/strategies. Three lines of inquiry can be covered in these assessment of risk mitigations:

1) What are the estimated safety benefits of human-factor-caused accident reduction?
2) What are the anticipated incremental costs of the proposed strategies or countermeasure? Would they be higher or lower than safety costs in service life?
3) What are the quantitative operational impacts if the proposed strategies are in service in real-world train operations?

2.4.1 Cost-benefit analysis

The proposed risk mitigation strategies offer potential safety benefits because it can reduce the corresponding human-factor-caused accident risk. Meanwhile, the installation and maintenance of these countermeasures are costly and increase capital and operating expenses. A benefit-cost analysis involves estimated safety benefits, incremental costs, net present value (NPV), and the benefit-cost ratios associated with proposed risk mitigation strategies. The main purpose of this systematic process of identifying and quantifying expected benefits and costs is to help provide decision-makers with economic information, evaluate trade-offs, and also serve as a reference for comparisons with alternative transportation investments.

The methodological framework for this benefit-cost analysis is based upon Benefit-Cost Analysis Guidance for Rail Projects published by the FRA (2016). The calculations are based on this FRA guidance, railroad experts' experience, and additional reference materials. Specifically, the safety benefits from the prevention of human-factor-caused accidents are estimated in monetary value with historical accident data and the estimation approach developed by FRA used in the PTC ruling making process (AAR, 2011; Peters

and Frittelli, 2012). The train accident information summarized here are from the FRA Rail Equipment Accident (REA) database. In terms of incremental cost, this research mainly uses the unit cost information based upon the collected survey from railroad experts and also involves the proposed countermeasures. In addition, the sensitivity of the cost-benefit ratio to certain variables can be developed to evaluate the uncertainties and variations behind the assessment results.

Analysis Period

FRA (2016) pointed out that the selection of an approximate analysis period is a fundamental consideration in any benefit-cost analysis (BCA). An analysis period is employed to capture these dynamics behind service-life safety benefits and costs. The FRA (2016) recommended that "the analysis period of a BCA consist of the full construction period of the project, plus at least 20 years after the completion of construction during which the full operational benefits and costs of the project can be reflected in the BCA." In this study of PTC economic analysis (FRA, 2009), 20 years is used as service life and a 20-year analysis of the costs and benefits associated with nationwide PTC implementation. As a similar topic, this study develops benefit-cost analysis with 20-year projected railroad safety benefits and 20-year costs as the objective variables in total.

Meanwhile, there are uncertainties about the future about how travel markets and patterns may shift, whether the PTC components used in the maintenance would be manufactured by the vendors. As a result, an exceedingly long-term analysis may lose reliability and perhaps even meaning. Therefore, the FRA (2016b) also recommends that "*project sponsors generally avoid analysis periods extending beyond 40 years of full operations*."

Converting nominal dollars into constant dollars

Monetary values of safety benefits and costs are used in the BCA and measured by the dollars. As a study involving a long-term period, it is essential to use constant dollars, instead of nominal dollars that are defined as the dollars without adjustment to reflect the effects of inflation. Due to the inflations in the real world, the purchasing power of dollars varies from year to year. For example, 1,000 dollars in 2009 will be expected to buy more goods of the same average quality than would 1,000 dollars in 2017.

In the study of inflation dynamics, Gali and Gertler (1999) measured inflation with the percent change in the Gross Domestic Product (GDP) deflator. To convert the nominal dollars into constant dollars, the GDP deflator is one general method and used in previous studies (FRA, 2009; 2016). The GDP deflators capture the changes in the value of a dollar over time by considering changes in the prices of all goods and services in the U.S. economy and are the data is collected from the World Bank (2018).

Table 2. 1. 2000-2017 U.S. GDP Deflators Provided by the World Bank (2018)

Year	GDP Deflator	Year	GDP Deflator
2000	80.90	2009	98.79
2001	82.74	2010	100.00
2002	84.01	2011	102.07
2003	85.69	2012	103.95
2004	88.05	2013	105.62
2005	90.88	2014	107.52
2006	93.67	2015	108.69
2007	96.12	2016	110.07
2008	98.05	2017	112.05

This study uses the dollar in 2017 as the unit in the estimations of safety benefits and costs in BCA. The GDP deflator is taken into consideration and the monetary values in each year are adjusted to 2017 dollars using the GDP inflator (World Bank, 2018).

Discount rate

The benefit-cost analysis uses the discount rate in the calculation of the benefits and costs that occur at different time points. The discount rate adjusts for the time value of money and allows for safety benefits, as well as following costs, to be valued in equivalent units. These equivalent units are called present values and are independent when they occur. The time value of money expresses the principle that costs and benefits that occur sooner in time are more highly valued than those that occur in the more distant future (FRA, 2016b). The discount rates of 7 percent and 3 percent per year are employed in both FRA reports (FRA, 2009; 2016) and would also be employed in this study. The calculations of safety benefits and costs with discount rate are as following equations are shown:

$$PV\_Benefits = \frac{FV_{Benefits}}{(1+d)^i} \quad (2-7)$$

$$PV\_Costs = \frac{FV_{Costs}}{(1+d)^i} \quad (2-8)$$

Where:

$PV\_Benefits$ and PV_Costs are the present discounted value in constant dollars;

$FV\_Benefits$ and FV_Costs are the future discounted value in constant dollars; and

d = annual discount rate; this study uses 3% and 7%.

2.4.2 Operational impact assessment

Operational impact analysis can be achieved with either qualitative assessment from expertise or quantitative assessment with simulation processes. Firstly, in the

quantitative assessment, each scenario is analyzed based on the proposed risk mitigation strategies and deep expertise. Secondly, the quantitative analysis employs a statistical simulation tool (e.g., Monte Carlo simulation) to quantitatively evaluate the impact on train operations, which may have a certain level of capacity impacts per expertise. A generic model of a known rail line is used to conduct this quantitative simulation under controlled conditions to determine any operational impacts on terminal capacity and operations. These contribute to a full assessment of operational impact in proposed risk mitigation actions. Train braking algorithm is one general principle in operational impact assessment.

CE-205 is one passenger train safe braking standard adopted by Amtrak (National Railroad Passenger Corporation) and commuter railroads (e.g., Caltrain, SunRail) in the United States (12-14). The CE-205 braking distance curve is based on the average performance of 1.1 mph per second deceleration rate. This rate is de-rated by 25% for safety factor to 0.88 mph per second in the calculation of stopping distances. In addition, the 8-second delay time is taken into account due to cab signal delay, brake propagation delay, and engineer reaction delay. The equation of CE-205 stopping distance is shown in Figure 2. 3. For example, if a train traveling with 20 mph applies brake and stops, the stopping distance is 568.032 ft. In the braking curves developed by Mokkapati and Pascoe (2011), the stopping distance with an 8-second delay is 270.73+29.34*8=505.45 ft. This braking algorithm is for train operation on level tangent track.

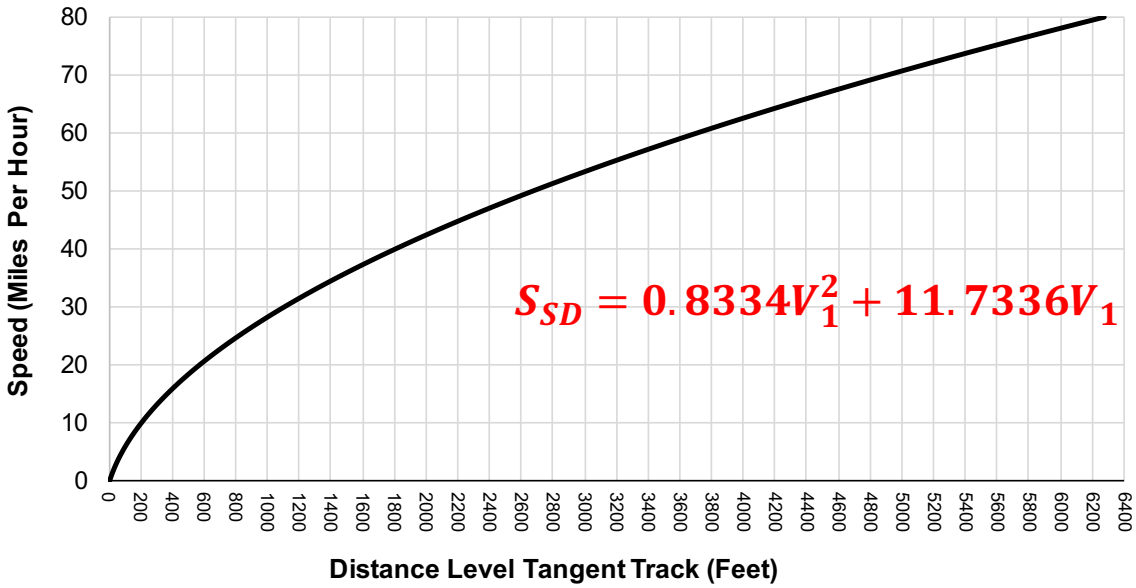

Figure 2. 3. CE-205 Braking Distance Curve

The above CE-205 braking algorithm is for train operations without a PTC system, in which the train engineer is responsible for speed reduction and positive train stop (PTS). In terms of braking applied by the PTC systems, the brake delay time in the PTC-induced braking algorithm is expected to be shorter than manual operation. Mokkapati and Pascoe (15) concluded that the brake delay time is related to locomotive positions and train length:

$$Td = CF * (0.0013 * (Train\ Length) + 1.8322\ s) \quad (2-9)$$

Where,

Td = the brake propagation delay time (seconds);

CF – the correction factor (e.g., 1.11 for the passenger trains with the locomotives at head end only and 1.08 for the push-pull passenger trains); and

Train length – the length of the entire train in feet.

Taking one passenger train consisting of 6 cars (1 locomotive at head end and 5 passenger cars) with a train length of 491 ft ($1 \times 66\text{ft} + 5 \times 85\text{ft}$) as an example, the brake delay time in PTC-induced brake algorithm would be 2.74 seconds.

CHAPTER 3

MODEL CALIBRATION AND APPLICATION WITH RESTRICTED SPEED TRAIN ACCIDENTS

Adapted from
Zhang, Z., & Liu, X. (2019). Safety risk analysis of restricted-speed train accidents in the United States. *Journal of Risk Research*, 1-19.

Zhang, Z., Liu, X., & Holt, K. (2019). Prevention of end-of-track collisions at passenger terminals via Positive Train Control. Transportation Research Record: *Journal of the Transportation Research Record*, 2673(9), 471-479.

Zhang, Z., Liu, X., & Holt, K. (2020). Prevention of End-of-Track Collisions in Passenger Terminals via Positive Train Control: Benefit-Cost Analysis and Operational Impact Assessment. Transportation Research Record: *Journal of the Transportation Research Record*, 20-04977

3.1 Introduction

Restricted speed is defined as a speed that will permit stopping within one-half the range of vision, but not exceeding 20 miles per hour (FRA, 2011a). Besides the federal regulations, railroad operating rules also set forth definitions of movements at restricted speeds. At present, most Class I railroads (a group of the largest railroads operating in the U.S., with each railroad's annual operating revenue over $433 million) use one of two "standard" rulebooks: the Northeast Operating Rules Advisory Committee (NORAC) rulebook, and the General Code of Operating Rules (GCOR). In these two guides, GCOR (2010) has almost the same definition of restricted speed as 49 CFR 236 Subpart G, while NORAC (2018) provides a stricter requirement in interlocking. More specifically,

restricted speeds in NORAC are required to not exceed 20 mph outside interlocking limits or 15 mph within interlocking limits.

However, railroad restricted speed is not a simple numerical value. Train movement must be made at a speed that allows for stopping within half the range of vision short of a variety of hazards, such as other trains, engines, railroad cars, stop signals, men or equipment fouling the track, as well as obstructions (GCOR, 2010; NORAC, 2018). Coplen (1999) pointed out that the violation of restricted speed rules was one of the most common types of rule compliance problems on U.S. railroads. Several rear-end train collisions occurring in 2011 and 2012, in which crewmembers failed to operate their trains under the required restricted speeds, were discussed by NTSB (2012) and the U.S. Federal Railroad Administration (FRA, 2012). One of them, a rear-end collision of two BNSF Railway (BNSF) trains in 2011, led to two fatalities and more than $8 million in estimated damage costs. The probable cause was the failure of the crew to comply with the signal indication and to stop short of the train because they had fallen asleep (NTSB, 2012). More recently, one end-of-track collision at Hoboken Terminal in New Jersey, September 29, 2016, occurred at restricted speeds and has provoked concerns from the public and rail industry. It led to one fatality, 110 injuries, and around $6 million in damage costs to the train, track, and facility. One probable cause was the failure of this train's engineer to stop the train after entering Hoboken Terminal with excessive speed (NTSB, 2018a).

Apart from human errors that can contribute to the occurrence of restricted-speed accidents, environmental conditions and terrain along the railway are also contributing factors in some accidents. More specifically, the range of vision, as one key part in the definition of restricted speed, varies with some key physical features in advance of the train,

such as a descending grade or a reduced visibility due to severe weather conditions. In some cases, the sensitive range of vision can result in trains not being stopped short of an obstruction or a switch not being properly lined, leading to an accident. Restricted speed is imposed on train movements under several conditions, such as:

1) At Automatic signals when the block ahead is occupied, a switch is not properly lined, or a defect detector is alarmed (either as a Stop and Proceed or Restricting as the least permissive aspect),
2) At Interlocking signals where the Call-On function (a two-step process which allows the dispatcher to display a signal into an occupied block) is enabled or where the Restricting aspect can be displayed,
3) At the end of PTC territory for mainline track exclusions and terminals,
4) Routes into non-signaled passing sidings,
5) Moves from PTC territory to yard limits which are defined by the yard limit signs at each end of the yard, and
6) En route failure of PTC system.

Restricted speed can be found on virtually every mile of PTC territory where Automatic Block Signaling (ABS) is used as the underlying train control system. In these systems, the most restrictive signal is Stop and Proceed at Restricted Speed, or Restricting. This applies to both interlocking and automatic signals, respectively. In interlocking, signals do not automatically display Restricting. Instead, interlocking signals have to be requested by the dispatcher and may require the use of a Call-On function.

Other areas with restricted speeds include areas approaching and within terminals.

Normally covered under a Mainline Track Exclusion Addendum (MTEA) (49 CFR Regulation 236.1019) waiver for non-PTC operation, this can be the result of insufficient Safe Braking Distance (SBD) to the end of the track from the Maximum Authorized Speed (MAS), operating practice, or limitations on signal aspects within the terminal. Similarly, trains are required to move at restricted speed while entering the yard limit area, which is defined by the yard limit signs.

Another common use of restricted speed is the most permissive aspect for movements in non-signaled sidings. In addition, similar to cab signals, when on-board PTC equipment fails during normal operations along the railroad, trains will operate at restricted speed until either the failure is corrected or other operating methods are imposed. Besides, there are some rare train operations under restricted speed and they are not discussed separately here. The proposed Concept of Operations in this study can be adapted to these rare restricted speed areas with few changes.

Although there is an increasing concern with restricted-speed operations and accidents, to our knowledge, there has been very limited analysis of restricted-speed train accident risk in the United States in the prior literature. This knowledge gap has motivated the development of this study, in which restricted-speed accident data is statistically analyzed for quantitative risk analysis. Due to the complexity of this subject and the content limit of this research, this chapter focuses on restricted-speed train accidents that are due to crewmembers' failure to comply with restricted speed rules, instead of all other causes (e.g., track, mechanical, signaling, and other human errors), in the United States.

3.2 Restricted-Speed Accident Risk Identification and Data Collection

In the United States, restricted-speed operation is a common type of train operation, which is on virtually every mile of the Absolute Block System (ABS) and extensively employed within terminals and yards. However, relying on train engineers to make operational decisions also introduces human-error-caused risk. For example, the National Transportation Safety Board (NTSB) issued a report in 2012 highlighting five rear-end collisions due to violations of restricted speeds (NTSB, 2012). In all five collisions, crewmembers failed to operate their trains at the required restricted speed.

Based on prior studies in accident risks (Nuclear Regulatory Commission, 1990; Aven and Renn, 2009; Liu, 2016a), the risk of restricted-speed accidents in this research is defined as the combination of expected accident frequency and expected accident severity. For example, the annual restricted-speed accident risk can be modeled as the product of the annual expected number of restricted-speed accidents and the expected accident consequences per accident. The risk analysis method and information garnered from it can potentially provide new insights into railroad safety and risk management related to restricted-speed operations. In addition to using the expected consequence (mean value) to represent the risk, this research also develops alternative risk measures (specifically the Conditional Value at Risk), to characterize low-probability-high-consequence restricted-speed train accidents under certain circumstances. Apart from a macro-level analysis of nationwide restricted-speed accidents, Fault Tree Analysis is also developed based upon specific accidents in order to explore the characteristics of individual accident cases. This developed qualitative analysis can contribute to identifying contributing factors. This study uses accident data for all types of accidents associated with the violation of restricted

speeds from 2000 to 2016. The accident data employed in this study comes from the FRA's Rail Equipment Accident (REA) database and traffic volume data source is the FRA Operational Safety Database. Accident narratives and causes are employed as the criteria to identify restricted-speed accidents. Narrative is a field in which a short text description of the accident was provided by the railroad correspondent. In these accidents' narratives, keywords such as "restricted speed" or "restricting signal" are adopted to collect restricted-speed accidents. In terms of accident causes, they were compiled into two fields of FRA's REA database, namely CAUSE and CAUSE2. CAUSE is defined as the primary cause of an accident and CAUSE2 is a contributing cause of the accident. Both CAUSE and CAUSE2 use a cause code (a coded variable with 389 values) in each field. Either of them having a restricted-speed-related cause code would mostly indicate a restricted-speed accident. Per railroad expert judgments, three cause codes, H603, H605, and H607, have a straightforward relationship with restricted-speed accidents due to human error (FRA, 2017b) and are used in our data collection. The definitions of yard limits and interlocking are stated in the Operating Rules (GCOR, 2010; NORAC, 2018) and Federal Regulations (FRA, 2011a). Yard limits are the main track area between yard limit signs and designated in the Timetable or special instructions. The leading end of movement within yard limits must operate under restricted speeds. Interlocking is an arrangement of signals that are interconnected by means of electric circuits, so that train movements over all routes are governed by signal indications succeeding each other in the proper sequence.

In addition, this chapter manually reviews the accident narratives to verify that the included accidents were indeed due to violation of restricted-speed operating rules (e.g., operating the train above 20 mph in the restricted speed territory). A general flowchart for

restricted-speed accident data collection is presented in Figure 3.1. In the restricted-speed accident dataset, 887 restricted-speed train accidents were identified and collected from 2000 to 2016 for the following empirical and statistical risk analysis. These 887 restricted-speed accidents include both freight-train accidents and passenger-train accidents on all types of tracks (e.g., main, yard, siding, and industry). Selected high-consequence restricted-speed accidents are listed in Appendix A.

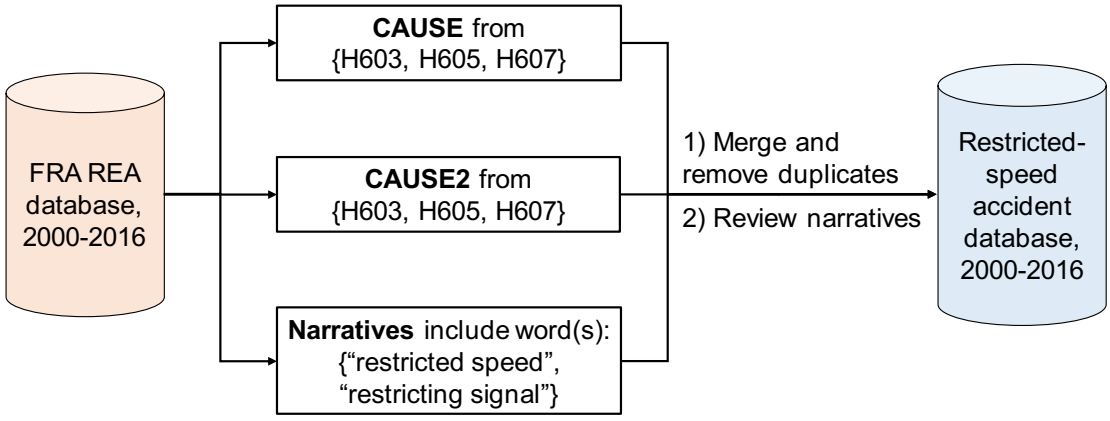

Figure 3. 1. Restricted-Speed Accident Collections

Based on the FRA data from 2000 to 2016, on average, there were 52 restricted-speed accidents per year in the United States. In the 17-year study period, those restricted-speed accidents have led to ten fatalities and 512 injuries. If the reportable damage cost (damages to track infrastructure, equipment, and signals) is adjusted to 2016 dollars using the GDP deflator (World Bank, 2017) with the consideration of inflation, the total cost of damage is around $146 million (at the 2016 dollar-value) in this period. Most of those restricted-speed accidents occurred in the form of either derailments or collisions, each accounting for 39%, respectively. Other accident types, such as obstruction by objects on

the track (e.g., bumper blocks, standing track inspector, standing ballast regulator), accounted for 22% of restricted-speed train accidents. The statistical analysis of accident frequency, severity, and risk (measured by casualty or damage cost) will be discussed in the following subsections (Figure 3. 2).

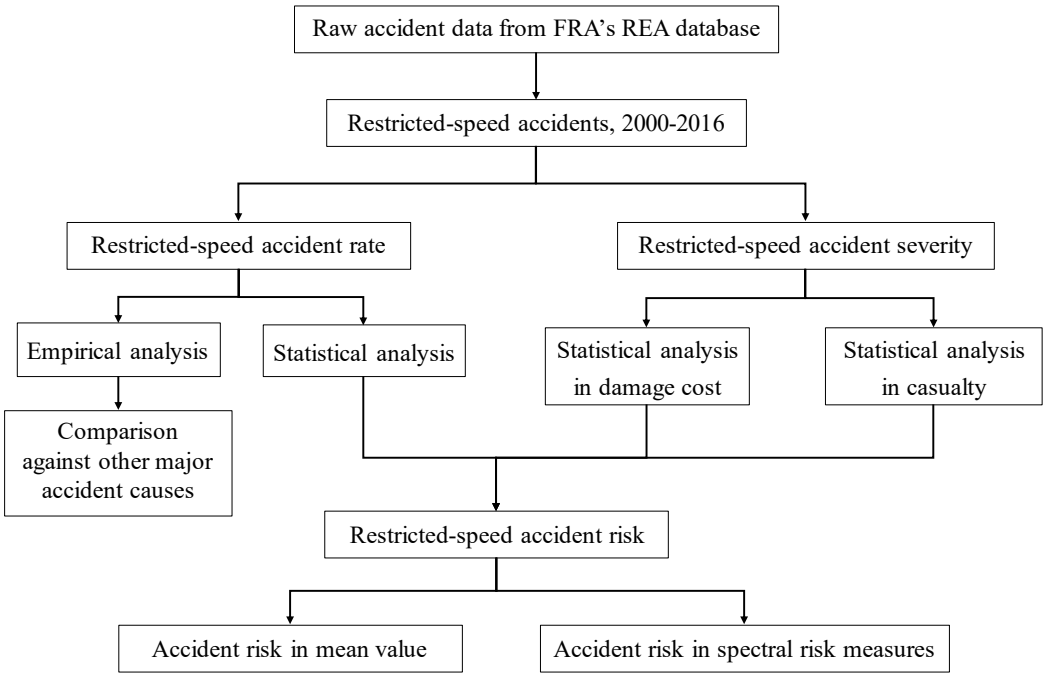

Figure 3. 2. Flowchart of Implemented Methodology

3.3 Restricted-Speed Accident Risk Analysis

3.3.1 Accident rate

Figure 3. 3 compares the empirical accident rate for restricted-speed train accidents with two other leading accident causes on U.S freight railroads: broken rails and track geometry failures. While broken rails were the leading accident cause in the United States for the last 17 years, the rate for this cause has declined steeply, dropping by around 50%. A significant safety improvement has also been observed for track-geometry-failure-caused accidents. The reduction in the rate of infrastructure-caused accidents is not

surprising. Over the past two decades, the U.S. railroad industry has invested extensively in advanced track detection technologies and risk-based maintenance strategies to increase infrastructure quality (Barkan et al., 2003). The graph shows no apparent indication that the rate of restricted-speed accidents has been either increasing or decreasing over the last 17 years. As a result of this dissimilar temporal trend, the rate of restricted-speed accidents has surpassed that of track-geometry-defect-caused accidents since 2013.

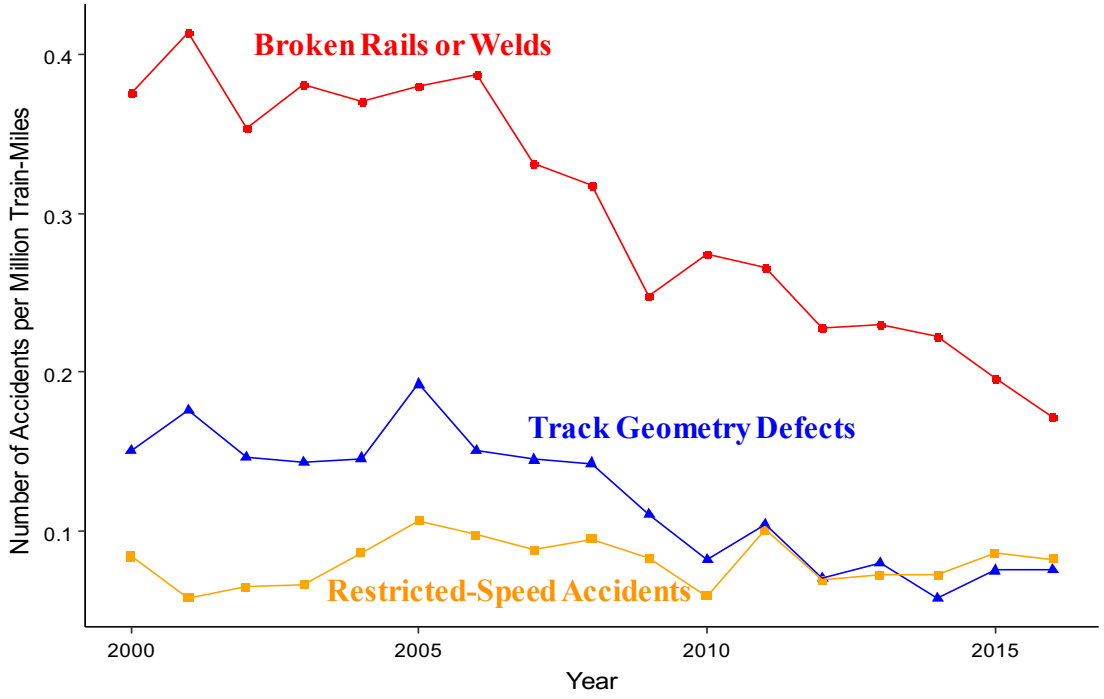

Figure 3. 3. Temporal Trend in Accident Rates for Three Accident Groups in the United States, 2000-2016

A statistical model can be developed to estimate the restricted-speed train accident rate. Based on a prior study, this study accounts for two potential contributing factors, the year and annual traffic exposure (Liu, 2016b). The year variable represents the temporal

change in the frequency of restricted-speed train accidents given certain traffic exposure. The annual traffic exposure variable tests whether and how the count of restricted-speed accidents varies with traffic volume in a given year. First, a Negative Binomial regression (NB) model is applied. As a generalization of Poisson regression, the NB model is for modeling count variables and also relaxes the assumption that the variance is equal to the mean made by the Poisson model. The NB model has been extensively applied to accident rate analysis for both highway transportation (Mitra and Washington, 2007) and railway transportation (Liu et al., 2017) and showed promising results with an acceptable goodness-of-fit. Therefore, this research employs it to model the number of restricted-speed accidents in the United States. Specifically, as shown in Equation 3-1 and Equation 3-2, the observed number of accidents (Y) is assumed to follow a Poisson distribution, in which the coefficient, λ, is assumed to follow a Gamma distribution. Thus, the NB model is also called the Poisson-Gamma mixture model (Hosmer et al., 2013). From this, the estimated number of accidents can be formulated as $\exp\left(\sum_{p=0}^{k} b_p X_p\right)M$. The basic framework is as follows (Liu et al., 2017): the model output is the number of accidents given traffic exposure, and the predictor variables are influencing factors that affect the accident rate.

$$Y \sim Poisson(\lambda) \tag{3-1}$$

$$\lambda \sim Gamma\left(f, \frac{f}{m}\right) \tag{3-2}$$

$$m = \exp\left(\sum_{p=0}^{k} b_p X_p\right)M \tag{3-3}$$

Where

Y = observed number of restricted-speed accidents;

m = estimated number of restricted-speed accidents;

b_p = p^{th} parameter coefficient;

X_p = p^{th} explanatory variable;

M = traffic exposure (e.g., train miles); and

f = inverse dispersion parameter.

In the study of restricted-speed accidents, it is assumed that accidents occur stochastically across the total traffic for a specific year with a Negative Binomial distribution, with a mean count per year (yi) as a function of year index and traffic volume:

$$y_i = \exp(\alpha + \beta \times T_i + \gamma \times M_i) M_i \quad (3\text{-}4)$$

Where

y_i = expected number of restricted-speed accidents in year i;

T_i = year index;

M_i = million train miles in year i; and

α, β, γ = parameter coefficients.

Three parameter coefficients, α, β, and γ, are estimated using the method of maximum likelihood (ML) (Hosmer et al., 2013). The model (4) has been fitted to the 2000-2016 restricted-speed accidents to estimate these three unknown parameter coefficients. The P-value of a parameter estimator represents the statistical significance of a predictor variable using the Wald test (Hilbe, 2007). A generally acceptable rule is that if a predictor variable has a P-value smaller than 5%, this variable is statistically significant. This model tests whether the restricted-speed accident rate changes with time. If the P-value of the index year is smaller than 0.05 and the coefficient is positive, it indicates that

accident rate increases with time (indicating diminishing safety). Otherwise, the accident rate reduces over time. If the P-value is greater than 0.05, it illustrates that there is no statistically significant trend in the accident rate during the study period. The analysis shows that there is an insignificant temporal change in the train accident rate under restricted speeds (P > 0.05). On the contrary, the parameter coefficient for the variable traffic exposure is significantly positive (γ =0.003, P < 0.05). This value illustrates that traffic exposure has a significant effect on the restricted-speed accident rate. A larger traffic volume is associated with a higher accident frequency. Using variables selections and updated modeling, a "final" model is $y_i = \exp(-4.067 + 0.003 \times M_i)M_i$. Table 3.1 shows the regression results and the last column is the P-value of a parameter estimator.

Table 3. 1. Parameter Estimates of Accident Frequency under Restricted Speeds, 2000-2016

Parameter	Estimate	Standard Error	Wald Chi-Square	P-value
α	-4.067	0.656	-6.251	<0.001
γ	0.003	0.001	2.420	0.016

A Pearson's test (Agresti and Kateri, 2011) is developed to evaluate the goodness-of-fit of the regression model. The test shows that the P-value is greater than 0.05 (P-value = 0.1432, degree of freedom = 16). Thus, the developed model adequately fits the empirical data in this study. The analysis shows that there is a non-linear relationship between the restricted-speed accident rate (yi/Mi) and traffic volume (train miles, Mi) (Equation 3-5). When traffic exposure increases, the restricted-speed accident rate per train-mile also

increases, probably due to the increased opportunities for train encounters (Nayak et al., 1983).

$$\frac{\partial(y_i/M_i)}{\partial(M_i)} = \frac{\partial(\exp(-16.380 + 0.003M_i)}{\partial(M_i)} = 0.003 \times \exp(-16.380 + 0.003M_i) > 0 \quad (3-5)$$

A sensitivity analysis is conducted here to estimate the restricted-speed accident rate given different traffic levels. If there is an annual 3% decrease of baseline traffic volume (the average traffic volume for 2000-2016, i.e. 647.5 million train miles), the number of accidents per million train miles will decrease from 0.076 to 0.073, which comprises a 5% accident rate reduction. Inversely, an annual 3% increase in baseline traffic volume can lead to a 5% accident rate boost in restricted-speed accidents.

3.3.2 Restricted-speed accident severity

Table 3.2 shows the distribution of the severity of restricted-speed accidents measured by casualties or damage cost per accident each year. A Wald-Wolfowitz runs test is used to check whether a dataset comes from a random process (Liu, 2016a). When the P-value in the test is greater than 0.05, one may conclude that there is no statistically significant temporal trend in the studied period. In the case of this particular study, the result of the runs test indicates that there is no significant temporal trend for either casualty (P-value = 0.605) or damage cost (P-value = 0.301). The annual fluctuation in accident severity is largely due to random variations. Therefore, the following risk analysis uses the average restricted-speed accident severities, which are 0.545 casualties per accident and around $165,000 in damages per accident.

Table 3. 2. Restricted-Speed Accident Severity per Accident, 2000-2017

Year	Casualties per accident	Damage cost per accident (in 2016 $)
2000	0.943	169,925
2001	0.250	120,911
2002	0.244	85,691
2003	0.674	109,047
2004	0.914	86,093
2005	0.918	163,999
2006	0.271	157,169
2007	2.517	174,517
2008	0.524	80,146
2009	0.500	86,738
2010	0.028	99,607
2011	0.349	126,784
2012	0.182	415,308
2013	0.489	456,671
2014	0.208	187,795
2015	0.164	117,877
2016	0.082	166,087
Average	0.545	164,963
Standard error	0.142	26,241
P-value in runs test	0.605	0.301

3.3.3 Accident risk analysis

The accident risks are summarized in Figure 3. 4. It is not surprising that accident risks calculated according to CVaR95% are always greater than mean value risks since CVaR stands for the 5% worst cases and provides insights into potentially high-severity accidents under restricted speeds. A Wald-Wolfowitz runs test was used again to test whether various accident risks follow any significant temporal trends. The statistical test results indicate that the accident risks for both two measures, R_{1i} (mean) and R_{2i} (CVaR), have no significant temporal trends in the study period.

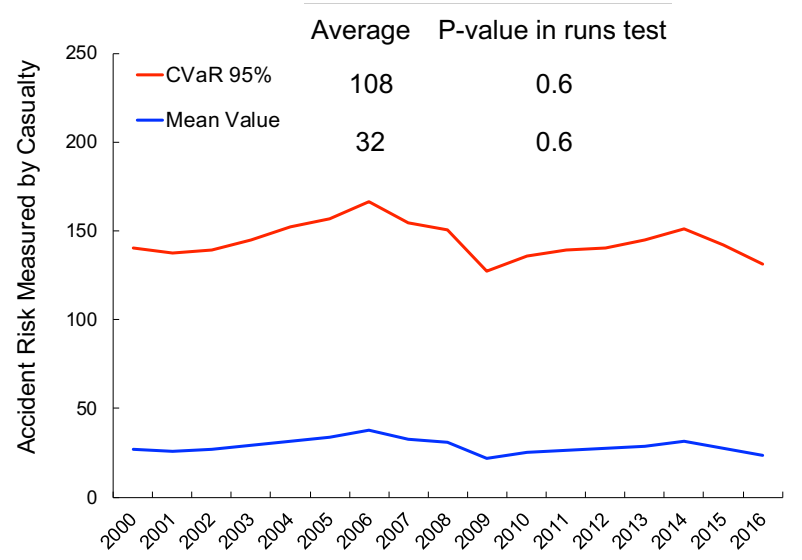

(a) Accident risk in casualty

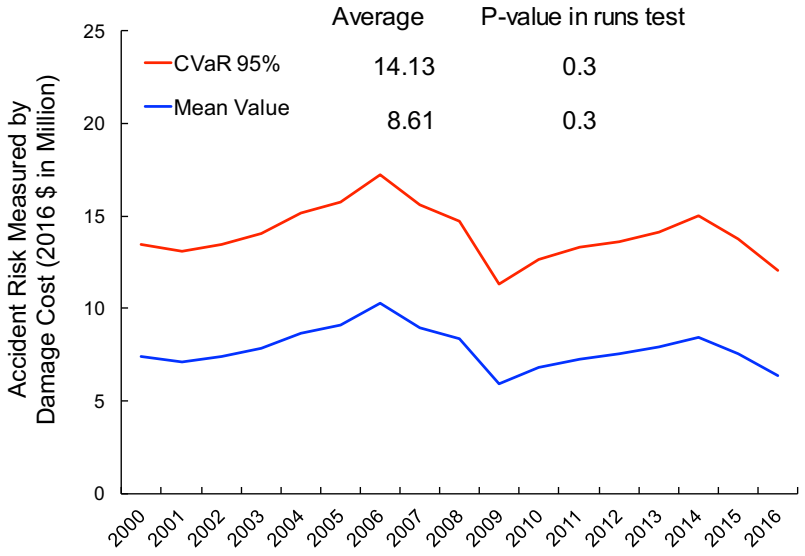

(b) Accident risk in damage cost

Figure 3. 4. Annual Restricted-Speed Accident Risk in Mean and CVaR, 2000-2016

In the period, on average, the annual restricted-speed accident risk totals 32 casualties or $8.61 million in damage costs to infrastructure and rolling stock. By contrast, on average, the worst 5% of restricted-speed accidents are expected to cause 108 casualties or $14.13 million in damage costs annually. Furthermore, the ratio of CVaR to mean value in casualties is over 3, which is larger than the ratio of CVaR to mean value in damage

costs. This indicates that accident risk measured by casualties may have a more significant "heavy-tail" in the worst accident consequences. This is also consistent with the empirical analysis, in which 85% of restricted speed accidents led to zero casualties whereas some severe accidents led to dozens of casualties. The risk analysis implies that the use of alternative risk measures can provide additional insights into certain types of low-probability-high-consequence restricted-speed train accidents. Depending on the question under consideration and decision makers' attitudes toward risk, specific risk measures can be used. Also, when potential risk mitigation strategies are evaluated and compared, using different risk measures could provide information about a specific strategy's effect on the risk profile, in terms of either overall average or worst-case scenarios.

3.3.4 Qualitative Analysis with Fault Tree Analysis

In this research, the co-occurrence of two intermediate events, which are a signal displaying a restricted-speed indication and the failure to comply with restricted-speed indication, would lead to restricted-speed accidents. These two intermediate events represent two primary determinants, in which each consists of a series of basic events. A signal displaying a restricted-speed indication can be deducted into four major restricted-speed scenarios, including Automatic Block Signal (ABS), interlocking, non-signaled siding, and terminal area. For example, restricted speed is imposed on ABS where the block ahead is occupied, a switch is not properly lined, or a defect detector is alarmed. Interlocking involves restricted speed operation where the Call-On function is enabled. Diverging either into non-signaled sidings from the signaled main track, or into the signaled main track from non-signaled sidings is one common form of restricted-speed

operations. Moreover, the Mainline Track Exclusion Addendum (MTEA) at terminal stations requires restricted-speeds operations. In terms of failure to comply with restricted-speed indications, three major event groups exist, including equipment failure, environmental conditions, and human error. Rolling stock failure, such as brake failure, may fail to stop the train short of the stopping point. In terms of environmental conditions, low visibility due to severe weather conditions (e.g., heavy snow, dense fog) and low adhesion due to vegetation or extreme environmental conditions (e.g., snow, ice) may be contributing factors. As for the human error, crewmembers' physical condition problems (e.g., use of alcohol, sleep issue, deteriorating vision), inattentive behaviors (e.g., texting), or communication problems (e.g., miscommunication or lack of communication between crews and dispatchers) may result in rule violation and thus an accident (Zhang et al., 2018b). In **错误!未找到引用源。** 3. 5, the bottom leaves of the fault tree are basic events and represent the lowest-level events that may contribute to the occurrence of the top event. To clarify, the Fault Tree Analysis covers not only the human factor as the primary cause but also equipment failure and environmental conditions as potential contributing causes in some cases.

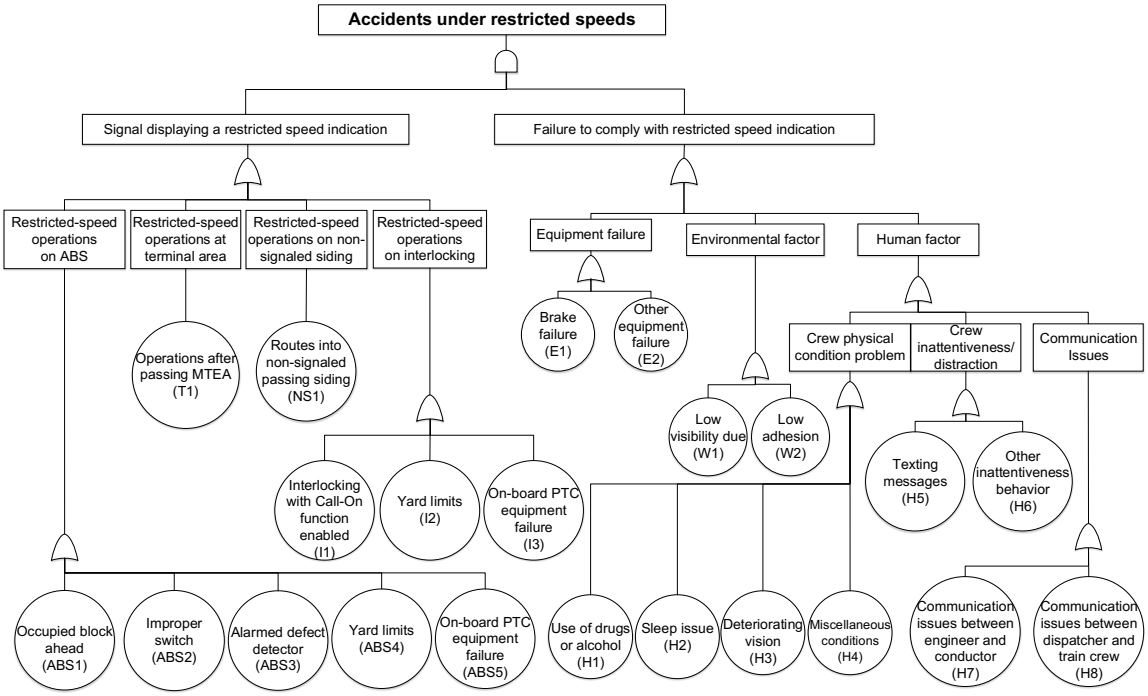

Figure 3. 5. Fault Tree for Train Accidents under Restricted Speeds

3.4 Restricted-Speed Accident Risk Mitigation with PTC Systems

Faced with unchanged restricted-speed accident risk in the last 17 years, it is not only important but crucial to develop and implement safety strategies at restricted-speed train operations. Based upon the findings from the above Fault Tree Analysis and reference information from multiple NTSB investigation reports (NTSB, 2012; 2018a; 2018b), This chapter focuses on the implementation of Positive Train Control (PTC) systems to effectively and reliably mitigate restricted speed train accident risks.

In order to confront human intervention failures in some cases, advanced train control systems such as Positive Train Control can be implemented to enforce positive stops and thereby prevent restricted-speed accidents. Positive Train Control (PTC) is a communication-based/processor-based train control system that is capable of reliably and

functionally preventing train accidents attributable to human error. By integrating the locomotive computer, wayside device, communication network, and back office, the PTC system can compare train real-time conditions against movement authority and speed restriction information to ensure train safety. Whenever a train crew fails to properly operate within specified safety parameters, the PTC system automatically applies the brakes and brings the train to a positive stop (Zhang et al., 2018a).

Federal regulations (FRA, 2011b) designate train operations at restricted speeds as a regulatory exemption from the PTC requirement and accordingly state that the PTC system is not required to perform its functions when a train is traveling under restricted speeds. For example, in both the NJT accident at Hoboken Terminal and LIRR accident at Atlantic Terminal, trains operating on terminating tracks were excluded from PTC installation. Meanwhile, NTSB reports (NTSB, 2013; 2018a; 2018b) pointed out that some restricted-speed accidents would have been prevented if a PTC system had been installed and used. Therefore, it is imperative that implemented mechanisms can automatically stop a train before the occurrence of such accidents, even if the engineer is negligent or disengaged, in order to promote the safety of restricted-speed operations. PTC may be a feasible option to achieve this function. Its cost-effectiveness in preventing restricted-speed accidents shall be carefully evaluated in a separate study.

3.4.1 Concept of Operations for PTC enforcement at restricted speed train operations

In order to confront human intervention failures in some cases, advanced train control systems such as Positive Train Control can be implemented to enforce positive

stops and thereby prevent restricted-speed accidents. Positive Train Control (PTC) is a communication-based/processor-based train control system that is capable of reliably and functionally preventing train accidents attributable to human error. Through integrating the locomotive computer, wayside device, communication network, and back office, the PTC system can compare train real-time conditions against movement authority and speed restriction information to ensure train safety. Whenever a train crew fails to properly operate within specified safety parameters, the PTC system automatically applies the brakes and brings the train to a positive stop (Zhang et al., 2018a).

Trains operating in PTC territory will accept a signal indicating restricting speeds as any other signal. While operating under restricted speeds, train speeds will be enforced at no greater than 20 mph (or 15 mph). This section gives detailed descriptions of how the proposed systems should operate and interact with its users and its external interfaces under a given set of circumstances. Seven major restricted speed scenarios are analyzed and proposed with each modification in the Concept of Operations. All of these individual parts contribute to comprehensible train operation under restricted speeds. Table 3. 3 gives a summary of the proposed modifications for each restricted-speed scenario. Major types of equipment are covered in this table, which excludes software in Back Office and locomotives. Detailed illustrations of the Concept of Operations are attached in Appendix B. In particular, substantial modifications are required in the train operations at stub-end terminals, in which end-of-track collision risks commonly exist with severe consequence. The following sections place an emphasis on the end-of-track collision risk and its mitigation at stub-end terminals.

Table 3. 3. Equipment Needed in Proposed Modifications (Excluding Software)

Scenarios	I-ETMS	ACSES
Stub end terminal	Station track mapping, WIU	Transponders
Through terminal	Station track mapping	Nothing else needed
Non-signaled siding	track mapping, WIUs (hand switch only)	Nothing else needed
Interlocking	Nothing else needed	Nothing else needed
ABS - Alarmed defect detector	Nothing else needed	Nothing else needed
ABS - Occupied block ahead	Nothing else needed	Nothing else needed
ABS - Misaligned switch	Nothing else needed	Nothing else needed
CTC	Nothing else needed	Nothing else needed
Yard limits	Track mapping, WIU (optional)	Nothing else needed

Apart from the aforementioned equipment, rear-end protection is also needed in some cases, such as interlocking, occupied block ahead in ABS. To prevent a rear-end collision, the following train would have to know the limits of movement based on the position of the rear of the train ahead. Rear-end protection would require a device, such as GPS, on the rear of the train with some means to stop the following train before a collision occurs. This would be a major upgrade to the current PTC system. PTC types in current operations do not identify the position of the end of trains nor do they confirm the integrity of trains. As such, there is no way to determine where the stopping point should be for trains operating within an occupied block. This type of train tracking is required for stand-alone systems and would require an extensive re-design of existing PTC systems that are considered outside the scope of this research. Otherwise, in blocks that are known to be occupied, trains would be enforced to a stop at the entrance of the block and await instructions before proceeding.

3.4.2 End-of-track collision at stub-end terminals

In the United States, there are over 35 passenger terminals with multiple terminating tracks ending at bumping posts and/or platforms (NTSB, 2018a). At these passenger terminals, the engineers' behavior plays a key role to safely stop the train before reaching the end of track. However, human errors and noncompliant behaviors (e.g. disengaged, incapacitated, or inattentive) may result in accidents. Train operations at stub-end terminals are one of the common restricted-speed scenarios in the United States. In the Safety Advisory 2016-03, train operations in terminals with stub end tracks are highlighted and "*stress to passenger and commuter railroads the importance of taking action to help mitigate human factor accidents, assist in the investigation of such accidents, and enhance the safety of operations in stations and terminals with stub end tracks*" (FRA, 2016).

Bumping post is a safety device placed at the end of terminating track to stop unauthorized movement and can provide limited protection for low impacts. Passenger stations commonly comprise multiple platforms and crowded people that are exposed to potential hazards resulting from noncompliant train operations. For example, New York Penn Station is the busiest passenger transportation facility in the United States and involves 21 tracks and 11 island platforms. It has a ridership of over 300,000 on the average weekday in 2016, among which LIRR contributes to around a ridership of 233,000 (LIRR, 2017).

In the past decade, there have been a series of end-of-track collisions in passenger terminals. For example, LIRR trains caused 15 collisions with bumping posts at passenger stations in New York between 1996 and 2010 and NJT also reported seven end-of-track collision accidents in the last 10 years (NTSB, 2018a). Most recently. the New Jersey

Transit (NJT) train accident at Hoboken Terminal (Figure 3. 6.a), New Jersey, on September 29, 2016, led to one fatality, 156 injuries, and around $6 million in damage costs. A similar end-of-track collision occurred at the Long Island Rail Road (LIRR) at the Atlantic Terminal (Figure 3. 6.b), New York, on January 4, 2017. The engineers in both accidents failed to stop trains before reaching the end of tracks at passenger terminals. A macro-level analysis of nationwide end-of-track collisions is summarized in Appendix A. The National Transportation Safety Board (NTSB) (2018a) stated that the safety issues identified from these two accidents also exist throughout the United States at many intercity passenger and commuter train terminals.

(a) NJT Accident (b) LIRR Accident

Figure 3. 6. Train Accidents of in Terminus Stations (NTSB, 2018a)

In spite of the potential risk and the increasing concerns, to the authors' knowledge, limited prior research has been conducted on end-of-track collisions at terminals in the United States. To narrow the knowledge gap, this section conducts an analysis of end-of-track collisions and presents an end-of-track collision prevention strategy through the

proposed PTC enforcement. In a special investigation report covering both the NJT accident at Hoboken Terminal and the LIRR accident at Atlantic Terminal (NTSB, 2018a), the NTSB pointed out one safety recommendation that "requires intercity passenger and commuter railroads to implement technology to stop a train before reaching the end of tracks" (R-18-001). Additionally, Moturu and Utterback (2018) stated that PTC can be one mitigation technique against end-of-track collisions. However, these studies contain conceptual oversights and there is a lack of detailed studies in specific modifications (e.g., what is needed and how to implement it) if the PTC system was enforced at passenger terminals. This knowledge gap has motivated the development of this chapter. The primary research objective of this chapter is to analyze the potential implementation of PTC to prevent end-of-track collisions at passenger terminals, with a focus on the Concept of Operations.

Concept of Operations with ACSES Enforcement on Terminating Tracks

In the ACSES-type PTC system, a set of transponders (two transponders in one set) located right before MTEA (Figure 3. 7.a) mark the end of the full ACSES territory at the end of a main track. When the train reaches this point, this set of transponders would inform the onboard ACSES system that it is entering "Out of ACSES Territory" and the ACSES system would go into a dormant state. The ACSES system being deactivated does not enforce any stop or speeds, but the ATC system enforces restricted speed at 20 mph or 15 mph (NORAC, 2018). The ATC system integrates with cab signals and involves speed enforcement. Specifically, with the ATC system, if the train movement violates speed requirements, an audible alarm would be activated. If the alarm is not acknowledged and

no brake is applied, a penalty brake application would be made automatically to reduce train speed. Although the maximum authorized speed at terminal tracks can be enforced by the active ATC system, a train moving under that maximum speed could still cause a collision. For example, a train moving at 5-mph can still cause an end-of-track collision, which cannot be prevented by the ATC alone. Thus, a safe positive (absolute) stop before the end of track continues to depend on the engineer's compliant behavior.

The proposed solution is to divide the terminal area into two zones and to install additional transponder sets at the second zone, as shown in Figure 3. 7.b. The first transponder set (T1 in Figure 3. 7.b) causes the train system to re-enter ACSES territory and provides positive train stop (PTS) information, identifying the end of the platform track as the stop target. In addition, it provides linking distance information to the next transponder set (T2). The first transponder set should be located at a distance greater or equal to the braking distance needed to stop the train safely. The second transponder set (T2 in Figure 3. 7.b) provides not only a PTS with the distance to the bumping post, but also the redundancy to the first set, resulting in better stopping accuracy.

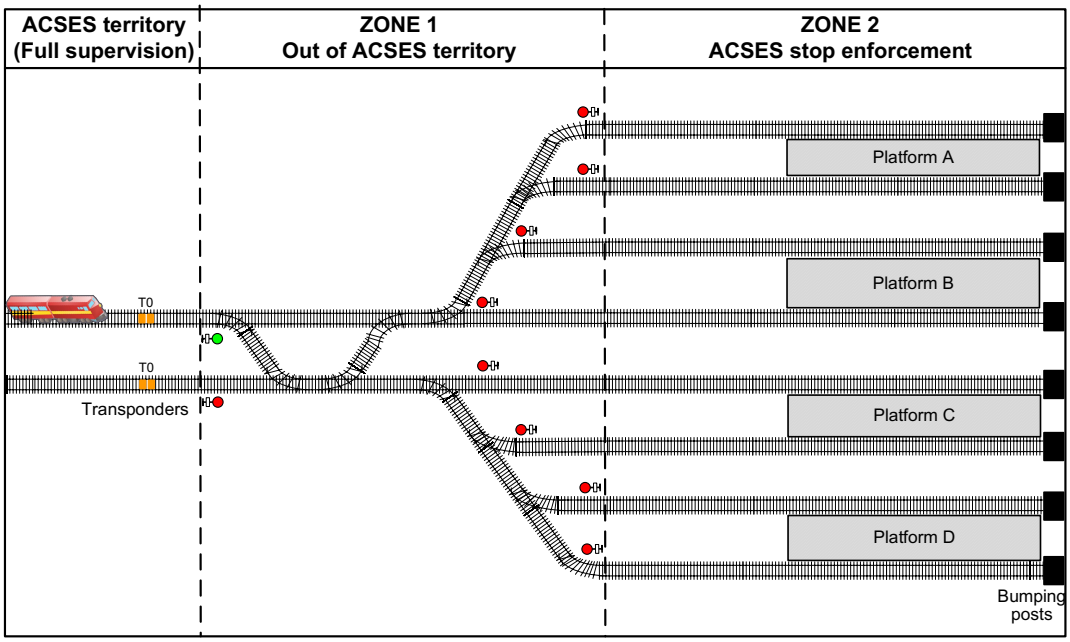

(a) Without ACSES enforcement

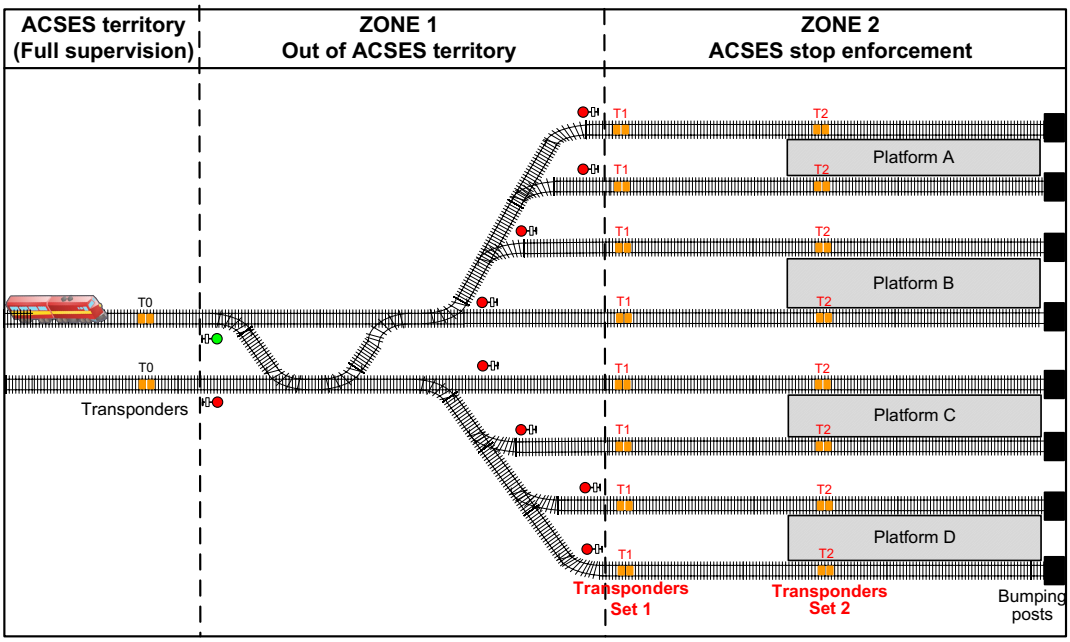

(b) With ACSES enforcement

Figure 3. 7. Stub-End Terminal (a) without ACSES and (b) with ACSES

As the train reads the first transponder set T1 in Zone 2, the ACSES system calculates a braking curve based on the real-time train speed and the present distance to the

target, such as a bumping post. If the system determines that sufficient braking distance exists at a given moment, the train operation will continue to be commanded by the engineer. If there is insufficient stopping distance, the active ACSES system will release a warning, which, if ignored by the locomotive engineer, would cause the system to slow the train so the train can safely stop short of reaching the end of the terminating track. When the train changes its direction and departs from the terminal, it will read the transponders T2 and T1 in the reverse direction. The message in these transponder sets for this direction will tell the train system that it is leaving ACSES territory until it reaches the location where ACSES territory with full supervision begins (Figure 3. 7.b).

Concept of Operations with I-ETMS Enforcement on Terminating Tracks

The I-ETMS system employs GPS navigation to track train movements and real-time location. In practice, many passenger terminals (e.g., Chicago Union Station) are either underground or are surrounded by crowded buildings that make reception of GPS signals difficult or impossible. As a result, it is challenging for the I-ETMS system to enforce a positive stop relying solely on GPS.

The proposed Concept of Operations is to map all the terminating tracks to obtain the distance between a point where the train can obtain a good GPS signal and the end of the track (Figure 3. 8.b). The distances from that point to each bumping post need to be measured over every possible route because there can be multiple routes with dissimilar route lengths.

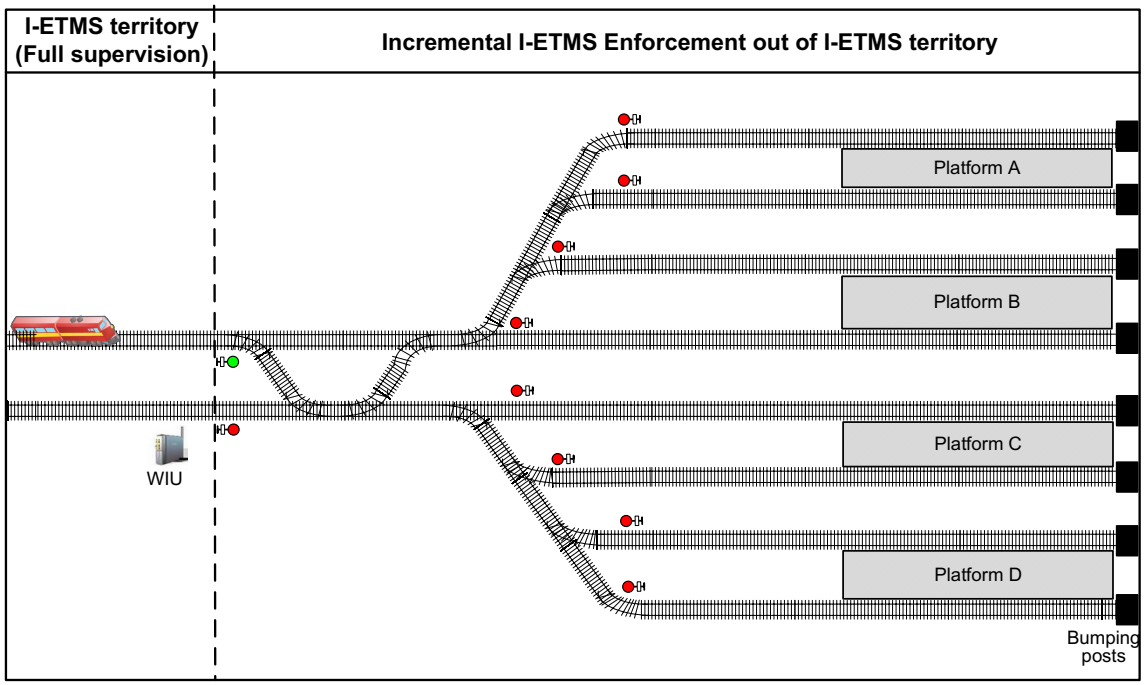

(a) Without I-ETMS enforcement

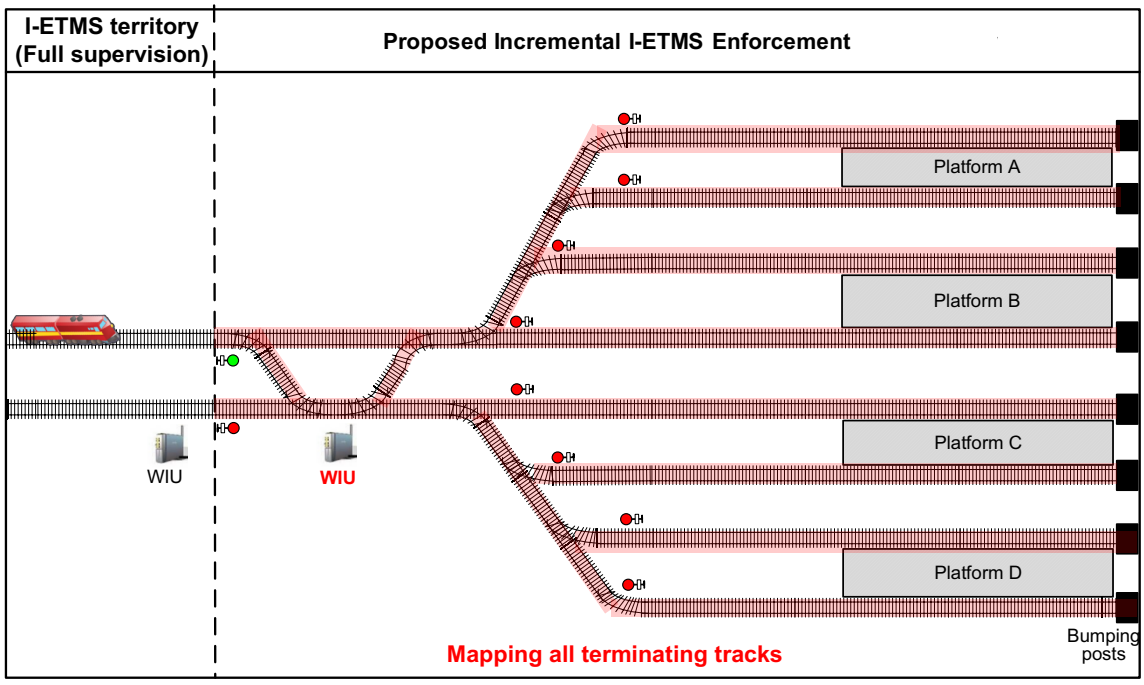

(b) With I-ETMS enforcement

Figure 3. 8. A Simplified Stub-End Terminal (a) without I-ETMS and (b) with I-ETMS Enforcement

When the I-ETMS system loses GPS signal, the distance that the train has traveled can be continuously measured through counting pulses from wheel sensors, which is known as “Dead Reckoning.” In addition to the traveled distance, the system should also know the distance to the bumping post. Therefore, it is essential to know the position of every switch in order to recognize which route the train would take and to determine how far to travel before enforcing a positive stop. To achieve this, the Wayside Interface Unit (WIU) would be required to be installed at the terminal to monitor all the switches within the terminal. The onboard system would query the WIU to obtain switch position information via data radio. Having obtained the determined route, the I-ETMS system receives the permissible distance that it can travel before reaching the bumping post. Correspondingly, the I-ETMS can calculate a braking profile based upon real-time train speed and the remaining distance to the stop target, and then a positive stop can be achieved before the end of the track.

The proposed PTC enforcement on terminating tracks may have certain engineering challenges, such as the close proximity of signals and switches in the terminal areas, the complexity of track-work, potential false penalty hits, and the reliability of transponder function for slow train movements. The studies of these engineering challenges, as well as the aforementioned cost-benefit analysis and operational impacts, are ongoing and will be presented in the future. In addition to end-of-track collisions, the prevention of train-to-train collisions in terminals may be a potential research area. If PTC is used to prevent this type of accident, the following train would need to know where the rear end of the lead train is located to calculate a braking profile to enforce a positive stop before hitting the rear end of the lead train. However, the current PTC systems cannot fully achieve these

functions. Therefore, future research might be worth developing implementable technologies to locate both the head end and rear end of each train, in support of train-to-train collision prevention. This enhanced positioning technology can also support the development of "moving block" systems.

3.5 Assessment of PTC-Based Risk Mitigation via Benefit-Cost Analysis

The developed benefit-cost analysis model in this section and operational impact assessment method in the following section can serve as methodological references for the economic analysis and operating capacity of other rail projects, respectively. Nationwide safety benefits and costs with the PTC enforcement at stub-end terminals (Zhang et al., 2019c) are estimated and compared against each other with two metrics: Net Present Value (NPV) and benefit-cost ratio.

3.5.1 Safety benefits of end-of-track collision prevention

Overview and accident data pool

The primary benefit of PTC implementation at stub-end terminals is the safety benefits or savings expected to accrue from the reduction in the number and severity of casualties arising end-of-track train collisions that would occur on equipped with PTC systems. Business benefits are also one common benefit in transportation project but in this research, the business benefits are excluded from the estimations of benefits due to two preliminary facts. Firstly, FRA (2009) recognized that the general PTC installation in the United States has uncertainty in the likelihood of business benefits and thus has not assumed any business benefits, beyond those from railroad accident prevention. Secondly,

the operational impact study indicates that the PTC implementations at stub-end terminals have a negligible impact on the capacity.

Therefore, in the BCA, benefits indicate the safety benefits related to accident preventions would accrue from a decrease in damages to property such as locomotives, railroad cars, and track, environmental damage, track closures, and evacuations. Benefits more difficult to monetize--such as the avoidance of hazardous material accident related costs incurred by Federal, state, and local governments and impacts to local businesses--will also result. These safety benefit categories were taken into account in the previous FRA study of PTC safety benefits (FRA, 2009). In the study of end-of-track collisions, these categories are still referred and covered in the calculation of safety benefits.

The safety benefits of end-of-track collisions are estimated in monetary value with historical accident data and the estimation approach developed by FRA used in the PTC ruling making process (Peters and Frittelli, 2012; GAO, 2013; AAR, 2017). The train accident information summarized here is from the Rail Equipment Accident (REA) database of the U.S. Federal Railroad Administration (FRA). In the FRA REA database, railroads are required to submit reports of accidents that exceed a monetary threshold for damage and loss (e.g., $10,500 in 2017) and the FRA compiles train accident data based on train accident reports. In addition to the basic accident information listed in Table 3. 4, more comprehensive information can be found in the FRA REA database, including operational factors, environmental factors, train characteristics, detailed damage states, and narratives.

Table 3. 4. End-of-Track Collisions in the United States, 2001-2017[1]

Date	Location [2]	Railroad[3]	Speed (mph)	Injury	Fatality	Damage Cost
Jan. 4, 2017	Atlantic Terminal, NY	LIRR	12	112	0	$5,348,864
Sept. 29, 2016	Hoboken Terminal, NJ	NJT	21	156	1	$6,012,000
Mar. 7, 2016	Port Washington Station, NY	LIRR	2	0	0	$1,713,104
Jun. 2, 2015	Hoboken Terminal, NJ	NJT	3	1	0	$23,802
Jan. 6, 2014	LaSalle Street Station, IL	NIRC	7	0	0	$25,554
Sept. 23, 2012	Jamaica Station, NY	LIRR	2	2	0	$12,000
Feb. 21, 2012	Port Washington Station, NY	LIRR	3	0	0	$42,334
Jun. 8, 2011	Princeton Station, NY	NJT	16	1	0	$53,500
May 8, 2011	Hoboken Terminal, NJ	PATH	13	35	0	$352,617
Mar. 21, 2011	Port Jefferson Station, NY	LIRR	12	2	0	$110,283
Jan. 27, 2011	New Canaan Station, CT	MNCW	7	0	0	$51,500
Jun. 27, 2010	Port Washington Station, NY	LIRR	0	0	0	$10,500
April 12, 2010	Grand Central Terminal, NY	MNCW	1	0	0	$31,500
Oct. 21, 2009	33rd Street Terminal, NY	PATH	6	2	0	$328,000
Jun. 12, 2009	Washington Union Station,	ATK	3	0	0	$19,500
Mar. 2, 2009	New Canaan Station, CT	MNCW	1	0	0	$20,000
Jun. 20, 2008	Far Rockaway, NY	LIRR	3	0	0	$20,500
Jul. 8, 2007	Penn Station, NY	NJTR	10	1	0	$90,600
Nov. 4, 2005	Port Washington Station, NY	LIRR	5	0	0	$15,800
Oct. 31, 2005	Hempstead Station, NY	LIRR	3	0	0	$11,600
Aug. 13, 2004	Grand Central Terminal, NY	MNCW	11	3	0	$50,000
Dec. 7, 2003	New Canaan Station, CT	MNCW	5	0	0	$28,674
Feb. 18, 2003	Port Washington Station, NY	LIRR	5	0	0	$7,900
Dec. 14, 2002	Hoboken Terminal, NJ	NJTR	0	0	0	$80,000
May 19, 2001	San Francisco Station, CA	PCMZ	2	0	0	$8,500
April 9, 2001	Flatbush Terminal, NY	LIRR	2	0	0	$8,210

Notes:
[1] Data sources: FRA REA database and NTSB railroad accident reports.
[2] Location: CA: California; CT: Connecticut; IL: Illinois; NJ: New Jersey; NY: New York.
[3] Railroad: LIRR: Long Island Rail Road; NJT: New Jersey Transit; MNCW: Metro-North Commuter Railroad; NIRC: Northeast Illinois Regional Commuter Railroad; PCMZ: Caltrain Commuter Railroad.

This section estimates the rail safety benefits for the period of 2001 – 2017, a span of 17 years. The estimate is based on a pool of 26 end-of-track collisions manually identified from the FRA REA database. As shown in Table 3. 4, the collected 26 end-of-track collisions occurring between 2001 and 2017 had led to 316 casualties (injuries and fatalities) and over $14,476,832 in damage costs to infrastructure and rolling stock only. In terms of either casualties or damage cost, the most severe accidents (the LIRR train accident at Atlantic Terminal and the NJT train accident at Hoboken Terminal) took place in the last two years and each led to over one hundred casualties and over $5 million in damage costs to rolling stock and infrastructure. Around 90% of these end-of-track collisions occurred on the east coast, such as Connecticut, New York, and New Jersey.

Methodology with cost factors

To estimate gross safety benefit, the estimation structure is plotted in Figure 3. 9. The categories include casualties, equipment damage, track and right-of-way damage, damage of the right-of-way, evacuations, wreck clearing, and train delays. (Figure 3. 9). The cost factors are the basis for the safety benefit estimations and are referred to the FRA report (FRA, 2009). For example, FRA (2009) estimated the cost of passenger train delays based on "285 passengers per train (a national average), an average duration of blockage of 2 hours (which implies passenger trains per day/12 are affected), an average per train delay of 15 minutes, and an average value of passenger time of $25 per hour". Then the average cost of passenger train delay was estimated at $148 ($=285 \times \$25 \times (\frac{1}{4}) \times (\frac{24}{2})$) in 1998 dollars, or $179 in 2009 dollars equivalently, which must be multiplied by the number of passenger trains per day. It was assumed that 33 trains per day and then the cost factor

for train delay would be $5,907 per accident. The amount in each cost factor is in 2009 dollars adapted from FRA (2009) and these cost units are typical values in general. The estimated safety benefits for PPAs below restricted speeds in 2009 constant dollars would be adjusted into 2017 constant dollars below.

To clarify, in addition to statistics from FRA 2009 report, the latest value of a statistical life (VSL) was provided in the FRA report (FRA, 2016b), in which VSL was set as $9.6 million. But in this section, to simplify the calculation of the total safety benefits involving train delay costs, right-of-way damage costs, evacuation costs, and so on, the unit cost of fatality is still using FRA 2009 report. The developed calculation method here can be adapted to any updated values if unit costs of all fields are provided or suggested.

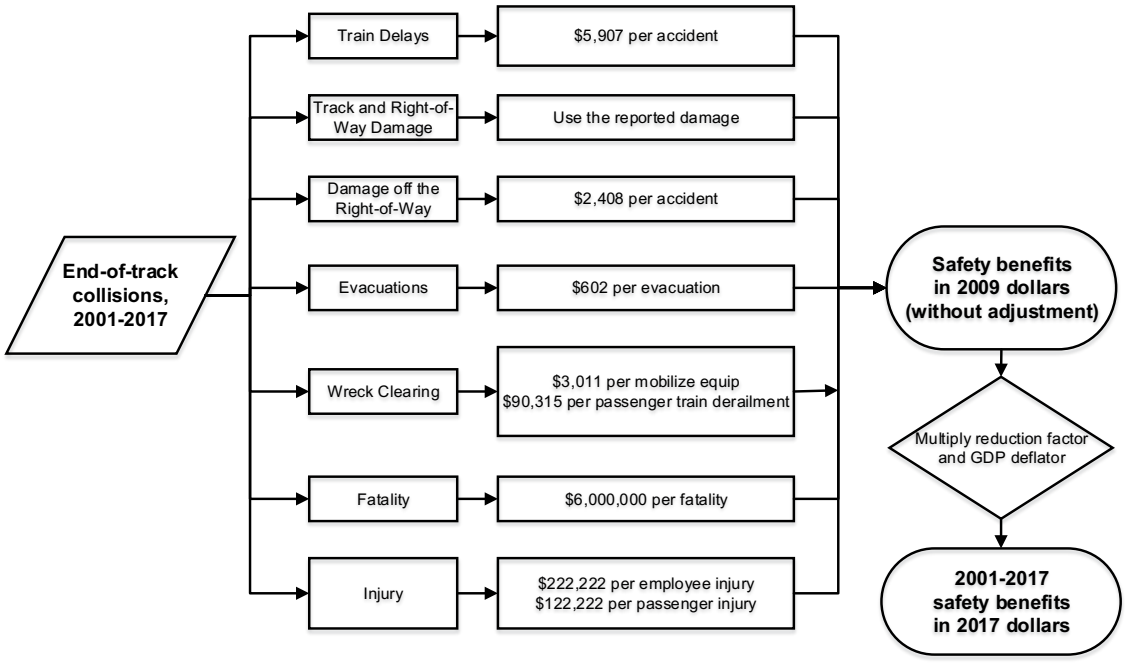

Figure 3. 9. Methodology for Estimating PTC Safety Benefit in End-of-Track Collisions (Adapted from FRA 2009)

Using the above methodology and collected end-of-track collisions from 2001 to 2017, the safety benefits (without adjustment) of end-of-track collisions can be estimated in 2009 constant dollars. Before the adjustment, the total safety benefit of preventing all restricted-speed-PPAs is approximately $62.0 million during this 17-year period (in 2009 dollars). From 2001 to 2017, there was one fatality caused by end-of-track collision, which was New Jersey Transit train accident at Hoboken Terminal in 2016.

Furthermore, in the prior PTC economic analysis (FRA, 2009), the reduction factor is considered and assumes that 25% of the estimated PPA safety benefits would be reduced through countermeasures that are already instituted. As reliable enforcement, it assumes that there is no reduction in PTC effectiveness in terms of preventing end-of-track collisions. Therefore, with 75% of PPA benefit reduction by other countermeasures, the estimated safety benefit would be discounted by 75%. In addition, current cost information uses the 2009 dollars as the unit. The inflation is taken into consideration and the damage cost in each year is also adjusted to 2017 dollars using the GDP inflator (World Bank, 2018), which was 98.793 in 2009 and 112.2 in 2017. The considerations of these two factors can be presented with the below equation:

$$B_j = b_i * \alpha * \frac{\beta_j}{\beta_i} \qquad (3-6)$$

Where

B_j = safety benefits in year j. In this study, year j = 2017;

b_i = safety benefits without adjustment in year i. In the previous part, year i = 2009;

α = reduction factor due to the mitigated risks by other countermeasures;

β_j, β_j = GDP inflator number is year i and year j;

Furthermore, the potential temporal trend was analyzed with the Wald-Wolfowitz runs test, a non-parametric statistical test that checks a randomness hypothesis for a two-value data sequence and has been employ in the previous studies (Liu, 2016; Zhang et al., 2019b). A Wald-Wolfowitz runs test shows that there is no significant temporal trend for safety benefits per year (P-value = 0.605). As a result, the expected annual savings due to end-of-track collisions are the average safety benefits per year based on the historical accident records, 2001-2017. In summary, the total safety benefit of preventing end-of-track collisions at stub-end terminals is approximately $52.8 million (in 2017 dollars) during this 17-year period. The expected annual savings due to end-of-track collisions prevention with PPA is $3.1 million (in 2017 dollars).

20-year projected safety benefits

In the prior PTC economic analysis, FRA (2009) considered some reduction factors and a phase-in schedule of safety benefits. The 20-year projected railroad safety benefits were estimated using 7 percent and 3 percent discount rate, which adjusts for the time value of money and allows for safety benefits, as well as following costs, to be valued in equivalent units. These equivalent units are called present values and are independent when they occur. The time value of money expresses the principle that costs and benefits that occur sooner are more highly valued than those that occur in the more distant future (FRA, 2016b). The discount rates of 7 percent and 3 percent per year are mentioned in both FRA reports (FRA, 2009; 2016). This section updates the total safety benefits using the collected end-of-track collisions from 2001 to 2017. The reduction factors and discount rates are from those used in FRA's prior study (FRA, 2009).

Also, the safety benefits will be phased-in as PTC systems are installed and applied with a promising service life. An estimated phase-in schedule of benefits comes from FRA (2009), based on the original deadline in 2015. Here, it assumes that the installations of PTC systems at terminals take 2 years with the identical phase-in percent (50%). Based on the above-mentioned safety benefit reduction factors and the phase-in schedule, 20-year projected safety benefits are calculated in Table 3. 5. In summary, the 20-year safety benefit of preventing end-of-track collisions at stub-end terminals is $33.7 million (2017 dollars, using 7% discount rate) and $46.0 million (2017 dollars, using 3% discount rate). The annual safety benefits are $1.7 million (2017 dollars, using 7% discount rate) and $2.3 million (2017 dollars, using 3% discount rate).

Table 3. 5. 20-Year Phase in Analysis of PTC Benefits in End-of-Track Collisions (in 2017 Dollars)

Discount Rates		7%			3%		
Year	Phase In Percent	Discount Factor	Annual Benefit	Discounted Annual Benefit	Discount Factor	Annual Benefit	Discounted Annual Benefit
2019	50%	0.86	$1,553,562	$1,343,676	0.94	$1,553,562	$1,461,747
2020	100%	0.80	$3,107,124	$2,499,237	0.91	$3,107,124	$2,835,789
2021	100%	0.75	$3,107,124	$2,324,291	0.89	$3,107,124	$2,750,715
2022	100%	0.70	$3,107,124	$2,161,590	0.86	$3,107,124	$2,668,193
2023	100%	0.65	$3,107,124	$2,010,279	0.83	$3,107,124	$2,588,148
2024	100%	0.60	$3,107,124	$1,869,559	0.81	$3,107,124	$2,510,503
2025	100%	0.56	$3,107,124	$1,738,690	0.78	$3,107,124	$2,435,188
2026	100%	0.52	$3,107,124	$1,616,982	0.76	$3,107,124	$2,362,132
2027	100%	0.48	$3,107,124	$1,503,793	0.74	$3,107,124	$2,291,268
2028	100%	0.45	$3,107,124	$1,398,528	0.72	$3,107,124	$2,222,530
2029	100%	0.42	$3,107,124	$1,300,631	0.69	$3,107,124	$2,155,854
2030	100%	0.39	$3,107,124	$1,209,587	0.67	$3,107,124	$2,091,179
2031	100%	0.36	$3,107,124	$1,124,916	0.65	$3,107,124	$2,028,443
2032	100%	0.34	$3,107,124	$1,046,171	0.63	$3,107,124	$1,967,590
2033	100%	0.31	$3,107,124	$972,939	0.61	$3,107,124	$1,908,562
2034	100%	0.29	$3,107,124	$904,834	0.60	$3,107,124	$1,851,306
2035	100%	0.27	$3,107,124	$841,495	0.58	$3,107,124	$1,795,766
2036	100%	0.25	$3,107,124	$782,591	0.56	$3,107,124	$1,741,893
2037	100%	0.23	$3,107,124	$727,809	0.54	$3,107,124	$1,689,637
2038	100%	0.22	$3,107,124	$676,863	0.53	$3,107,124	$1,638,948
Total		9.46		$28,054,461	14.31		$42,995,393

3.5.2 Cost calculations of PTC implementation at stub-end terminals

PTC installation cost at stub-end terminals

The above calculation of safety benefits covers the nationwide stub-end terminals in the United States. Equivalently, the incremental cost of proposed PTC enforcement at terminal stations should also be estimated at the national scale. Firstly, the unit costs (e.g., labor costs, material costs) are based on discussions with railroad experts and vendors over the course of risk experience in estimating PTC component costs. Secondly, the collected unit costs involve a lower end and higher cost in order to take account of cost variations. For example, the higher end costs are used for the conditions with more difficulties in practices. More detailed unit cost information and explanations are presented in Task 4. Cost Calculation of PTC Implementation under Restricted Speeds.

- **Track mapping cost (for I-ETMS only)**. The track mapping cost in Table 3.6 covers the collection of data points, preparation of GIS database, and preparation of sub-division files. The collected unit cost information also acknowledges the floating elements of track mapping. More specifically, at the terminal stations, the number of possible routes and the complexity of terminating tracks lead to the fluctuation in the track mapping cost; on open road, number of switches and number of highway-rail grade crossings would have an effect on the exact track mapping cost per track mile. In summary, and the low end and high end for terminating track mapping are $7,500 and 20,000, respectively.

Table 3. 6. Incremental Cost Information for Track Mapping

Track Mapping	Cost Per Track Mile	
	Low	High
Terminals	$7,500	$20,000

- **WIU (for I-ETMS only) and transponder (for ACSES only)**. The cost information of three categories of WIUs, stand-alone WIU, integrated WIU at intermediate location (Int. Loc.), and integrated WIU at control point (CP), are summarized in Table 3.7. Each type of WIU involves three major parts, namely cost, miscellaneous material, and labor fee to install. In particular, the labor to install a WIU is floating and driven by the amount of design, wiring, and testing that is required. For example, the larger the terminal, the more switches there are and hence the more wiring and testing needed. For those locations where the signal system is run by a vital microprocessor controller, there is less wiring to be done. In conclusion, the total cost of a stand-alone WIU are from $25,500 to $31,500, integrated WIU (intermediate location) are from $12,000 to $15,000, and integrated WIU (control point) are from $17,000 and $21,000. In some cases of requesting additional WIUs, radio tower may be also needed with $20,000 in material part and $4,000 in labor fee. Similarly, the overall cost of transponder covers material cost of transponder, miscellaneous materials, and labor to install and ranges from $3,300 to $3,600 due to the varying location and complexity of transponder installation (Table 3.7).

Table 3. 7. Incremental Cost Information for WIU and Transponder

Type of Hardware	Cost Ea.	Misc. Mtl.	Labor to Install		Total	
			Low	High	Low	High
Stand Alone WIU	$12,000	$1,500	$12,000	$18,000	$25,500	$31,500
Integrated WIU (Int. Loc.)	$6,000	$1,000	$5,000	$8,000	$12,000	$15,000
Integrated WIU (CP)	$8,000	$1,000	$8,000	$12,000	$17,000	$21,000
Transponder	$2,500	$500	$300	$600	$3,300	$3,600

Notes: Cost Ea.: Unit cost for each hardware; Misc. Mtl.: Cost for miscellaneous materials.

- **Design cost**. The construction of database and measurements are essential in the design of PTC implementation at stub-end terminals. In I-ETMS-type terminals, design cost mainly involves the preparation of sub-division file with necessary measurement. In the ACSES-type terminal, some design work is needed to plug the collect information and program into the transponder. The design cost per railroad experts' judgment is estimated as $50,000 in terminals with less than 5 terminating tracks and $100,000 in the terminals with over 5 terminating tracks.
- **Test cost**. In addition to equipment, material, and labor to install the hardware, train testing is necessary in most cases once the implementation is done. In the testing train, crew and train are needed to run the practical test and the cost is around $6,000 per shift.
- **Maintenance cost**. Based upon both prior FRA report (FRA, 2009) and railroad experts' experience, the annual maintenance costs are assumed to be 10%~15% of installed system costs at the end of the previous year.

In NTSB accident report (NTSB, 2018), it pointed out that there are at least 35 passenger train terminals with multiple tracks that end at a bumping post and/or platform, and all of the terminal operators have requested an exclusion from applying a positive train control (PTC) system. However, no literature provides detailed, exact count for the number of stub-end terminals, as well as the numbers of terminating tracks in each terminal in the nationwide railroad system. Using 45 as the number of stub-end terminals, in which PTC systems are proposed to enforce their functions, an approximate cost amount can be derived that can provide a loose reference information. As Figure 3. 10 shows, the ACSES-type PTC system and I-ETMS-type PTC system are considered with their approximate parameters. In this case study, the gross installation cost for 39 ACSES systems and 6 I-ETMS systems is estimated at $6.9 million to $7.4 million. To be clarified, these installation cost amounts do not involve maintenance cost, which is correlated with the number of years.

An Excel-based calculator is developed to estimate the gross incremental installation cost (without maintenance cost) for both ACSES-type PTC system and I-ETMS-type PTC system. A nationwide PTC implementation cost at stub-end terminals can be easily calculated once the exact number of stub-end terminals with detailed parameters being accessible with this calculator. Moreover, any railroad or Corridor can also derive its cost estimations via this calculator and essential parameters, such as the number of stub-end terminals, number of terminating tracks in each terminal, the length of terminating tracks, etc.

Cost Calculator for PTC Enforcement at Stub-End Terminals — **Updated by November 2018**

Required
Null
Outcome

Required Inputs

Scenarios	Quantity	Number of Tracks	Total Length of Tracks (mile)	Train Testing (shift)	Number of WIU needed	Type of WIU	Additional Radio Tower is Needed?
Stub End Terminal with ACSES System	24	4	2.5	2			
	15	8	5	2			
Stub End Terminal with I-ETMS System	3	4	2..5	2	1	Stand Alone WIU	NO
	3	8	5	2	1	Stand Alone WIU	NO

Outcomes

Scenarios	Cost ($)	
	Low End	High End
Stub End Terminal with ACSES System	6,019,200	6,278,400
Stub End Terminal with I-ETMS System	843,750	1,161,000
Total	**6,862,950**	**7,439,400**

Figure 3. 10. Installation Cost Calculator for Multiple Stub-End Terminals

20-year projected PTC implementation cost with maintenance cost

This section calculates a life cycle cost over a service life of 20 years. The length of this service life (20 years) is based on an FRA study of PTC economic analysis in 2009. Annual maintenance costs are assumed to be 10%~15% of installed system costs at the end of the previous year. 10% is used in the low-end cost estimation and 15% is used in the high-end cost estimation. Similar to previous safety benefit calculations, the net present value is considered in cost calculation and thus the discounted life-cycle costs are calculated using both 3% and 7% annual discount factors, which is consistent with previous FRA study (FRA, 2009).

Table 3. 8. 20-Year Service Life Cost of PTC Implementation at Stub-End Terminals

(a) Lower-End

Year	Phase In Percent	Installed Costs	Maintenance Costs	7%			3%		
				Discount Factor	Annual Cost	Discounted Annual Cost	Discount Factor	Annual Cost	Discounted Annual Cost
2019	50%	$3,086,100	$308,610	1.00	$3,394,710.00	$3,394,710	1.00	$3,394,710.00	$3,394,710
2020	100%	$3,086,100	$617,220	0.93	$3,703,320.00	$3,444,088	0.97	$3,703,320.00	$3,592,220
2021	100%	$0	$617,220	0.87	$617,220.00	$536,981	0.94	$617,220.00	$580,187
2022	100%	$0	$617,220	0.82	$617,220.00	$506,120	0.92	$617,220.00	$567,842
2023	100%	$0	$617,220	0.76	$617,220.00	$469,087	0.89	$617,220.00	$549,326
2024	100%	$0	$617,220	0.71	$617,220.00	$438,226	0.86	$617,220.00	$530,809
2025	100%	$0	$617,220	0.67	$617,220.00	$413,537	0.84	$617,220.00	$518,465
2026	100%	$0	$617,220	0.62	$617,220.00	$382,676	0.81	$617,220.00	$499,948
2027	100%	$0	$617,220	0.58	$617,220.00	$357,988	0.79	$617,220.00	$487,604
2028	100%	$0	$617,220	0.54	$617,220.00	$333,299	0.77	$617,220.00	$475,259
2029	100%	$0	$617,220	0.51	$617,220.00	$314,782	0.74	$617,220.00	$456,743
2030	100%	$0	$617,220	0.48	$617,220.00	$296,266	0.72	$617,220.00	$444,398
2031	100%	$0	$617,220	0.44	$617,220.00	$271,577	0.70	$617,220.00	$432,054
2032	100%	$0	$617,220	0.41	$617,220.00	$253,060	0.68	$617,220.00	$419,710
2033	100%	$0	$617,220	0.39	$617,220.00	$240,716	0.66	$617,220.00	$407,365
2034	100%	$0	$617,220	0.36	$617,220.00	$222,199	0.64	$617,220.00	$395,021
2035	100%	$0	$617,220	0.34	$617,220.00	$209,855	0.62	$617,220.00	$382,676
2036	100%	$0	$617,220	0.32	$617,220.00	$197,510	0.61	$617,220.00	$376,504
2037	100%	$0	$617,220	0.30	$617,220.00	$185,166	0.59	$617,220.00	$364,160
2038	100%	$0	$617,220	0.28	$617,220.00	$172,822	0.57	$617,220.00	$351,815
Total				11.33		**$12,640,666**	15.32		**$15,226,817**

(b) Higher-End

Year	Phase In Percent	Installed Costs	Maintenance Costs	7%			3%		
				Discount Factor	Annual Cost	Discounted Annual Cost	Discount Factor	Annual Cost	Discounted Annual Cost
2019	50%	$4,068,450	$610,268	1.00	$4,678,717.50	$4,678,718	1.00	$4,678,718	$4,678,718
2020	100%	$4,068,450	$1,220,535	0.93	$5,288,985.00	$4,918,756	0.97	$5,288,985	$5,130,315
2021	100%	$0	$1,220,535	0.87	$1,220,535.00	$1,061,865	0.94	$1,220,535	$1,147,303
2022	100%	$0	$1,220,535	0.82	$1,220,535.00	$1,000,839	0.92	$1,220,535	$1,122,892
2023	100%	$0	$1,220,535	0.76	$1,220,535.00	$927,607	0.89	$1,220,535	$1,086,276
2024	100%	$0	$1,220,535	0.71	$1,220,535.00	$866,580	0.86	$1,220,535	$1,049,660
2025	100%	$0	$1,220,535	0.67	$1,220,535.00	$817,758	0.84	$1,220,535	$1,025,249
2026	100%	$0	$1,220,535	0.62	$1,220,535.00	$756,732	0.81	$1,220,535	$988,633
2027	100%	$0	$1,220,535	0.58	$1,220,535.00	$707,910	0.79	$1,220,535	$964,223
2028	100%	$0	$1,220,535	0.54	$1,220,535.00	$659,089	0.77	$1,220,535	$939,812
2029	100%	$0	$1,220,535	0.51	$1,220,535.00	$622,473	0.74	$1,220,535	$903,196
2030	100%	$0	$1,220,535	0.48	$1,220,535.00	$585,857	0.72	$1,220,535	$878,785
2031	100%	$0	$1,220,535	0.44	$1,220,535.00	$537,035	0.70	$1,220,535	$854,375
2032	100%	$0	$1,220,535	0.41	$1,220,535.00	$500,419	0.68	$1,220,535	$829,964
2033	100%	$0	$1,220,535	0.39	$1,220,535.00	$476,009	0.66	$1,220,535	$805,553
2034	100%	$0	$1,220,535	0.36	$1,220,535.00	$439,393	0.64	$1,220,535	$781,142
2035	100%	$0	$1,220,535	0.34	$1,220,535.00	$414,982	0.62	$1,220,535	$756,732
2036	100%	$0	$1,220,535	0.32	$1,220,535.00	$390,571	0.61	$1,220,535	$744,526
2037	100%	$0	$1,220,535	0.30	$1,220,535.00	$366,161	0.59	$1,220,535	$720,116
2038	100%	$0	$1,220,535	0.28	$1,220,535.00	$341,750	0.57	$1,220,535	$695,705
Total				11.33		**$21,070,503**	15.32		**$26,103,175**

Using the calculated amounts in the above section as an example, the 20-year projected PTC implementation cost can be derived. Table 3.8.a and Table 3.8.b present low-end service costs and high-end service costs, respectively. In addition, a phase-in schedule is also assumed that the installations of PTC systems at terminals take 2 years with the identical phase-in percent (50%). Based on the installation cost, maintenance cost, and the phase-in schedule, 20-year projected costs are calculated in Table 3.8. In summary, the 20-year low-end costs of PTC implementations at stub-end terminals are $12.6 million (2017 dollars, using 7% discount rate) and $15.2 million (2017 dollars, using 3% discount rate). The 20-year high-end costs of PTC implementations at stub-end terminals are $21.1 million (2017 dollars, using 7% discount rate) and $26.1 million (2017 dollars, using 3% discount rate). The maintenance costs exceed the initial procurement costs over the 20-year period, as shown in Table 3.8.

3.5.3 Cost-benefit analysis

Cost-Benefit analysis results in ratio and NPV

To evaluate the benefit-cost analysis, two metrics are used here: Net Present Value (NPV) and benefit-cost ratio. NPV is equal to the benefits minus costs over a specified service life (e.g., 20 years) and the benefit-cost ratio is equal to the benefits divided by the costs. These two major outputs were employed in previous studies. For example, the FRA developed GradeDec, a highway-rail crossing investment analysis tool to provide grade crossing investment decision support (FRA, 2018b).

In this research, the NPV of PTC implementation at stub-end terminals is calculated as the sum of the safety benefits of reduced end-of-track collisions, minus the total cost

associated with the PTC installation and maintenance over the service years (20-year) during which the safety benefits and costs are expected to accrue. This measure has been used in the previous study of the benefit-cost analysis of infrastructure improvement for derailment prevention (Liu et al., 2010) and the benefit-cost analysis of heavy haul railway track upgrade (Liu et al., 2011). As shown in the below equation, the monetary values of benefits and costs were discounted to constant (year 2017) dollars:

$$NPV = \sum_{i=1}^{Y} \frac{B_i - C_i}{(1+d)^i} = \sum_{i=0}^{Y} \frac{B_i}{(1+d)^i} - \sum_{i=1}^{Y} \frac{C_i}{(1+d)^i} \quad (3-7)$$

Where:

Y= time span over which the NPV is calculated; In this study, Y=20;

B_i = safety benefits of reduced end-of-track collisions in year *I;*

C_i = Costs of PTC implementation at stub-end terminals in year *i*; and

d = annual discount rate; this study uses 3% and 7%;

The benefit-cost ratio (BCR) is also an indicator used in the cost-benefit analysis. It was used in the calculation of nationwide PTC economic analysis (FRA, 2009) and can be calculated via Equation 3-8:

$$BCR = \frac{\sum_{i=0}^{Y} B_i}{\sum_{i=0}^{Y} C_i} \quad (3-8)$$

Where:

B_i = safety benefits of reduced end-of-track collisions in year *i* ;

C_i = Costs of PTC implementation at stub-end terminals in year *i*; and

Y= time span over which the NPV is calculated; In this study, Y=20.

With two indicators that were commonly used in cost-benefit analysis, the analysis results were summarized in Table 3.9.

Table 3. 9. Cost-Benefit Analysis of PTC Implementation in Stub-End Terminals

		7% Discount Rate		3% Discount Rate	
		20-year total values	**Annualized values**	**20-year total values**	**Annualized values**
Safety Benefits		$33,650,157	$1,682,508	$46,047,583	$2,302,379
Incremental Costs	Low End	$12,640,666	$632,033	$15,226,817	$761,341
	High End	$21,070,503	$1,053,525	$26,103,175	$1,305,159
NPV	Low End	$12,579,654	$628,983	$19,944,408	$997,220
	High End	$21,009,491	$1,050,475	$30,820,765	$1,541,038
Benefit-Cost Ratio	Low End	1.7	1.7	1.8	1.8
	High End	2.8	2.8	3.1	3.1

The average annual NPV would be around $0.8 million (2017 dollars, using 7% discount rate) and $1.3 million (2017 dollars, using 3% discount rate). In other words, the benefit-cost analysis shows the safety benefits exceed the installation costs and maintenance costs for a 20-year service life. Moreover, the benefit-cost ratio is around 2 or even more, which indicates that the 20-year safety benefits would be approximately 2 times the 20-year costs. To conclude, the PTC implementation at stub-end terminals yields a significant economic advantage (benefits higher than costs), provided that it is kept for a reasonable lifetime (e.g., 20 years or longer). It was also noticed that the total costs are "recovered" in terms of benefits in around 5 years. In other words, starting from the 5th

year of PTC implementation at stub-end terminals, the total safety benefits would be greater than total costs (summation of installation and corresponding maintenance costs).

Per the developed cost calculator in this study, either the number of stub-end terminals or the parameters in each scenario can be updated based on more practical data or railroad-specific data information in the future. The cost-to-benefit analysis only provides an exemplary case for the nationwide PTC enforcement at stub-end terminals.

Sensitivity analysis

Developed BCA will include some level of uncertainty attributable to the use of preliminary cost estimates, difficulty of modeling future traffic levels, or use of other imperfect data and incompletely understood parameters. When describing the assumptions employed, BCA should identify those that are subject to especially large uncertainty and emphasize which of them has the greatest potential influence on the outcome of the BCA.

If key data elements are uncertain, the BCA should include a sensitivity analysis illustrating how its results would change if it employed alternative values for those elements. In this section, a sensitivity analysis is developed to investigate the impacts of discount rate, service life, and maintenance costs on the NPV calculation and benefit-cost ratio. FRA guidance (FRA, 2016b) suggested that the benefit-cost analysis should include a sensitivity analysis if key data elements are uncertain. This study uses the aforementioned nationwide PTC implementation as an example and takes the previous results as a base case. A sensitivity analysis is applied to illustrate how its results would change if this analysis employed alternative values for those elements (e.g., discount rate, service life,

and maintenance costs). Also, the section simplifies the cost outputs via a medium value, instead of presenting both low end and high end.

The above base cases use 3% and 7% as two discount rates, which are referred to two FRA reports (FRA, 2009; 2016). It is evident that the use of different discount rates has a substantial impact on the results (Figure 3.11). Lower discount rate would have a larger annualized NPV. A 3% discount rate resulted in a positive, larger NPV at any service life within 20-40 years considered. On the other hand, a 15% discount rate still has positive NPV but the values of NPV are relatively smaller.

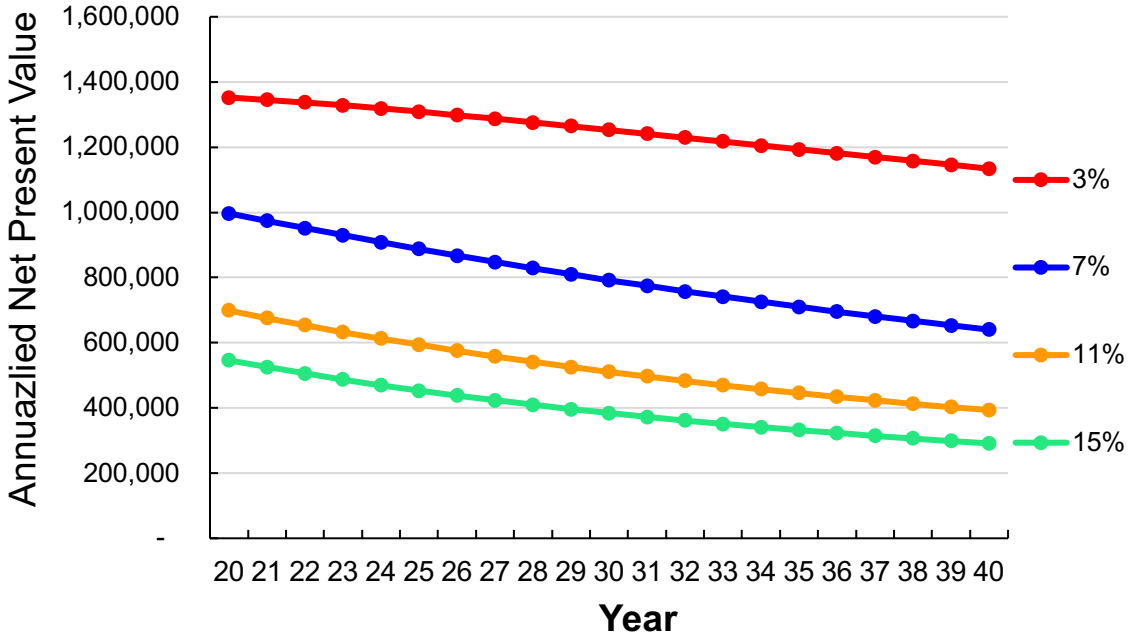

Notes: To simplify the sensitivity analysis, the cost part takes the mean value of high-end cost and low-end cost.

Figure 3. 11. Sensitivity Analysis of NPV Affected by Discounted Rate

Also, with more extended study time period (service life), the annualized NPV decreases steadily. This is consistent for all discount rates considered in this sensitivity analysis. It indicates that the economic advantages of PTC implementation at stub-end

terminals are decreasing (but still positive) for a longer service life perspective, but the relative metric in terms of the comparison between safety benefits and costs is stable or even increasing a little.

The above analysis assumes the annual maintenance costs to be 10%~15% of installed system costs at the end of the previous year. This subsection considers 6 different ratios of maintenance cost to installation costs, namely 5%, 15%, 20%, 30%, 35%, and 40%. The use of different maintenance cost ratio has a substantial impact on the results (Figure 3. 12). A lower maintenance costs ratio would have a larger annualized NPV and larger benefit-cost ratio, relatively. A 5% maintenance costs rate resulted in a positive, larger NPV at any service life within the 20-40 years considered. The use of a 20% discount rate still has positive NPV but the values of both the NPV are relatively smaller. On the other hand, the use of a 40% discount rate shows a negative NPV, which indicates that the total benefits in a service life would be lower than total costs once the annual maintenance cost is equal or greater than 40% of installed PTC costs.

Overall, with a more extended study time period (service life), annualized NPV decreases steadily. This indicates that the economic advantages/disadvantages of PTC implementation at stub-end terminals decrease with a longer service life perspective. Moreover, higher maintenance cost ratios are also studied and when the maintenance cost ratio is larger than 36%, the NPV would be a negative value. This indicates that when the annual maintenance cost is larger than 36% of installed PTC costs, the total benefits in a service life would be lower than total costs.

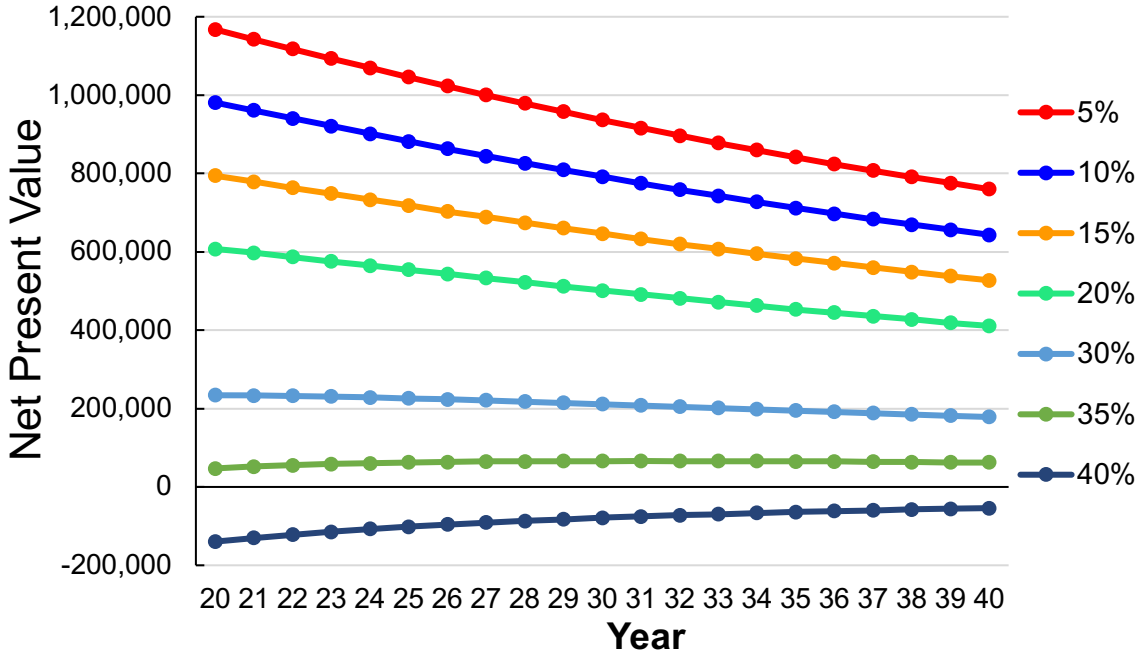

Notes: the cost part takes the mean value of high-end cost and low-end cost.

Figure 3. 12. Sensitivity Analysis of NPV Affected by Maintenance Cost Ratio

3.6 Assessment of PTC-Based Risk Mitigation via Operational Impact Analysis

This section studies the operational impacts of operating practices based upon the proposed restricted speed PTC enforcement. According to the design and procurement of all improvements or modifications to PTC from the Concept of Operations document developed in the previous subsection, an operational impact assessment for ACSES and/or I-ETMS is conducted in this research. Several scenarios will be studied to fully describe the operational impact on capacity and run-time for each case.

Firstly, in the macro-level assessment, each scenario is analyzed based on the proposed Concept of Operations and deep expertise in PTC technology. Secondly, the quantitative analysis employs statistical simulation tool (e.g., Monte Carlo simulation) to quantitatively evaluate the impact of PTC on operations at stub-end terminals, which may

have a certain level of capacity impacts per expertise. A generic model of a known rail line is used to conduct this quantitative simulation under controlled conditions to determine any operational impacts on terminal capacity and operations. These two steps contribute to a full assessment of operational impact in PTC enforcement at restricted speeds. A Washington Union Station-based case study demonstrates a practical evaluation of the "without PTC enforcement" and "with PTC enforcement".

3.6.1 Monte Carlo simulation process

The quantitative operational impact analysis of terminal capacity can be achieved with Monte Carlo simulation involving the aforementioned key principles. One simulation is the imitation of the real-world process of a train operation over time in the stub-end passenger terminal. The simulation method can serve well as a representation of the dynamic behavior of a system by moving it from state to state in accordance with pre-defined constraints, and a considerably large iteration of simulation (e.g., 1,000,000 or more) can consider the stochasticity that exists in the practical train operations within the service life. As a very early study in the quantitative analysis of terminal train operational impact, train operating duration on terminating track is employed as the key assessment criterion based on prior research (Woodburn, 2017). Time operation duration can demonstrate both actual train arrival time and train delay incurred en route via comparing the actual to the planned since this is closely linked to network capability and resilience. Furthermore, considering the variations and uncertainties (e.g., engineer attentiveness, brake efficiency, environment conditions, rail adhesion, system processing speed), the Monte Carlo simulation takes account of these by assuming the brake delay time and

steady-state brake rate follows Normal Distributions. The mean value of these factors in Normal Distribution would follow the aforementioned braking algorithms and the variance would be justified based upon railroad expertise. This study mainly investigates and compares three scenarios: terminal operation without PTC system (benchmark), terminal operation with an ACSES-type PTC system, and terminal operation with an I-ETMS-type PTC system.

Base case simulations

In the base case, the train approaching into terminal is operated by the train engineer and no train control system can apply penalty brake even if the train movement is noncompliant. These simulations are executed based on the train operational methods currently used in the terminating stations. In general, three major phases are involved in this base case, which are train movement under restricted speeds (without slowing down, t_{E_r}), brake delay involving reaction time (t_{E_d}) and steady-state braking duration (t_{E_s}) (Figure 3. 13.a). Then the total time duration for a train approaching into the terminal and stopping at the targeted point before bumping post is t_E:

$$t_E = \sum_{i \in \{r,d,s\}} t_{E\_i} \tag{3-9}$$

Where

t_{E_i} = time durations for engineer operation; and

$i = r$ for train operation under restricted speed and before applying brake; $i = d$ for brake delay; $i = s$ for steady-state brake.

I-ETMS-type PTC system involved terminal simulations

Similarly, the proposed I-ETMS system in terminating station would be monitored with respect to its speed limits and authority. Only if any violation in the event of human errors happens, the PTC would apply the braking enforcement to stop the train safely before hitting the bumping posts. In addition, this practical operational impact analysis section also takes the PTC component reliability into account. Three main types of I-ETMS component failure are covered and are likely to result in different scenarios. The occurrence of onboard locomotive system failure would lead to the failure of PTC braking application. In this case, the train movement would still be controlled by the engineer. If WIU or data radio fails, the onboard system would not know the exact distance to the bumping post and would have to take the worst-case (shortest) distance. Therefore, the train approaching terminal with WIU failure or data radio failure is consist of four phases, which are train movement under restricted speed (t_{I_r}), reaction time (t_{I_d}), effective braking time with steady-state brake (t_{I_s}), restarting & second movement time (t_{I_re}).

$$t_I = \begin{cases} \sum_{i\in\{r,d,s\}} t_{0\_i} & \begin{array}{c} if\ train\ operation\ is\ compliant\ or \\ PTC\ has\ failure \\ (excluding\ WIU\ fialure\ or\ radio\ failure) \end{array} \\ t_{E\_r} + \sum_{i\in\{d,s,re\}} t_{I\_i} & \begin{array}{c} if\ PTC\ enfoces\ with\ WIU\ falure \\ or\ radio\ failure \end{array} \\ t_{E\_r} + \sum_{i\in\{d,s\}} t_{I\_i} & \begin{array}{c} if\ PTC\ enforces\ due\ to \\ noncompliant\ behavior \end{array} \end{cases} \tag{3-10}$$

Where

t_{E_i} = time durations for engineer operation;

t_{I_i} = time durations for I-ETMS enforcing brake; and

$i = r$ for train operation under restricted speed and before applying brake; $i = d$ for brake delay; $i = s$ for steady-state brake.

ACSES-type PTC system involved terminal simulations

These simulations are executed by involving proposed PTC enforcement at stub-end terminal. With a reliable PTC system, the train movement would be monitored with respect to its speed limits and authority. If any violation in the event of human errors happens, the PTC systems (e.g., ACSES system) would apply the braking enforcement to stop the train safely before hitting the bumping posts. On the other side, the train movements would be operated by train engineer if noncompliant behavior is detected. In other words, the train stopping before the end of terminating track would rely on the engineer's operation.

In addition to the first condition in Figure 3. 13.b, the ACSES component failures (e.g., transponder failure, onboard transponder antenna failure, and onboard computer failure) also play a key role in the simulation of ACSES's operational impact. As introduced before, the occurrence of any ACSES-type PTC system component failures would cut off PTC system and train stopping at targeted point still relies on the locomotive engineer. Figure 3. 13.b depicts the process of train stopping at designated point for two cases, namely train stopping at targeted point with ACSES function (no component failure) and train stopping operated by engineer because of either compliant train movement or ACSES system involving component failure(s). The total time operation duration in ACSES-involved terminal (t_A) has two conditions:

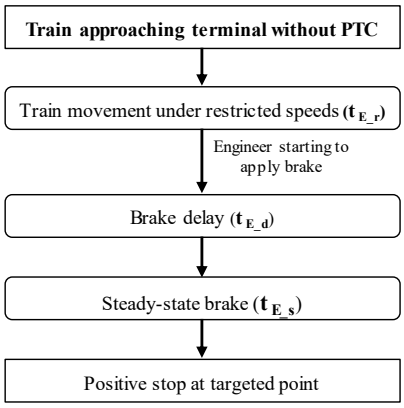

(a) Terminal Train Operation without PTC (Base Case)

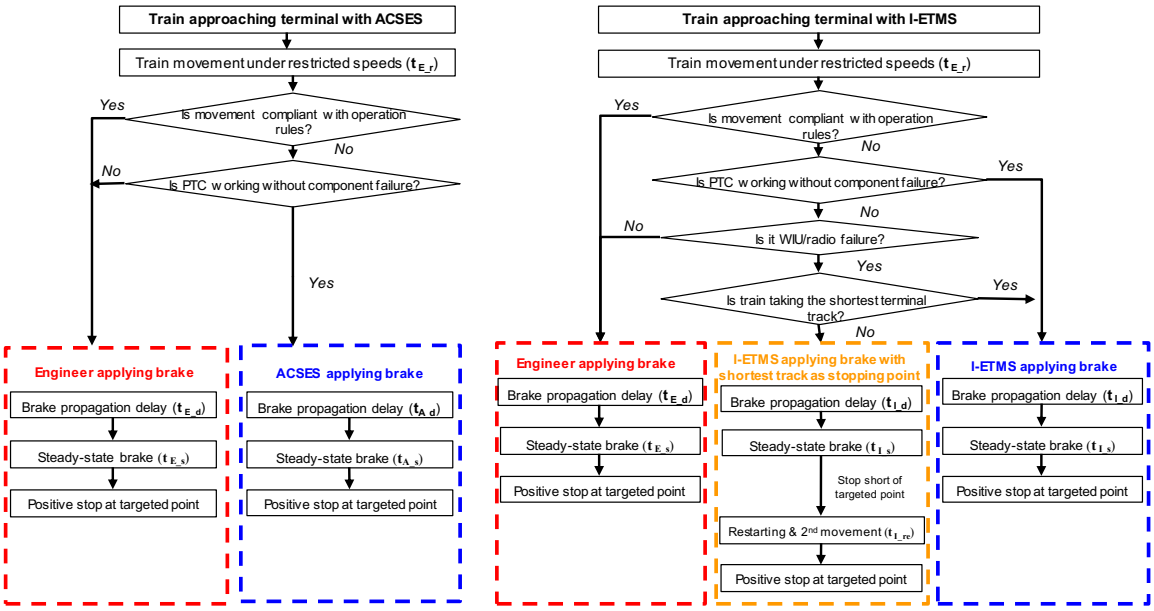

(b) Terminal Operation with ACSES-Type PTC (c) Terminal Operation with I-ETMS -Type PTC

Figure 3. 13. Flowchart of Train Movements in the Terminal Areas (a) without PTC System; (b) with ACSES System; and (c) with I-ETMS System

$$t_A = \begin{cases} \sum_{i \in \{r,d,s\}} t_{E\_i} & \text{if train operation is compliant or PTC has componenet failure} \\ t_{E\_r} + \sum_{i \in \{d,s\}} t_{A\_i} & \text{if PTC enforces due to noncompliant behavior} \end{cases} \quad (3\text{-}11)$$

Where

$t_{\_i}$ = time durations for engineer operation;

t_{A_i} = time durations for ACSES enforcing brake; and

$i = r$ for restricted speed operation; $i = d$ brake delay; $i = s$ steady-state brake.

Time duration assumptions with uncertainties

The time length in each zone involves uncertainties and depends on various factors. For example, the reaction time varies with the degree of engineer's attentiveness. The time length of effective braking time depends on the total weight of the train, brake shoe friction, track adhesion, and other factors. Therefore, each stochastic time length is assumed to follow a certain statistical distribution (Table 3.10). For example, it assumes that the brake propagation delay time follows Normal distribution. Train brake applied by PTC systems will have T_d calculated in the above equation as the mean value in the Normal distribution, while train engineer applying the brake will have greater mean value and variance due to longer reaction time and larger uncertainties from manual operation. For restarting and the second movement in terminal with I-ETMS system, the time length varies with the track length difference between the targeted track and the shortest track that is implemented as worst-case distance if PTC equipment fails.

Table 3. 10. Statistical Distribution Assumptions for Time Length

Type		Distribution	Effecting factors
Without PTC system	Brake delay time	t_{E_d} ~ *Normal distribution*	Engineer's attentiveness; etc.
	Steady-state braking time	t_{E_s} ~ *Normal distribution*	The efficiency of braking, etc.
With PTC system	Brake delay time	t_{A_d}, t_{I_d} ~ *Normal distribution*	PTC system processing speed and signal transmitting speed; etc.
	Steady-state braking time	t_{A_s}, t_{I_s} ~ *Normal distribution*	Remaining distance from PTC being in function to end of track; environment (e.g., adhesion), etc.
	Restarting & 2nd movement time, for I-ETMS only	t_{I_re} ~ *Uniform distribution*	The speed to raising air pressure in the brake pipe; time to compare stopping point against targeted point, the track length error between real track and shortest track, etc.

3.6.2 Case Study in Operational Impact Assessment

To explicitly disclose the operational impact assessment of PTC enforcement at stub-end terminal, this section develops a case study based upon the track layout and train operations at Washington Union Station. Washington Union Station is a major railroad terminal station and involves 22 tracks, 13 of which are terminating tracks. It mainly provides services for Amtrak, Maryland Area Regional Commuter Rail (MARC), and Virginia Railway Express (VRE). Amtrak operates around 85 trains daily that consist of primarily Northeast Corridor services (e.g., Acela Express and Regional trains), serving over 5 million passengers in 2017 (Amtrak, 2018). The track layout of Washington Union Station is as shown in Figure 3.14.

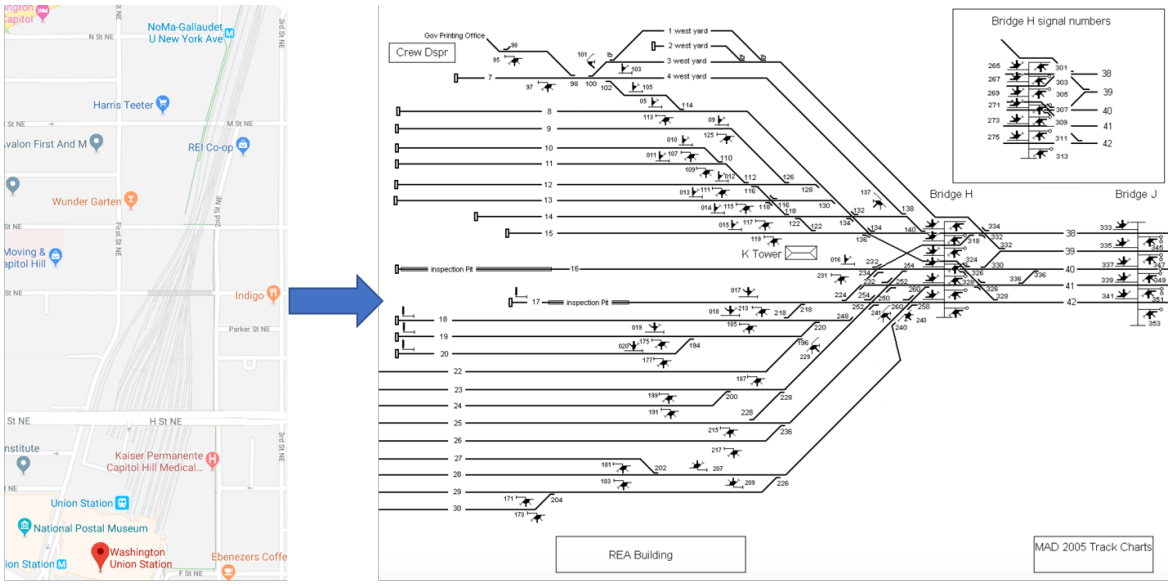

Figure 3. 14. Washington Union Station Track Layout

For the trains that approach into the terminal station, it also refers to the train schedule in Washington Union Station, which mainly provides ridership for Amtrak and MARC (Maryland Area Regional Commuter). It assumes 300 trains approaching the terminal daily. The analysis of the terminal explicitly examines simulated operations covering a 50-year period (equivalent to 5,475,000 train operations) in the terminal. During this period, the time durations needed from passing the last signal bridge (Bridge H in Figure 3.14) to stopping safely before the end of tracks are simulated and captured with Monte Carlo simulation. In this example, it is assumed that the maximum authorized speed (MAS) is 15mph (22ft/s), which is the maximum speed after entering Washington Union Station. The Washington Union Station involves 13 terminating tracks, where the starting point is K Signal Bridge. The track lengths of terminating track with MTEA vary between 2,460 ft and 2,760 ft in this case study.

In addition to the assumption in the distribution of time lengths, the probability of a specific scenario occurrence is also listed in Table 3.11. Some assumed probabilities are based on experts' experience and previous study (FRA, 2014). For example, the rate of PTC failure to enforce braking (failures per 1,000 hours of train operation) was assumed to range from 0.0606 to 0.606 in an FRA report (FRA, 2014) that studied PTC risk assessment. But it does not provide direct reference information about PTC component failure. In addition, to the authors' knowledge, quite limited published reports or studies that are publicly accessible discuss the PTC component failure or PTC reliability. The probability of failed on-board computer, WIU, or radio in PTC system would be assumed to have the same magnitudes with previous research in FRA report (2014). In addition, they are also partially based upon railroad expertise. Specifically, it assumes that the probability of an on-board computer being failed is 0.0001 per PTC enforcement in train approaching terminal and the probability of a WIU or radio being failed is 0.0001 per PTC enforcement in train approaching terminal too. In particular, the probability of transponder failure (0.00001) is even lower than other components due to the redundancy provided by the second set. Although, to the authors' knowledge, there is no publicly available information about complete PTC component reliability. Railroads and vendors can easily update and achieve their practical operational impact assessment results with their own PTC component reliability data and the assessment tool developed in this research. Moreover, the probability of the train taking the shortest terminal track in terminal is calculated based upon the track lengths in the terminal, which is equal to 0.1538= (2/13).

Table 3. 11. Assumptions in the Occurrence of Specific Scenarios

(a) In I-ETMS

Parameters	Definition	Assumed Values
P_{11}	The probability of a train being compliant with operation rule (e.g., following 15mph as MAS)	0.95
1- P_{11}	The probability of a train being incompliant with operation rule	0.05
P_{21}	The probability of an on-board computer in I-ETMS system being failed (for "practical" I-ETMS only)	0.0001
P_{22}	The probability of a WIU or radio in I-ETMS system being failed (for "practical" I-ETMS only)	0.0001
1- P_{21} -P_{22}	The probability of no failure in I-ETMS system (for "practical" I-ETMS only)	0.9998
P_{31}	The probability of the train taking the shortest terminal track in terminal	0.1538
1-P_{31}	The probability of the train not taking the shortest terminal track in terminal	0.8462

(b) In ACSES

Parameters	Definition	Assumed Values
P_{11}	The probability of a train being compliant with operation rule (e.g., following 15mph as MAS)	0.95
1- P_{11}	The probability of a train being incompliant with operation rule	0.05
P_{211}	The probability of ACSES system with transponder failure (for "practical" ACSES only)	0.00001
P_{212}	The probability of ACSES system with other component failure(s), such as onboard computer failure, onboard transponder antenna failure (for "practical" ACSES only)	0.0002
1- P_{21}	The probability of no component failure in ACSES (for "practical" ACSES only)	0.99979

Statistics of simulation results

Following the aforementioned assumptions in time length, tracks, and train information, as well as drawn flowchart in train operations, a 50-year terminal operation in the calculation of total time needed to stop a train safely in the terminal areas is developed and summarized in Table 3.12. Here it assumes that this terminal has 300 trains approaching into terminal every day and equivalently 5,475,000 trains every year. Based

on the simulation results, the five objective scenarios (namely without PTC, with perfect ACSES, with practical ACSES, with perfect I-ETMS, and with practical I-ETMS) have quite similar mean time lengths (around 86 seconds). But the maximum traveling times in terminal track have obvious difference, which are 196.4 seconds for terminal with practical I-ETMS system, 94.2 seconds for terminal without PTC, and 95.3 seconds for other scenarios. It indicates that the time length distribution for terminal with practical I-ETM system may have "heavy-tail" characteristics and significantly small part of samples have a high value. CVaR has primarily been employed in financial engineering (Soleimani et al., 2014), social sciences (Cotter and Dowd, 2006), highway hazardous materials transportation (Toumazis and Kwon, 2016), and recently rail transport of hazardous materials (Hosseini and Verma, 2017) and has been proven as a useful alternative risk measure to capture the "worst-case" or "largest-case" of a certain scenario.

CVaR is the weighted average of all outcomes exceeding the confidence interval (α-quantile and $\alpha \in (0,1)$) of a dataset sorted from worst to best. For example, CVaR(99%) of the time length is the mean (average) of all the numbers of casualties within the longest 1% of train operation in terminal tracks in terms of time length.

In this study, α is set as 99.995% and the CVaR (99.995%) represents the average of the longest 0.005% of train operating time in terminals (around 550 train operation simulations). According to the results listed in Table 3.12, the longest 0.005% of train operating time in terminals without PTC is 93.9s, which is smaller than that in terminals with practical I-ETMS systems subjected to potential component failure (148.2s). Other scenarios, such as an ACSES system, or a "perfect" I-ETMS system without failure, have similar operation duration (95.1s) with the benchmark.

Table 3. 12. Train Operating Time Duration (in Second) at Washington Union Station-alike Terminal with CE-205 Braking Curve

Scenarios		Mean	Min	CVaR (99.995%)	Max
Terminal without PTC (benchmark)		86.1s	78.1s	93.9s	94.2s
Terminal with ACSES	"Perfect" system without component failure	86.1s	78.1s	95.1s	95.3s
	"Practical" system with probable component failure	86.1s	78.1s	95.1s	95.3s
Terminal with I-ETMS	"Perfect" system without component failure	86.1s	78.1s	95.1s	95.3s
	"Practical" system with probable component failure	86.2s	78.1s	148.2s	196.4s

Notes: [1] Train operation duration time indicates the time length that the train spends on terminating tracks, from passing Signal Bridge H to stopping at the targeted point.

Mean Time to Train Approaching Delay in Terminal with I-ETMS

With a special interest in the distribution of train approaching durations in the terminals with "practical" I-ETMS that is subject to probable component failure(s), the means time to train approaching delay is investigated in this section. It is found that the probability that train traveling time in terminal with PTC is between 100 seconds and 160 seconds is 2.28×10^{-6} (Table 3.13). It indicates that on average, one of 438,000 train movements in terminals (equivalently 4.0-year train operations) needs 100 - 160 seconds. In other words, such train operation occurs once in 4.0 years. For more severe delayed train approaching, the probability with over 160 seconds in travel time is only 1.92×10^{-6}. It means that such severe delayed train approaching would take place every 5 years in approximate. Although the likelihood of such "slow" train operation at terminal is quite small, it is able to block the path of other trains and delay them from either entering or

leaving their tracks. In busy passenger terminals such as Washington Union Station, the delay impacts could be significant, although the occurrence probability is quite low.

Table 3. 13. Long-Tail Operating Time Length in Terminal with I-ETMS

Frequency Type	**Simulated Time Interval**	
	[100s, 160s]	**[160s, +∞]**
Frequency per train operation	2.28×10^{-6} /train operations	1.92×10^{-6} /train operations
Frequency per year	0.25 /year	0.22 /year
Mean time to such time duration	4.0 years	4.8 years

Note: Here it assumes that this terminal has 300 trains approaching into terminal every day and equivalently 109,500 trains every year.

Above simulation results focus on a single, independent event of a train entering terminal with PTC that is likely to have equipment failure. In practice, WIU failure or radio failure could last for several minutes or even hours and can lead to consistent abnormal train operation status, in which PTC is able to take the worst-case distance and be delayed from reaching a point within the platform area where it would be able to discharge passengers. This practical situation can be even more serious for the train operation in busy passenger terminals.

Sensitivity analysis of PTC component failure

In this section, a preliminary sensitivity analysis of PTC component failure is conducted with two motivations:

a) To account for the uncertainties and variations of PTC component failure probabilities, in particular under a variety of vendors offering nationwide PTC components.

b) To understand how changes in practice or failure prevention technology mitigation affect the overall operational impact and terminal capacity.

Considering the relatively significant impact of system component failure in I-ETMS, this section would focus on the terminal with "practical" I-ETMS only. In the previous case study, it assumes that both the probability of an on-board computer in the I-ETMS system being failed and the probability of a WIU failure and/or radio failure in the I-ETMS system being failed is 0.0001 and the probability of no failure in I-ETMS system is then 0.9998. In addition, this chapter also considers 0.00001, 0.00002, 0.00005, 0.0002, 0.0005, 0.001, 0.01, and 0.1. The distributions of train operating time duration at terminals are summarized in Figure 3.15. For I-ETMS with onboard computer failure (Figure 3.15.a), the three measurements (e.g., mean, CVaR, and max) almost remain constant in general while the probability of onboard computer failure changes between 0.00001 and 0.1. However, considering the major effect is from the probability of WIU failure and/or radio failure, this chapter concentrates on the sensitivity analysis of train terminal operating time duration with varying probabilities of WIU failure and/or radio failure. According to simulation results (Figure 3.15.b), the probability of WIU failure and/or radio failure does not have an impact on the mean value of train operating time duration, while it does have some effect on the "worst-case" measures (e.g., CVaR and Max). For example, when the probability of WIU failure and/or radio failure is only 0.001 (10 times of original case), the CVaR (99.995%) and maximum value would increase 14.6% ($\frac{169.8-148.2}{148.2}$) and 3.3% ($\frac{202.9-196.4}{196.4}$), respectively. While for the probability of WIU failure and/or radio failure being 0.00001 (0.1 times of original case), the CVaR (99.995%) and maximum value would decrease 19.6% ($\frac{119.1-148.2}{148.2}$) and 6.7% ($\frac{183.2-196.4}{196.4}$), respectively. In particular, while

the probability of WIU failure and/or radio failure is assumed to be 0.00001, values of CVaR (99.995%) are quite close to the value of terminal without PTC systems. It indicates that even for the worst 110 train operating time durations, their average value is quite close to the benchmark and the operational impact would be significantly minor compared with the original case study. However, the maximum value for any value of probability of WIU failure or radio failure is still quite large (over 160 seconds). To further study these most severe cases, the mean time to frequency is also investigated here.

If the "moderate delay" is defined as train terminal operation duration between 100 second and 160 seconds and the "severe delay" is defined as train terminal operation duration over 160 seconds, Table 3.14 summaries the distributions of mean time to these delayed train terminal operations under different probabilities of WIU failure or radio failure. When the probability of WIU failure or radio failure is 0.001 or even higher, the mean time to either moderate delay or severe delay is lower than 1 year approximately, which is significantly more frequent than the original case (probability = 0.0001). In addition, as the probability of WIU failure or radio failure is reduced to 0.00001, the mean time to either moderate delay or severe delay would be decades of years, which is a substantially rare event. It highlights the lower probability of WIU failure or radio failure, the longer mean time to train delayed operations at terminals with proposed PTC system. In other words, it highlights that the probability of WIU failure or radio failure has a distinct impact on the mean time to train delays and lower failure probability (equivalently high reliability) would essentially have more rare train delay events and significantly reduce adverse operational impacts.

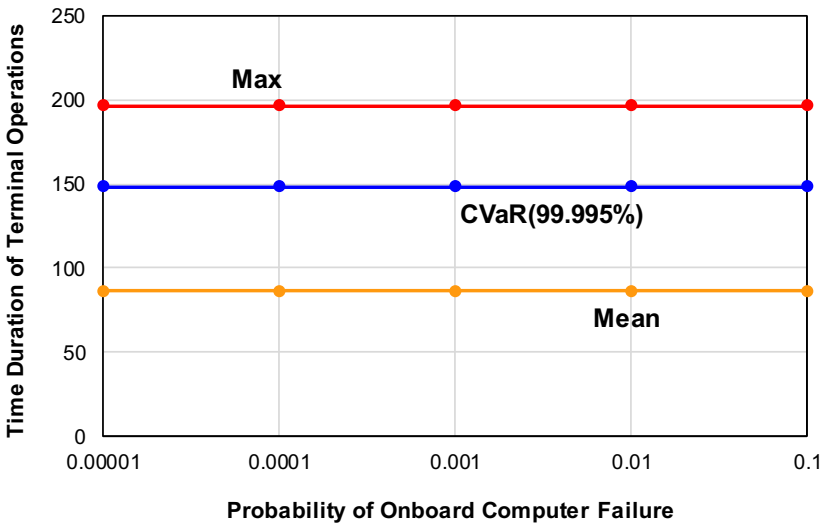

(a) Onboard computer failure probability

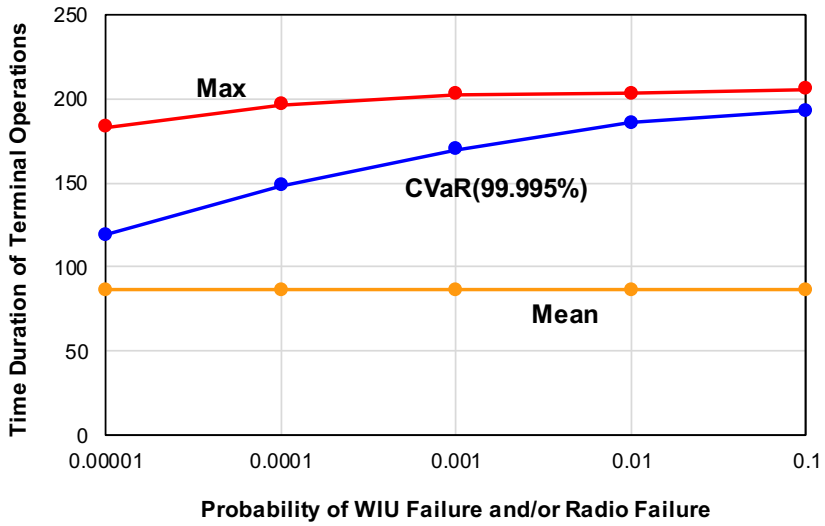

(b) WIU failure or radio failure probability

Figure 3. 15. Sensitivity Analysis for Train Operating Duration (in Second) Affected by (A) Onboard Computer Failure Probability (b) WIU Failure or Radio Failure Probability

This sensitivity analysis of train terminal operations under the varying probability of WIU failure or radio failure would serve as a reference for interested railroads and

vendors with comparative information in the impact of PTC terminal enforcement that is subject to component failure.

Table 3. 14. Statistics of Train Operating Time Duration (in Second) under Varying Probabilities of WIU Failure or Radio Failure

Probability of WIU Failure or Radio Failure	Mean Value	CVaR (99.995%)	Maximum Value	Mean Time to Train Delay	
				Moderate Delay [100s, 160s]	Severe Delay [160s, +∞]
0.1	86.4s	192.7	206.1	0.004 year	0.005 year
0.01	86.2s	185.5	203.5	0.03 year	0.07 year
0.001	86.2s	169.6	203.1	0.4 year	0.5 year
0.0005	86.2s	163.4	197.4	0.8 year	1.1 year
0.0002	86.2s	158.5	196.0	2.1 years	2.5 years
0.0001	86.2s	148.2s	196.4	4.0 years	4.8 years
0.00005	86.2s	131.8	191.4	8.4 years	8.9 years
0.00002	86.2s	121.9	188.6	19.1 years	23.8 years
0.00001	86.1s	119.3	182.7	35.7 years	44.4 years
Without PTC system (benchmark)	86.1s	93.9s	94.2s	-	-

Explanation of the operational impact analysis results

Negligible operational impacts from the "perfect" PTC system enforcement at stub-end terminals may potentially result from low probability of noncompliant train operations, rare component failure, and insignificant difference between engineer-induced braking curve and PTC-induced braking curve simultaneously. In passenger terminal stations, train speed is low due to restricted speed rules. Thus, the impact of PTC braking curve characteristics as mentioned in above section would be little during train operations at terminus stations.

In real-world PTC systems, component failure may occur, although it is rare event. In ACSES and I-ETMS systems, PTC component failure would cut off PTC function and leave the engineer in command of train movement under the Concept of Operations, except for the failure of WIU and/or failed radio. The I-ETMS system with failed WIU and/or radio can still enforce restricted speeds and prevent the train from hitting the bumping post. However, since WIU and radio are employed to monitor and transmit the position information of the switches, the failure would result in missing the planned route and the exact distance to bumping post. As a result, it would take the worst-case distance, or the shortest distance, to the bumping post as the braking curve calculation. This can lead to stop enforcement well short of the targeted point. In general, the train would be delayed from reaching a point within the platform area to be able to discharge passengers. In addition, this delay increases the time that the train would occupy individual track segments and the end of the train would be blocking the path of other trains, delaying them from either entering or leaving their tracks, which is likely to lead to congestion. In busy passenger terminals such as Washington Union Station or during rush hour periods, the delay impacts could be relatively significant. However, simulation analysis demonstrates that the adverse impact could not be significant to terminal operation in general, since WIU/radio failure resulting in taking the non-shortest track is such a rare event. Stopping well short of the targeted point requires the simultaneous occurrence of three events at least: noncompliant train movement, WIU/radio failure, and taking the longer terminating track. Thus, the probability of all three events occurring is extremely low. Furthermore, PTC with very high reliability (low component failure probability) would notably reduce the occurrence of train delay and minimize the adverse operational impacts.

3.7 Chapter Summary

This chapter presents preliminary assessments of the safety benefits, incremental costs, and operational impacts of PTC implementation at stub-end terminals that aims to prevent end-of-track collisions and enhance the safety levels at passenger terminals. The quantitative analysis consists of two major parts: benefit-cost analysis and operational impact assessment. The nationwide benefit-cost analysis concludes that taking 20 years as the service life, the annualized NPV is around $0.8 million (2017 dollars, using 7% discount rate) and around $1.2 million (2017 dollars, using 3% discount rate). The benefit-cost ratio is 1.7~2.8 (using 7% discount rate) and 1.8~3.1 (using 3% discount rate). In other words, the safety benefits may exceed the incremental costs if PTC is enforced to prevent end-of-track collisions over a 20-year period under specified circumstances and assumptions. The potential reason is that major PTC components have already been installed to achieve PTC functions in active territories, while the proposed PTC implementation aims to extend PTC functions to terminus stations with limited increments. Quantitative operational impact assessment is achieved with Monte Carlo simulation and considers two key potential factors: train braking curve and PTC component failure. The case study discloses that compared to “without PTC implementation”, the operational impact in PTC enforcement should be negligible, except for the rare occurrence of WIU failure or radio failure in the I-ETMS-type PTC system that would result in a stop well short of the targeted point and potentially delay both onboard passengers and inbound/outbound trains.

CHAPTER 4

ARTIFICIAL-INTELLIGENCE-AIDED TRESPASSING RISK MANAGEMENT

Partially Adapted from
Zhang, Z., Xu, J., Liu, X. and Zaman, A. (2020). Artificial Intelligence-Aided Railroad Trespassing Data Analysis: Methodology and A Case Study. (Working Paper)

Zhang, Z., Casazza A., Liu, X., Turla, T. (2019). Railroad Trespassing Risk Management: A Literature Review. In *Proceedings of the American Railway Engineering and Maintenance of Way Association Annual Meeting*, Minneapolis, MN.

4.1 Introduction

Train derailments and collisions are well-publicized events and have received significant attention from researchers and policymakers seeking to reduce their occurrence. Less attention has been devoted to trespassing, despite trespassing making up the majority of rail-related fatalities when compared to derailments and collisions combined. The U.S. railroad system is comprised of approximately 830 railroads, 134,000 miles of track, and 210,000 railroad crossings (FRA, 2018d). Trespassing accidents along right-of-way (ROW) and at highway-rail grade crossings constituted over 90% of rail-related deaths over the past ten years (FRA, 2018d). More specifically, there were 855 trespass-related fatalities in 2017, which demonstrates an increase of 18 percent from 2012 (FRA, 2018d). In addition to fatalities, these incidents resulted in other serious consequences, such as nonfatal injuries, train derailments, hazardous material spillage, train delays, and traffic congestion. From 2012 to 2016, trespassing accidents cost the United States approximately

$43 billion (FRA, 2019a), a sum that does not cover indirect costs (e.g., emotional distress or productivity losses). The FRA (2016a) concluded that the vast majority of trespassing deaths each year are preventable if effective countermeasures are implemented.

Amongst the limited studies of railroad trespassing, most researchers encountered challenges due to limited data resources and uncertain data quality. The vast majority of publicly available data refers to trespassing casualties or grade crossing accidents, and not to incidents. For example, the FRA published severe trespassing accident data reported by railroads, such as casualty-involved trespassing data in Form 6180.55A and collisions at grade crossings in Form 6180.57. However, the majority of rail trespassing behaviors do not lead to injuries, fatalities, or even accidents, and are not typically recorded in the FRA accident database, due to the absence of immediate harms. However, the FRA (2014) pointed out that more data on incidents that do not result in casualties would be valuable to railroad safety researchers. While the accident/incident reports submitted to the FRA by railroads have proven to be extremely helpful to railroad researchers, the study of trespassing near-miss events can bring incremental benefits. Not all trespassing events cause damage, but they indicate certain behaviors that may lead to severe consequences if they occur repeatedly. Learning from these trespass events, using statistical analysis and behavioral analysis, is critical for determining how to better educate the public on trespassing safety, how to better enforce laws, and how to engineer safer areas to prevent trespassing on railroad tracks. The increasing availability of video data within the rail industry makes the collection of trespassing data more feasible.

There are two types of video surveillance systems: Closed Circuit Television (CCTV) cameras that are known as analog and IP cameras that are also known as network

cameras. Both CCTV cameras and IP cameras can be found throughout railroads, observing yards, bridges, grade crossings, and stations, and both can transmit video to their desired destination. Deployment of camera systems continues to increase in the United States, following the 2015 Fixing Americas Surface Transportation (FAST) Act, which mandated the installation of cameras throughout passenger railroads to promote safety objectives (Congress, 2015a). Based on the Fast Act, the Safety Advisory 2016-03 issued by the FRA (2016a) contains recommendations related to inward-facing and outward-facing cameras to help mitigate human factor accidents. In addition, the Transportation Security Authority (TSA) provided funding for surveillance and sensors in transit and passenger rail areas recognized as being higher risk (Elias et al., 2016). For example, Caltrain in Palo Alto, California has installed CCTV cameras at safety-critical grade crossings to actively monitor and prevent illegal incursions through an integrated alert system (Palo Alto Online, 2018). various types of security monitoring systems were developed in Korea. Park and Lee (2010) presented a novel security monitoring system to detect critically dangerous situations, such as when a passenger falls from the station platform or when a passenger walks on rail tracks. These systems provide valuable sources of video big data for railroads, but making full use of the data accurately and efficiently is challenging. Most camera systems are reviewed manually by railroad crews, train police, or local police, which is labor-intensive and expensive. Limited resources and operator fatigue (Dee et al., 2008) can potentially lead to missing trespassing events. To address this challenge and also to leverage the untapped potential of the big data in railroad trespassing prevention, this research develops a novel Artificial Intelligence (AI)-aided algorithm that is capable of localizing and identifying trespassing events in both archival

video data and live video streams with acceptable processing speed and accuracy. You Only Look Once (YOLO), an emerging, state-of-the-art object detection algorithm developed by Redmon (2016, 2018), is utilized in the trespassing detection methodology to achieve high-accuracy trespassing detection with relatively low computation time. With this practice-ready technology, over two months of video data from one highway-rail grade crossing are processed and over 3,000 trespassing events are detected and analyzed in this study. These detected events, along with recorded trespassing video clips, can contribute to the development of practical trespassing risk mitigation strategies. Furthermore, a developed AI-based trespassing detection tool can be adapted to other trespassing-critical locations (e.g., grade crossing, right-of-way) throughout the railroad system to support railroad safety decisions and ultimately save lives.

The ultimate contribution of this chapter is to mitigate the safety risks from trespassing accidents, which account for a large proportion of rail-related deaths and injuries, with an economical, autonomous method. To achieve this, this research consists of the following parts:

1) Develop a deep learning-based algorithm to automatically detect trespassing events from archive videos and live streaming videos in a cost-effective and reliable way
2) Establish a practice-ready tool that can implement this methodology with low computational costs and high efficiency
3) Collect and analyze the trespassing events from studied videos and locations to understand trespassing characteristics and violators' characteristics
4) Propose the preliminary safety strategies and educational information to increase the safety level in specific grade crossings or rights-of-way

This study focuses on two general railroad trespassing areas: grade crossing and the ROW. Thus, a trespasser in this study is considered to be any person who enters or remains on railroad property that he or she is not legally authorized to access, including railroad equipment or facilities located on or near railroad property and rights-of-way (ROW). The trespassers can be pedestrians, bicyclists, cars, trucks, or other categories of highway users. The application of the detection methodology developed in this study would serve to improve the safety of the train crew, rail passengers, and road users, protect the general population and environment from the risks associated with hazmat shipments, and aid in the relief of congestion by reducing the number of incidents and delays due to those incidents.

4.2 Literature Review

4.2.1 Trespassing on railroad property

To the authors' knowledge, most trespass-related studies typically use publicly accessible accident data, as well as demographic and economic data. However, Stanchak and DaSilva (2014) concluded that much of the academic literature on trespassing risk is inconclusive because of the issues caused by limited data resources and uncertain data quality. Although FRA accident data (e.g., FRA Form 6180.55A - Railroad Casualties and FRA Form 6180.57 – Highway Rail Accidents) and demographic and economic data are extensively used, the much greater volume of trespass incidents, near-miss events, and unsafe acts are not well studied. Accidents only account for a small portion of the data that is needed in safety risk analysis. Meanwhile, near misses and unsafe acts can play a

significant role in safety. The definitions of accident, incident, and near miss are clarified below:

- Accident: an unwanted, undesired, unplanned event, which results in a loss of some kind (personal injury or property damage);
- Incident: an unplanned, undesired event that adversely affects completion of a task;
- Near miss: incidents where no property was damaged and no personal injury was sustained, but where, given a slight shift in time or position, damage and/or injury could easily have occurred.

An accident is an event with a harmful outcome and a near miss is an event resulting in no harm. Thus, this study only presents accidents and near misses that have obvious differences to avoid confusion. The near-miss management system is considered a critical component of a safety management system. The level of railway safety against trespassing, which has been so far achieved by assessing the historical data using various factors, as well as the existing safety programs and reduction strategies, are not adequate, and could be improved by some innovative future research directions, such as intelligent transportation systems (ITS), which could detect any unsafe conditions on the tracks or rights-of-way (Dong, et al., 2011). The distribution of causes of near misses with different levels of severity was presented by Wright and Van der Schaaf (2004). They focused on testing the common hypothesis that there exists a similarity in the severity of accidents and near misses. The results indicated no significant differences in the severity outcomes, which is slightly in favor of the hypothesis, but is specific to its domain data. However, there are many fewer publications focused on detecting near-miss events for any mode of transportation. There is a definite need for an increase in research analyzing near-miss

trespassing accidents with behavioral analysis, in order to figure out how to prevent highway-rail grade crossing and right-of-way accidents more efficiently. Even after a person attempts to trespass, if the near-miss detection systems work efficiently enough and if there is enough time to react, casualties can be prevented.

Ultimately, recorded near-miss events can provide detailed characteristics of trespassing for behavioral risk analysis. Even though forms of noncompliance have been hypothesized, a lack of actual behaviors captured at the time of violation has hindered further study. In the study of Signal Detection Theory in grade crossing, Raslear (2015) raised the concern that models have only been tested against limited data and there is a need for more information about motorist behavior. Thus, the detected near-miss data via either AI-based technology or "Close Calls" can be used to support the development of a specific behavior risk analysis that can contribute to identifying the factors that prompt such noncompliant decisions and establish a comprehensive framework for evaluating the impact of proposed countermeasures.

Overall, there is a definite need for research analyzing near-miss events in order to figure out how to mitigate highway-rail grade crossing and right-of-way risks more efficiently. A near-miss management system is considered as a critical component of a railroad safety management system. However, there are fewer publications focused on near-miss events due to the lack of near-miss data and the lack of a data collection methodology. There are only four near miss-involved literatures (Figure 4.1), which are limited in scope due to considerable costs of data collection. To overcome this limitation, a generic methodology aiming to collect trespassing events (including near misses) and reinforce trespassing risk reduction is proposed in this research.

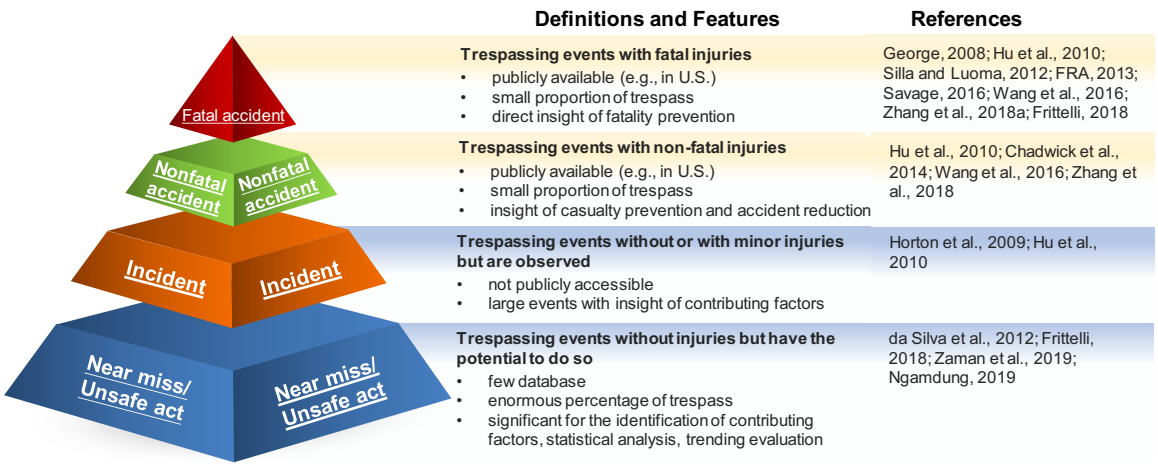

Figure 4. 1. Pyramid Chart for Trespassing Events in Fatal Accident, Nonfatal Accident, Incident, and Near Miss

4.2.2 Railroad trespassing detection technologies and methodologies

Previous studies have employed various technologies to detect trespassing over railroad infrastructure in the past decade. DaSilva et al. (2012) demonstrated an automated prototype railroad infrastructure security system installed at a bridge in Pittsford, New York (Figure 4.2). This location was selected due to its numerous accounts of trespassing and fatalities. The key component of this system is the dual-technology motion detector that combines stereo Doppler microwave technology with a passive infrared sensor. Although this motion sensor can be activated by an approaching trespasser, the system still needs attendants to observe videos from the installed camera and determine whether there is indeed a trespasser. A similar trespass detection sensor was developed and installed in Brunswick, Maine (Volpe Center, 2017). However, these technologies are based on the conglomeration of several devices which makes them susceptible to component failure, resulting in downtime (DaSilva et al., 2012).

In one recent study of an overpass bridge going over a grade crossing (Ngamdung, 2019), the overpass utilization was collected using an automated pedestrian counter, while the pedestrian trespass under the bridge was manually coded based on video data. However, the manual counting of trespassing events for 100 hours of video is expected to have considerable labor costs. Meanwhile, in one recent study on railroad trespassing, Topel (2019) concluded that manual detection from surveillance is labor-intensive and expensive, and instead suggested automated detection as one way to potentially reduce the need for human monitors. In order to detect and collect trespassing events in an efficient, reliable way, an Artificial Intelligence-based trespassing detection methodology is proposed in this research to detect trespassing events from vast amounts of video data.

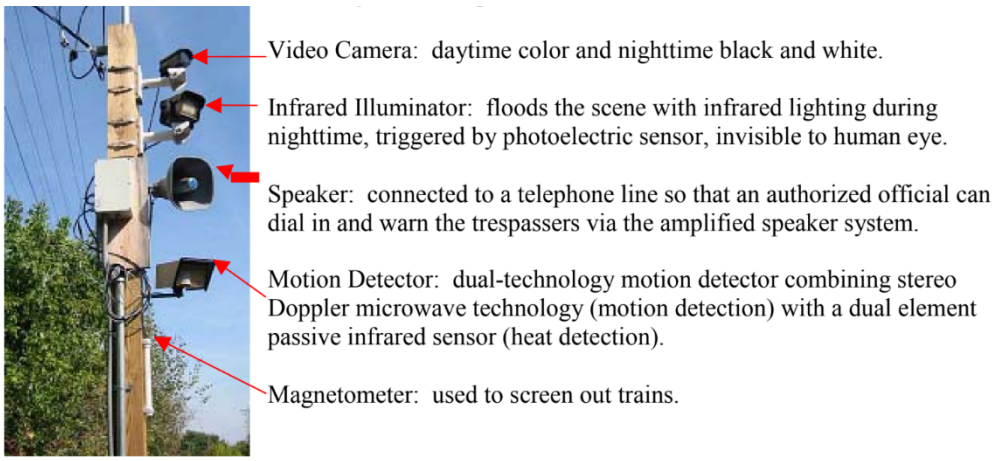

Figure 4. 2. Pole Configured with Monitoring and Detection Components from DaSilva et al. (2012)

4.3 Overview and Identification of Trespassing Safety Risk

Railroad Trespassing is defined as an event when any unauthorized person or vehicle enters or remains on a railroad right-of-way, equipment, or facility (FRA, 2018d). Railroads own their rights-of-way and have a reasonable expectation of operating on their property without the presence or interference of unauthorized persons. Pedestrians and motorists are only permitted on railroad property where an authorized crossing (either roadway or pedestrian) intersects with the railroad right-of-way at a grade crossing, provided that highway traffic control signals and other signages are obeyed. Railroads have continuously struggled with the issue of trespassing at highway-rail grade crossings and rights-of-way (ROW), which can have serious consequences, such as fatalities and injuries, train derailments, hazardous material spillages, train delays, and traffic congestion. There are two types of trespasses in the United States:

- In the case of trespass along ROW, trespassers are illegally on private railroad property without permission. They are most often pedestrians who walk across or along railroad tracks as a shortcut to another destination. Some trespassers are loitering or engaged in recreational activities such as jogging, hunting, bicycling, snowmobiling, or operating off-road, all-terrain vehicles (ATV) (FRA, 2016c).
- In the case of trespass at highway-rail grade crossings, where a public or private road, street, sidewalk, or pathway intersects railroad tracks at the same level, such sites can include passive crossbucks, flashing lights, two-quadrant gates, long gate arms, and median barriers, in various combinations. Lights and/or gates are activated by circuits wired to the track (track circuits). Any movement

> over the grade crossing zones while the red signal is flashing would be identified as a trespassing violation and may bring hazards to trains and highway users. The highway users include automobiles, buses, trucks, motorcycles, bicycles, farm vehicles, pedestrians, and all other modes of surface transportation, motorized and un-motorized.

Prior research has largely focused on evaluating common countermeasures and understanding the factors that influence trespassing. The solutions to prevent trespassing accidents/incidents fall under the traditional safety concept of the 3 E's (Engineering, Enforcement, Education) (Chadwick et al., 2014). In terms of influencing factors, the occurrence of trespassing events is correlated with several organizational factors, environmental factors, personal factors, and psychological factors. A trespassing accident can occur due to a number of organizational, environmental, social environmental, personal, and psychological factors. Per the collected influencing factors in trespassing studies, they can be categorized into four major groups: pre-crash behavior, crash characteristics, mental health, and environments. Table 4.1 presents a summary of cited references. In particular, age and gender are most widely studied in the literature. Compared to females and seniors, most fatalities from trespassing are young males, who tend to lack awareness of potential dangers in a specific traffic situation (George, 2008; Silla and Luoma, 2012; FRA, 2013).

Table 4. 1. Literature by Influencing Factors

Factor	Observation	References
Weather	Fewest accidents occurred during the harsh cold weather and accidents seem most prevalent in summer.	Savage, 2007; Stanchak and da Silva, 2014; Savage, 2016
Age	In New Zealand, 50% of train-related pedestrian deaths and 40% of injuries involved people aged between 10 and 19 years.	Lobb et al., 2003
	In the U.S., most fatalities in rail-pedestrian crashes were young people.	Caird et al., 2002; George, 2008; FRA, 2013; Savage, 2016; FRA, 2018d
	In Finland, the largest age group at each location was adults, followed by youngsters and children.	Silla and Luoma, 2012;
Gender	The vast majority of decedents in railroad-trespasser incidents continue to be male.	Caird et al., 2002; Raub, 2007 ; George, 2008; Silla and Luoma, 2012; FRA, 2013
Race	81 percent of decedents in the current study are White, which is 9 percent higher than the national average.	FRA, 2013
Alcohol and/or Drugs	At least 52.4 percent of all incidents involved alcohol and/or drugs.	FRA, 2008; George, 2008; Silla and Luoma, 2012; FRA, 2013
Use of headphones or other electronic devices	Trespassers who are wearing headphones or talking on cell phones are more likely to sustain fatal injuries.	Wali et al., 2018
Walking, sitting, or lying on or near the railroad tracks	Most fatal train crashes happened when individuals were walking, sitting, or lying on or near the railroad tracks.	Savage, 2007
Traffic flow and waiting time	Higher traffic flow and longer waiting times at the highway-rail grade crossings may also be responsible for restless behavior, thus motivating the intention to trespass.	Stefanova et al., 2015
Travel time and/or distance	A potential decrease in travel time and/or distance also motivates trespassers.	Skladana et al., 2018
Time	A majority of fatalities were observed on weekends at night-time.	Radbo and Anderson, 2005; Savage, 2007
	Summer has the highest percentage of trespassing incidents.	FRA, 2018d
Physical act	The actions with the highest average percentage of incidents across all three years are walking and lying down.	FRA, 2018d

Based on historical data analysis, the FRA (2013) concluded that the reported decedents' mean age at time of death was 37.9 years; two out of every three railroad trespassing fatalities involved individuals between the ages of 20 and 49. Meanwhile, the average age of victims may be younger in New Zealand where 50% of train-related pedestrian deaths and 40% of injuries involved people between 10 and 19 years of age (Lobb et al., 2003). In addition, it is noted that alcohol and drug use is one causal factor which has received much focus. George (2008) and the FRA (2008; 2013) concluded that over half of all incidents involved alcohol and/or drugs. In particular, only around 29% of the fatalities reported were free from the influence of both alcohol and drugs (FRA, 2008). Although the information only specifies the presence of alcohol/drugs, but not the exact cause, the FRA (2008) has clarified that the percentage of alcohol/drug use seems to be higher among suicide fatalities when compared to other trespassers.

4.4 Trespassing Collection Methodology with AI-Aided Detection

4.4.1 Methodology

Overview of You Only Look Once (YOLO)

You Only Look Once (YOLO) uses features learned by a single deep convolutional neural network to detect objects. Most deep learning-based object detection algorithms, such as the R-CNN family, have a complex detection pipeline, in which bounding box generation, object classification, duplicate detection elimination, and bounding box refining and rescoring are executed sequentially. Instead, YOLO sees the entire image or video frame and implicitly encodes contextual information about classes as well as their appearance (Redmon et al., 2016). In this algorithm, object detection is redefined as a regression

problem to spatially separate bounding boxes and associated class probabilities with one single Convolutional Neural Network. The generic architecture of YOLO and R-CNN are presented in Figure 4.3.

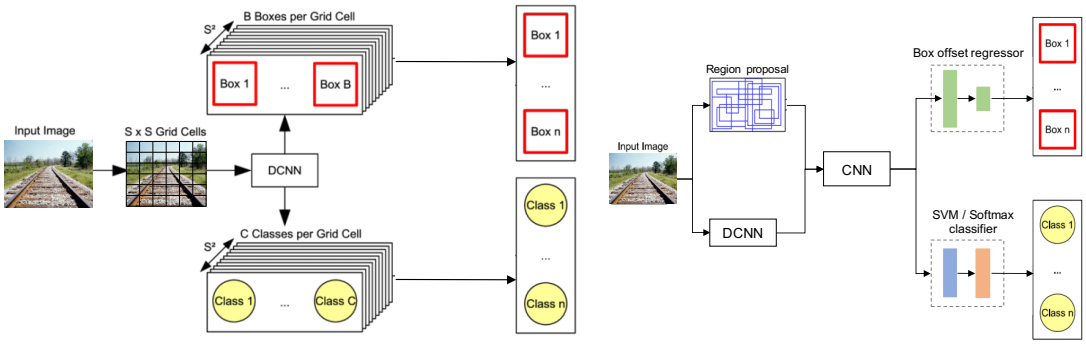

(a) YOLO (b) R-CNN

Notes: In R-CNN, DCNN is for pre-training and CNN is fine-tuned for region features.

Figure 4. 3. Architecture for Object Detection in (a) YOLO and (b) R-CNN (Altenberger and Lenz, 2018)

YOLO's performance as a single-stage detector can be extremely fast compared to other deep learning-based methods and can be good for real-time processing with limited computational resources. In addition to its fast real-time processing ability, YOLO assesses the whole image during training and test time and thus it implicitly encodes contextual information about classes as well as their appearance, instead of limiting the classifier to the specific region and missing the larger context, as occurs when using some R-CNN family methods. Overall, YOLO leads to fewer false positives in background areas and Redmon et al. (2016) stated that YOLO demonstrates less than half the number of background errors compared to Fast R-CNN. Further, YOLO reasons globally about the image or frame when making a prediction. Unlike sliding window or region proposal-based

techniques, YOLO has access to the whole image when predicting boundaries. With the additional context, YOLO demonstrates fewer false positives in background areas. After the updates from YOLO to YOLOv3, the accuracy of YOLO's algorithm has improved significantly and can achieve a similar accuracy level to the most advanced, complex methods. Therefore, in this study, YOLO's fast speed in video/image processing and detection prediction can satisfy the need for real-time object detection, as well as archive videos, with stable accuracy. The following sections will introduce the basic principles of YOLO. For more details on this object detection method, refer to Redmon et al (2016).

Unified detection

YOLO applies a single neural network to features from the entire image to predict each bounding box across all classes simultaneously. In general, to enable end-to-end training and real-time speeds with reasonable precision, YOLO divides the input image into an $S \times S$ grid. Each of these grid cells (the total number of which is S^2) predicts B Boundary boxes and detects one object only, regardless of the number of boundary boxes. Each boundary box has five elements, which are x, y, w, h, and the confidence score. Specifically, x and y are the coordinates of the box center relative to the bounds of the grid cell and w and h are the bounding box width and height normalized by the image width and height, respectively. The confidence score reflects the level of confidence that the bounding box contains an object and how accurate the box is that it predicts. It is defined as $\Pr(Object) * IOU_{pred}^{truth}$, in which IOU is the intersection over the union between the predicted box and the ground truth. Hence, if no object exists in the cell, the confidence score should be 0, otherwise it would be equal to IOU. The ultimate objective for each

grid cell is to predict the class probabilities per grid cell in an image. Class-specific confidence scores can be calculated as the product of the bounding box confidence score and conditional class probability,

$$Final\ score = \Pr(Class_i) * IOU_{pred}^{truth} = \Pr(Class_i|Object) * \Pr(Object) * IOU_{pred}^{truth} \quad (4\text{-}1)$$

Where:

$\Pr(Class_i)$ is the probability that the object belongs to $Class_i$;

$\Pr(Class_i|Object)$ is the probability that the object belongs to $Class_i$, given that an object is present; and

$\Pr(object)$ is the probability that the bounding box contains an object.

Network design and feature extractor

The network in YOLOv1 has 24 convolutional layers followed by 2 fully connected layers (FC). The figure below presents the network design in the creation of YOLO by Redmon et al. (2016), which uses PASCAL VOC (2015) as the evaluation detection dataset. It assumes that the number of grid cell S^2 is 7^2, the number of bounding boxes for each grid cell is 2, and the number of classifiers is 20. Then, the final prediction is a $7 \times 7 \times 30$ tensor (as shown in Figure 4. 4).

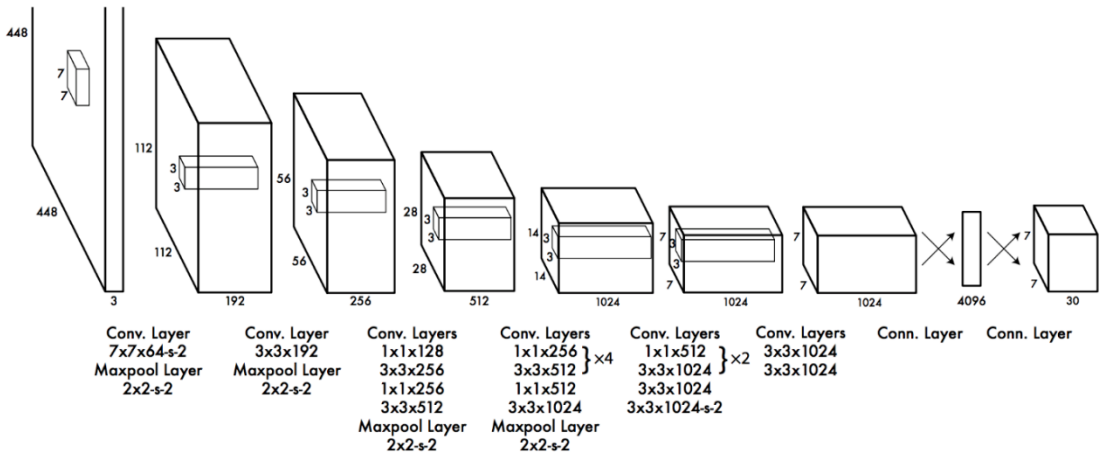

Figure 4. 4. Feature Extractor of YOLOv1 (Redmon et al., 2016)

Improvements in YOLOv3

Although YOLOv1 is a powerful tool for real-time object detection, it has some limitations. For example, YOLOv1 still lags behind some state-of-the-art detection methods in terms of accuracy and it struggles to precisely localize some objects, especially small ones. To overcome these major drawbacks in YOLO, YOLOv2 (Redmon and Farhadi, 2017) and YOLOv3 (Redmon and Farhadi, 2018) proposed some updates to YOLO. The primary AI system in this study is YOLOv3, which is the third, most recent object detection algorithm in the YOLO family. Considering the similarity between YOLO and YOLOv3, this section will not introduce YOLOv3 from scratch. Instead, Figure 4.3 demonstrates the major updates to YOLOv3 from YOLOv2. For example, in terms of classification, instead of using the softmax function and mean square error in calculating the classification loss, YOLOv3 uses independent logistic classifiers and binary cross-entropy loss for each label, in order to calculate the probability that an input belongs to a

specific label. This can reduce the computation complexity from the softmax function. For more detailed updates to YOLOv3, refer to Redmon and Farhadi (2018).

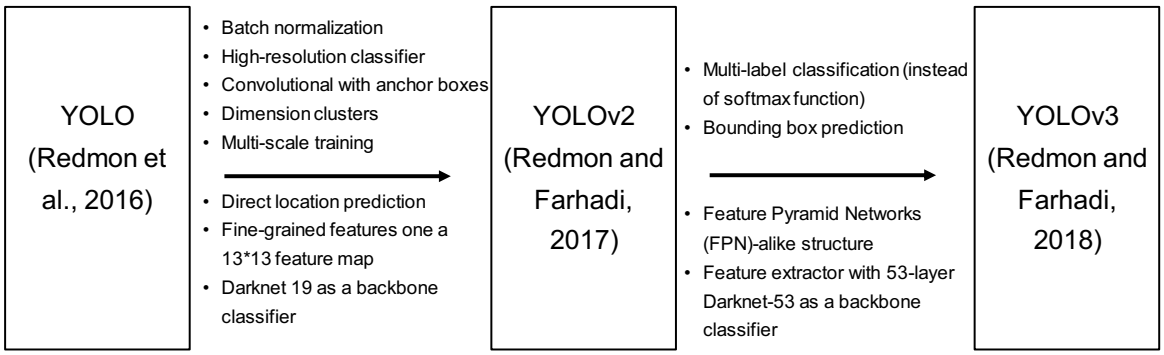

Figure 4. 5. Updates from YOLO, YOLOv2, to YOLOv3

One of the major updates in YOLOv3 is the use of Darknet-53 as feature extractor. Redmon and Farhadi (2018) point out that Darknet-53 is more powerful in terms of accuracy and more efficient in terms of operation speed, than ResNet, such as ResNet-101. Compared to the Darknet-19 that is used in YOLOv2, using Darknet-53 can achieve small object detections, as well as more accurate detections with deeper layers. YOLOv2 commonly struggles with small object detections, due to the loss of fine-grained features as the layers downsample the input. However, Darknet-53, used in YOLOv3, has only one global average pooling layer before the input, along with 53 convolutional layers. For the improvement of accuracy and processing speed, a residual block, consisting of several convolutional layers and shortcut paths, is employed to add up the old features and to make it easier for the network to learn the features stably, especially for deep networks. Appendix C presents the loss function used in YOLOv3.

Common Objects in Context (COCO)

YOLO and common R-CNNs are compatible with existing, large-scale training datasets, such as the Common Objects in Context (COCO) dataset. This dataset consists of over 200,000 labeled images of everyday scenes, built for use in object recognition research, and gives computer vision algorithms valuable training data to recognize commonly seen objects, such as people, cars and trains (Lin et al., 2014). These features, coupled with YOLO, allow for rapid deployment of AI to object recognition tasks.

A key part of Mask R-CNN's performance is the training dataset, which allows it to recognize objects. The COCO dataset, consisting of more than 200,000 labeled images of everyday scenes, built for use in object recognition research, was utilized for this purpose. It is selected because of its depth (over 330,000 images and over 200,000 labeled images), diversity (80 object categories) and timeliness through its continual growth and refinement (Lin et al., 2014). Additionally, the COCO dataset includes pre-generated boundaries around recognized images, allowing for better object recognition. By providing the YOLO with this dataset, it can recognize people, cars, trains and other objects within the ROI.

4.4.2 YOLO-Based Trespassing Detection Framework

There are five major phases in trespassing detection with YOLO and computer vision: video frame input, region of interest designation, YOLO-based object detection, object tracking, and output collection and follow-up actions. Figure 4. 6 presents a systematic illustration of this detection technology. The developed detection tool can be applied to two safety-critical scenarios: right-of-way and highway-rail grade crossings.

- Railroad right-of-way is defined as railroad property with no intersection or crossing. For trespassing along right-of-way, any unauthorized movements of people or vehicles within the right-of-way would be deemed illegal at any moment and identified as trespass violations.
- A highway-rail grade crossing is the intersection between the highway and railway, where active signals are commonly installed to alert highway users to an approaching train. Trespassing at a highway-rail grade crossing is defined as when pedestrians and vehicles enter the crossing zone while the signal lights are activated, though the highway users' behaviors in other cases would be permissible.

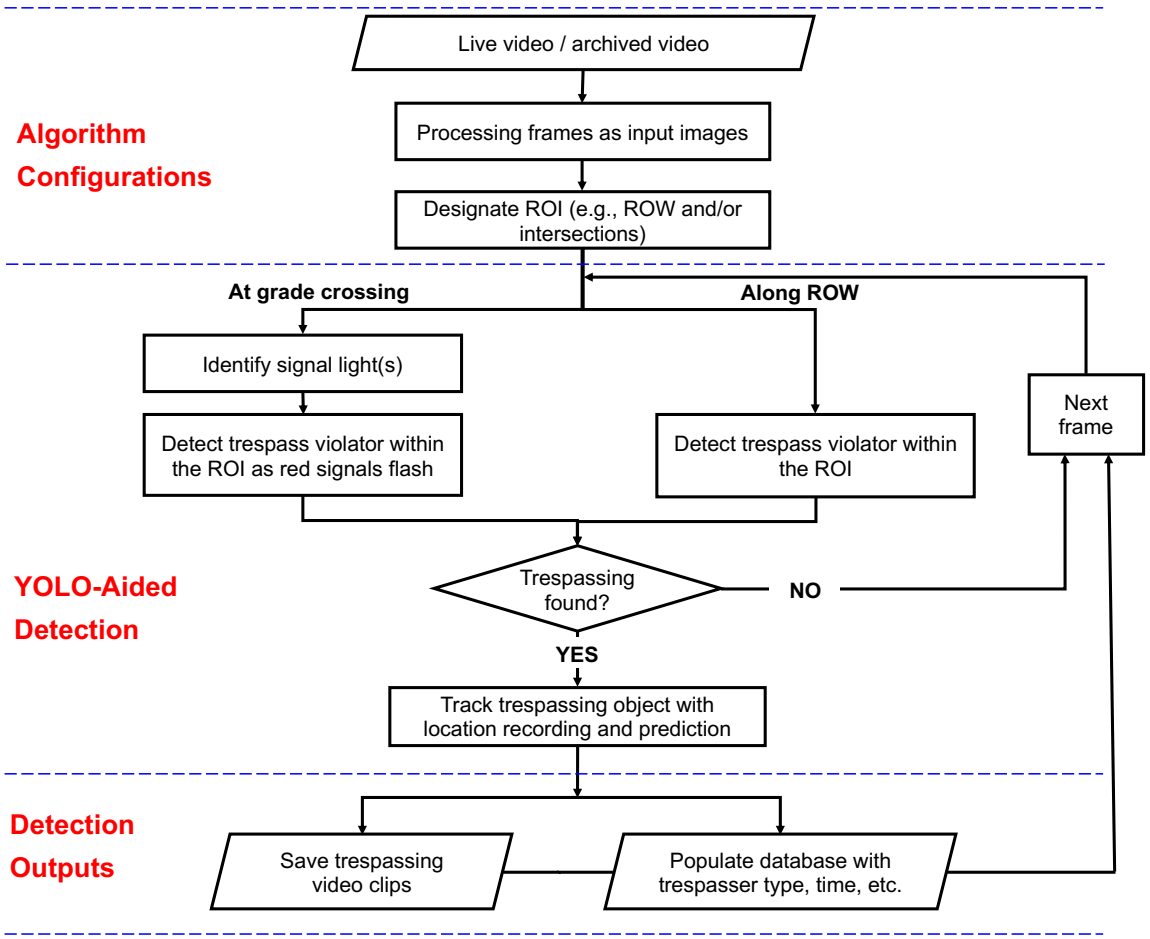

Figure 4. 6 General AI Framework for Railroad Trespass Detection

4.4.2.1 Configurations

Detection of trespassing events in video feeds involves a wide variety of configurations of environmental variables and technical features from either live data streams or archived videos of railroads (Table 4. 2). An AI-based methodology built for trespass detection must have several fundamental performance qualities.

Table 4. 2. Essential Configurations in Trespassing Detection

Configuration Factors	Brief Requirements	Influencing Aspects
Video frame rate	GPU computation ability, measured in frame per second, should be greater than the video frame rate in order to guarantee at least real-time processing.	Video quality
Graphics Processing Unit (GPU) computation ability		GPU types and computation ability
Center locations of red signals	Provide the exact pixel information in one frame where the signals are located	Grade crossing design and red signal installations
Pixel size of red signal (e.g., 7×7)		Red signal lamp size and video quality
Threshold α for gray color difference between two red signal lamps	The absolute intensity difference between the two red signal lamps is greater than α for both daytime and nighttime. In general, α is set as 0.3.	Video color quality, red signal brightness
Region of Interest in grade crossing	The location of the polygon in each frame	Grade crossing location and design
Region of Interest in ROW		ROP location in video frame

Video input preparations

The first step of the developed AI framework is to import either live video streams or archival video data. Frames are extracted from videos and processed as the input image in the AI framework. Instead of reading every frame within a video, the algorithm should be tuned in order to achieve an optimal trade-off between processing speed and accuracy. To be processed in real time or an even shorter time, the number of frames per second in tuned videos should be smaller than the number of frames/images that the graphics processing unit (GPU) is able to process in one second. Accuracy should be maintained with a sufficient number of frames.

Designation of ROI

The region of interest (ROI) is defined as the area that pedestrians and highway users are prohibited from entering. In right-of-way, zones involving rail track and ballast should be identified as the ROI and any intrusion without railroad permission is forbidden. In terms of highway-rail grade crossing cases, the ROI is defined as the part of the road and rail intersection where highway users are prohibited from entering during flashing red stop signals. To designate the ROI in trespassing cases, a user can sequentially select the outer limits of the trespass area in the static image of the video. Since this study focuses on videos from fixed cameras only, one pre-defined ROI, as an enclosed polygon, is practicable for all image processing in one location.

Activated signal light detection

In highway-rail grade crossing trespass detection, one precondition is the identification of activated red signals. From the computer vision perspective, the identification of a red signal can be achieved with red pixel values in one small zone where the red signals are located. Zhang et al. (2018b) provided a red signal indication method, in which the intensity difference of two lamps emitting red lights in the stop signal was the reference for stop signal detection. More specifically, two small square windows in RGB (red, green, blue) color scale are extracted from the left signal lamp and the right signal lamp, respectively (Figure 4.7). The equation below is used to convert two signal lamps' RGB into grayscale:

$$\Phi(x_{RGB}) = x_{GRAY} = (0.2989) \times x_R + (0.5870) \times x_G + (0.1140) \times x_B \quad (4\text{-}2)$$

where x_R, x_G, x_B, x_{GRAY} are color values for red, green, blue, and gray, respectively.

If the absolute intensity difference δ between the two lamps is greater than a threshold (α), the status of the signal light is identified as "on," while correspondingly the status is identified as being "off" if the absolute intensity difference δ is smaller than the threshold. The threshold α of color difference can be configured based upon training video data. Previous studies (Zhang et al., 2018c; Zaman et al., 2018; 2019) have proven that this method is feasible in the testing of trespassing detection algorithms for both daytime and nighttime conditions.

Figure 4. 7. Intensity Difference of Stop Signal (Zhang et al., 2018c)

4.4.2.2 YOLO-based trespass detection

Trespasses along rights-of-way and at highway-rail grade crossings are two trespassing scenarios. Along the right-of-way, any unauthorized pedestrians or vehicles detected in the ROI are deemed to be trespassing. On the other hand, the highway-rail grade crossing will only trigger trespass event detection if the signal lights and crossing gates are activated. This categorization represents the two fundamentally different types of locations where trespassing occurs. Both scenarios are analyzed using the same generalized trespass detection framework, except for the fact that the trigger of the signal light serves as a precondition for highway-rail grade crossing.

With pre-defined ROI and red signal identification, the YOLO-based algorithm can analyze frames of the live video feed or archival video data. A key part of YOLO's performance is the training dataset, which allows it to recognize objects. This study uses COCO, a large-scale object detection dataset, for the training data. The COCO dataset includes over 330,000 images, more than 200,000 labeled images, and 80 object categories.

Due to its depth, diversity, and continuous growth and refinement, the COCO dataset has been employed in object recognition research and gives computer vision algorithms valuable training data to recognize commonly seen objects (Lin et al., 2014). These features coupled with YOLO allow for the rapid deployment of AI in object recognition tasks.

As shown in the conceptual diagram of trespassing detection, the YOLOv3 network is fed with input images, which are frames from live video streams, and outputs tensors with bounding box coordinates and objectness scores. The dimension of an output tensor is:

$$S \times S \times [B \times (5 + C)] \tag{4-3}$$

Where

$S \times S$ is the scale of input images;

B is the number of boxes that each grid predicts (e.g., 3);

5 is the box coordinates (tx, ty, tw, th) and objectness score (the level of certainty); and

C is the number of classes (e.g., person, car, truck).

In addition to convolutional layers, residual blocks are used for better feature learning. A residual block consists of several convolutional layers and shortcut paths. Different from a classic CNN network, which learns features one by one, residual blocks, with the residual added to certain hoc layers, can add up an old feature with a simplified learning feature. This makes it easier for the YOLOv3, with very deep networks, to learn the features stably without a complete complex feature.

In general, to execute a detection, the image (a certain frame from the video stream) is divided into a grid of $S \times S$ (left image). Each one of the S^2 cells will predict N possible bounding boxes and the objectness score (the level of certainty) of each of them, such that $S \times S \times B$ boxes are generated and calculated. The vast majority of these boxes will have a very low probability, which is the reason why the algorithm proceeds to delete the boxes that are below a certain minimum threshold of probability. The remaining boxes are passed through a non-max suppression, which eliminates possible duplicate objects and thus only leaves the most exact of them (Figure 4. 8).

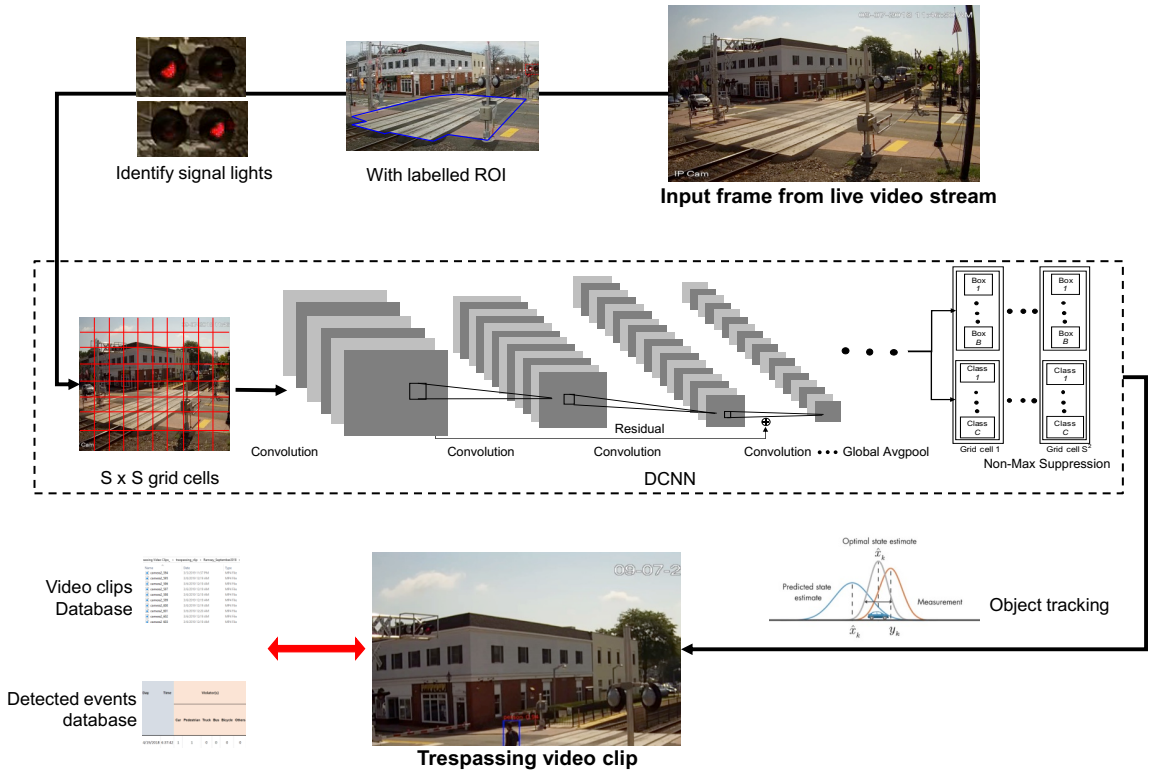

Figure 4. 8. Conceptual Trespassing Detection System Using Artificial Intelligence

4.4.2.3 Object tracking

A limitation of the YOLO network is that it cannot inherently remember and track objects from frame to frame. Detection results from the YOLO network can only provide the detected object information from each individual image (frame). It is a challenge to distinguish these "new" objects from the "old" objects that also exist in the previous frames, which comprises the huge discrepancy between image processing and video analysis. The distinct consequence of erroneous categorization is that the number of trespassing occurrences increases rapidly due to recurrent counting of objects in frames. Therefore, the proper categorization of detected objects is crucial to ensure detection accuracy in trespassing video analysis.

Object tracking is based on the position of objects. The position of each object in one frame is recorded and a mask window including all possible positions where objects may appear in the next frame is predicted using a Kalman Filter (Kalman, 1960). In the next frame, if there is an object detected in the predicted area from the last frame, these two detected objects are identified as the same object. This process is repeated for each analyzed frame of video to maintain continuous object tracking. If the predicted location is out of ROI, it means that this object has already left the ROI or the image. Consequently, the algorithm can stop tracking it and then generate output for this detected object.

4.4.2.4 Trespassing detection outputs

If an illegal object is detected within the ROI, a subroutine of the AI will execute the commands with several outputs (Figure 4. 8). A clip of the trespass event is recorded and metadata (e.g., trespassing type, time, video file name, etc.) is stored in a trespass event

database. This metadata is automatically generated by the AI, demonstrating that the context of the image can be extracted and interpreted. Trespass data can provide valuable information about hazardous environments and trespassing behaviors that can inform education, enforcement and engineering strategies for trespass prevention. Additionally, the aggregation of these trespass events has the potential to enhance future railroad risk analyses. Furthermore, in the implementation of AI-based trespassing detection technology, combining computer vision techniques and the YOLO algorithm, detection accuracy can be increased through configuration and testing. Additional datasets, including diverse environmental conditions (e.g. rain, snow, day, night and fog) and distortions (e.g., video artifacts, shadows) should be tested to verify its performance under varying circumstances.

4.5 Trespassing Data Collection Framework Application

This section aims to develop a location-specific case study with large volumes of trespassing data that are automatically detected and collected by the AI-aided technology. Data analyses are developed to quantitatively support railroads and railroad communities in better understanding trespassing behaviors and influencing factors, and thus to develop efficient countermeasures in the selected grade crossing location. In addition, such grade crossing video data is also accessible from railroads and online resources. For example, the VirtualRailFan, a web portal recording live camera videos at grade crossings and rights-of-way from 66 cameras in 22 states, provides live streaming 24 hours a day, 7 days a week with high definition (HD) video cameras. In this chapter, both automatic detection technology and trespassing data analysis play a critical reference role for trespassing prevention and mitigation in terms of engineering, education, and law enforcement.

4.5.1 Overview of selected grade crossing

To validate the functionality of the proposed AI-based trespassing detection technique, a grade crossing located in New Jersey is selected as a case study, although the developed methodology can also be applied to rights-of-way. The selected crossing experiences about 110 activations per day, with the majority being commuter trains. One train station with three parking lots, two to the west of the train tracks and one to the east, are adjacent to the grade crossing. Several restaurants, markets, and two schools are located along the busy downtown street (Figure 4.9). Trespassing in the selected grade crossing is commonplace and fatalities have occurred in the past decade. Per the FRA Form 6180.57 (FRA, 2019b), at least four grade crossing accidents have occurred at the selected grade crossing since 2010, two of which led to fatalities (Table 4. 3). Per observations from videos and field visits, grade crossing trespasses occur there every day.

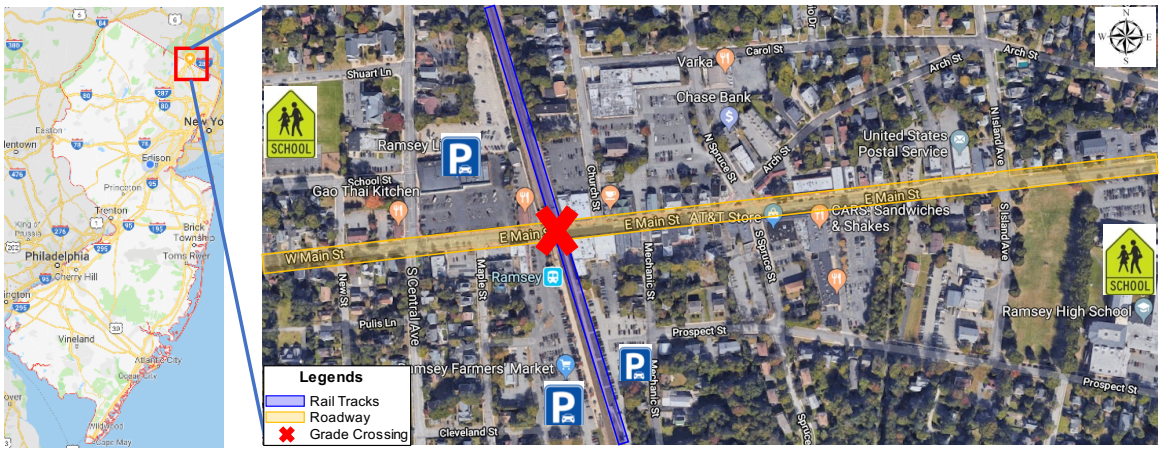

Figure 4. 9. Aerial View of Selected Grade Crossing

Most violations do not involve damage or injuries, and accidents are (fortunately) too few to provide a significant statistical sample to support decision making about

investing in safety improvements. However, the few accidents that have occurred were preceded by trespassing, and gathering data on near misses will dramatically increase the data available to formulate solutions to this problem. This lack of data is the prime motivation for the AI-aided trespassing detection methodology developed in this research.

Table 4. 3. 2010-2016 Four Grade Crossing Trespass Accidents in Selected Location from FRA 6180.57 Database

Date	August 4, 2010	May 21, 2010	September 15, 2012	June 9, 2016
Time	7:43 AM	11:52 AM	12:00 PM	6:45 AM
Weather Condition	Cloudy	Clear	Clear	Clear
Train Speed	29 mph	40 mph	70 mph	68 mph
Highway User(s)	Pedestrian	Truck	Auto	Pedestrian
Circumstance of Accident	Rail equipment struck highway user	Rail equipment struck highway user	Rail equipment struck highway user	Rail equipment struck highway user
Action of highway user	NA [1]	Stopped on crossing	Stopped on crossing	Went around the gates
Number of fatalities	1	0	0	1

Notes: [1] NA: No relevant information in the database.

4.5.2 AI-aided detection technology configuration and processing

Video data preparation and computing devices

During the data collection, one IP camera is mounted on a utility pole located approximately 30 feet northwest of the grade crossing, as shown in Figure 4. 10. The camera's view can cover all activities in the grade crossing, as well as at least 5 feet on either side of this location.

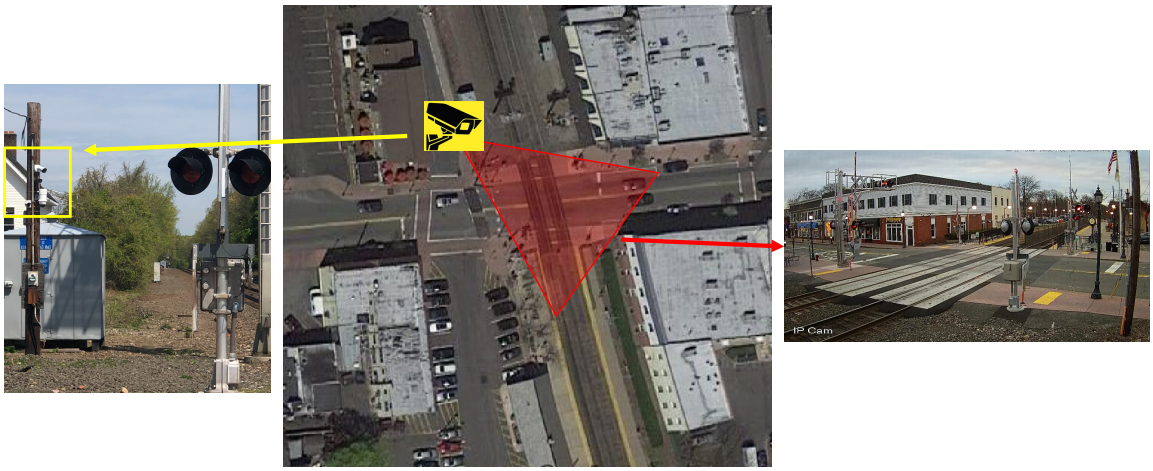

Figure 4. 10. IP Camera Placement at Selected Location

In this case study, 1,632 hours (68 days) of raw video data is processed to support the AI-aided methodology validation, data collection, and trespassing risk analysis. The video data is in MP4 format with 30 frames per second and a resolution of 1920 pixels by 1080 pixels. With limited data availability, three time periods are studied in an aim to cover diverse season conditions. The periods are as follows:

- April 19-25, 2018 (7 days)
- September 2018 (30 days)
- January 2019 (31 days)

Two computing devices are used in this study. One is a NVIDIA Jetson TX2 developer kit that is equipped with Pascal GPU with 256-CUDA cores and 8 GB memory capacity. The other device is the more powerful GPU – NVIDIA Tesla V100-DGXS, in which 5120-CUDA cores work with 32GB memory capacity. Per the pre-test, the processing speeds of the Jetson TX2 and NVIDIA Tesla V100 are around 0.45 seconds per image and 0.06 seconds per image, respectively, with the developed YOLO-based algorithm. Therefore, to achieve reliable real-time object detection from Ramsey video

data, the video frame reading rates for the two processing tools should be about 2 frames per second and 16 frames per second, respectively, so that trespassing events in the videos can be detected with acceptable accuracy.

ROI and red signal

In the grade crossing case study, only pedestrians and vehicles that entered the ROI after the signal lights would trigger the detection of trespassing events. In other words, red signals are used in the algorithm to differentiate between legal passes and illegal passes. The selected grade crossing employs proactive, advanced grade crossing systems, in which flashing red lights and gates are equipped to warn and block highway users. As shown in Figure 4. 11, ROI in the crossing is represented by the polygon with blue lines. The right-of-way around the grade crossing is excluded in this case study due to an explicit focus on grade crossing risk. In this 1920×1080 video frame, the borders of ROI can be drawn through connecting a series of endpoints: (914, 556), (143, 720), (252, 767), (148, 790), (776, 933), (919, 861), (1245, 900), (1563, 954).

The on/off state of the stop signal is derived by focusing on the stop signal post. The stop signal consists of a left lamp and a right lamp with a size of 3×3 pixels emitting red light (Figure 4. 11). In this 1920×1080 video frame, the centers of left red signal and right red signal are (380, 1551) and (380, 1601). The on/off state of the red signal is identified based on the error of two median values of the lamps' gray color values. Accounting for both daytime and nighttime conditions, the intensity difference threshold of α has been fixed at 0.3 after trial and error.

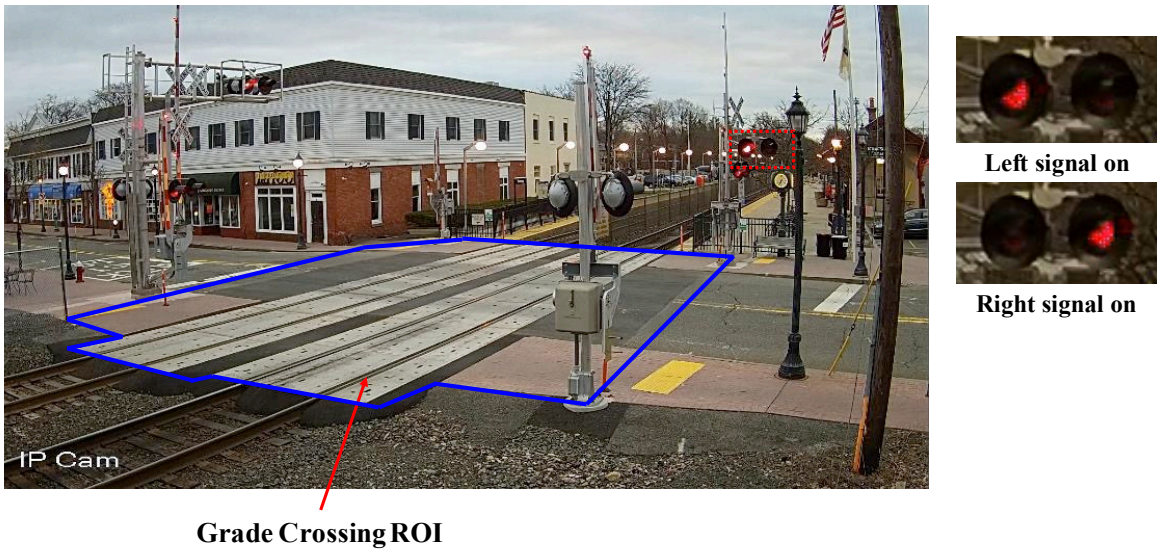

Figure 4. 11. ROI and Identification of Red Signals in Grade Crossing

4.5.3 YOLO algorithm configuration

The computing device, NVIDIA Jetson TX2 developer kit, is able to process one video frame in 0.45 seconds. The video frame reading rate is tuned to 2 frames per second in order to achieve a non-later than real-time processing ability.

Video frames

The size of input images in this YOLOv3 model is first resized to 416 x 416. Therefore, the algorithm needs to resize the original frames while preprocessing. Channels are set to 3, which indicates that this model processes 3-channel RGB input images.

Batch hyper-parameter

The batch parameter indicates the batch size used during training and testing. In this case study, the training batch size is 64 and the test batch size is 1. This means that 64 images are used in one iteration to update the parameters of the neural network and the test only uses 1 image.

Subdivisions

It is challenging for GPU to process a batch size of 64 or more with common memory. Fortunately, Darknet allows the specification of a variable, called subdivision, which processes a fraction of the batch size at one time on the GPU. In this research, the training subdivision is 16 and the testing subdivision is set to 1.

Learning rate

The parameter learning rate controls how aggressively the algorithm should learn based on the current batch of data. Typically, this is a number between 0.01, 0.001, and 0.0001. This research uses 0.001 as the learning rate.

COCO classification

Regarding COCO classification, there are 80 classes in the COCO dataset. This research focuses on 6 of them: 'person', 'bicycle', 'car', 'motorbike', 'bus' and 'truck'.

4.5.4 Trespassing data collection and algorithm validation

Trespassing data collection and preparation

In the raw video data covering two months and one week, over three thousand trespassing events are detected and corresponding video clips are documented. The basic information pertaining to these collected trespasses, such as date and time, or the classifiers of trespassing violators (e.g., pedestrian, car, truck, bus), are recorded automatically by the AI tool. Several fields, such as daylight period and weather conditions, can be recorded via public data sources (e.g., https://weather.com), and traffic volume in terms of vehicles and pedestrians can also be recorded using a computer vision-based algorithm and raw videos.

Table 4. 4. Recorded Fields in Trespassing Database

Field Name	Definition	Type
Year	Time in Year, 2018 and 2019	Numerical
Month	Time in month, April, September, and January	Numerical
Week	Time in week, Monday, Tuesday, Wednesday, Thursday, Friday, Saturday, and Sunday	Categorical
Hour	Time in hour, 0 to 24	Numerical
Weather	Weather conditions, including clear, cloudy, rain, fog, snow	Categorical
Daylight Period	Daylight period conditions, including dawn, day, dusk, dark	Categorical
Pedestrian	Number of pedestrian violators in trespassing event	Numerical
Car	Number of car violators in trespassing event	Numerical
Truck	Number of truck violators in trespassing event	Numerical
Bus	Number of bus violators in trespassing event	Numerical
Motorcycle	Number of motorcycle violators in trespassing event	Numerical
Bicycle	Number of bicycle violators in trespassing event	Numerical
Vehicle	Number of vehicle violators in trespassing event (e.g., car, truck, bus, motorcycle, etc.)	Numerical
Before / After	Violation before train coming or after train passing	Categorical
Gate Angle	Position of gate(s) during trespassing measured by the angle with ground. 0 degree indicates a fully closed gate and 90 degree indicates an open gate.	Numerical
Male	Number of male trespassers	Numerical
Female	Number of female trespassers	Numerical
Gender	Gender of trespasser, male, female, or both	Categorical
Food	Trespasser with food or not	Categorical
Cell	Trespasser with cell phone or not	Categorical
Headphone	Trespasser with headphones or not	Categorical
Violation Way	The way violator violates, including around pedestrian gates, under pedestrian gates, around vehicle gates, under vehicle gates, or other	Categorical
Narratives	Short words to describe the violation event	Text

Further, additional information (e.g., violator gender, gate angle, use of cell phone or headphones) regarding trespassing events may be essential. To automatically detect these, a combination of high-resolution/frame rate cameras and more sophisticated and computationally complex deep learning AI is required. However, on average, around 35 trespassing events are documented in one-day's raw video and manually watching it only takes 6 minutes (=$350\ seconds = \ 35\ clips\ \times 10\ seconds\ per\ clip$), which is only 0.4% of the one-day raw video duration (1,440 minutes). Therefore, the developed AI-aided tool can perform as a decision support tool and the generated video clips can contribute to additional information with efficient usage of railroad resources. Future research can focus on developing advanced functions to record these additional fields in a cost-effective way. Table 4.4 summarizes variables recorded in the trespassing database.

Algorithm validation

In this study, in addition to the raw video data, a grade crossing data supplier manually watched the same video segments from April as the developed system and recorded 407 trespassing events. This data is used to validate the accuracy of the AI-aided trespassing detection tool.

In the AI-based algorithm outputs, 422 trespassing clips are originally detected. After the manual check, 407 of these are validated as true trespasses and 15 are false trespasses. This means that all trespasses manually collected were detected by the developed AI algorithm without any missed detections, while several false detections were generated. Sensitivity and precision are common for computer vision detection in the literature (Le et al., 2016; Alsalam, et al., 2017) and are employed to evaluate the algorithm developed in this research. Sensitivity, measured by the proportion of actual positives

(trespassing events) that are correctly identified, is 100% ($= \frac{407}{407}$), and the precision is 96.4% ($= \frac{407}{407+15}$). Through watching trespassing clips from April, September, and January, some potential reasons behind false positives are extreme weather conditions that affect the video quality (Figure 4. 12. a) and sunlight noises on signal faces (Figure 4. 12. b). Future work would focus on the mitigation of noises from red signals and camera via hardware actions and algorithm enforcement. Only the positive trespasses in the selected location are covered in the following analysis.

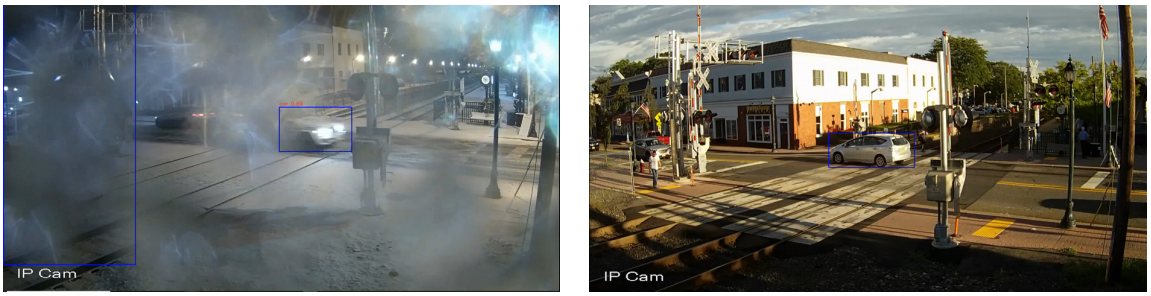

Figure 4. 12. False Detections Due to (a) Extreme Weather and (b) Noises from Sunlight

4.6 Trespassing Safety Risk Analysis with Case Study

4.6.1 Exploratory data analysis overview

With the implementation of the AI-aided algorithm, 3,004 positive trespassing events were captured and recorded in the current database from two-months-and-one-week's worth of raw video data. A detailed summary of the trespassing database is presented in Table 4.5. On average, there were 158 trespassing pedestrians and 74 trespassing vehicles per day in the studied period. In terms of solely the collected traffic volumes, the traffic counts of vehicles have similar values (around 25,000 per week) for

the three time periods selected, while the pedestrian counts have significant differences. September and April have much greater numbers of pedestrians per week (18,000 and 13,000 respectively), which are around one-and-a-half times that in January (around 9,000 per week).

Based upon the number of trespasses (e.g., frequency, pedestrians, and vehicles) per day between different months, April and September 2018 have more frequent daily trespassing events and greater numbers of daily trespass pedestrians and vehicles than January 2019. For example, compared to September 2018, the number of trespass pedestrians per day and the number of trespass vehicles per day decrease 28% ($=\frac{129-180}{180}$) and 33% ($=\frac{59-88}{88}$) in January 2019, respectively. One potential reason is that winter is expected to involve fewer outdoor activities. Based on the collected traffic information, the total number of pedestrians at this location in January (38,792) is half of that in September (73,100). In the previous trespassing accident study, Savage (2016) similarly observed that fewer trespassing accidents occurred during winter months. Another potential justification for the majority declining trend in the number of trespass vehicles is a safety action taken by the New Jersey Department of Transportation (NJDOT). In November 2018, the anti-gridlock box design, a road marking meaning DO NOT BLOCK, was painted at the intersection between the highway and roadway. This is consistent with the results showing that the number of trespass vehicles per 1,000 vehicle traffic counts in January (19) is significantly smaller than that in April (23) or September (25), as represented in Table 4.5. In particular, the pedestrian trespass rate, defined as the number of trespassing pedestrians per 1,000 pedestrians, in January (103) is higher than that in September 2018 (74). This discrepancy discloses that the relatively smaller number of daily trespass pedestrians in

January 2019 mainly results from the much lower pedestrian volume in the cold season, which was also pointed out by Savage (2016). However, the likelihood of each pedestrian trespassing this grade crossing in the colder weather would be greater than during warmer seasons. To the authors' knowledge, no prior study has investigated the trespass pedestrian rate during colder weather, potentially as a result of limited data. However, through the study of pedestrian street crossing behavior and safety in Toronto under different weather conditions, Li and Fernie (2010) concluded that pedestrians were more likely to violate the "Don't Walk" signal and became riskier in inclement winter weather.

Table 4. 5. Summary of Trespassing Events in Two Months and One Week

	April 19-25, 2018		September, 2018		Janaury, 2019		Sum	
	Count	Percentage	Count	Percentage	Count	Percentage	Count	Percentage
Total Number of Trespassing	407	100%	1,614	100%	983	100%	3,004	100%
Number of Trespassings per Day	58		54		32		44	
By Daylight (Total Number)								
Dark	35	8.5%	121	7.5%	443	45.1%	602	18.0%
Dawn	25	6.2%	95	5.9%	30	3.0%	152	4.6%
Day	309	75.8%	1,317	81.6%	423	43.1%	2,077	62.3%
Dusk	39	9.5%	81	5.0%	87	8.8%	210	6.3%
By Train Occurance (Total Number)								
Before Train Passing	125	30.6%	455	28.2%	353	36.0%	944	31.1%
After Train Passing	282	69.4%	1,159	71.8%	629	64.0%	2,097	68.9%
Total Number of Trespass Pedestrians	1,342	100%	5,404	100%	3,997	100%	10,743	100%
Number of Trespass Pedestrians per Day	192		180		129		158	
Number of Trespass Pedestrians per 1,000 Pedestrians	105		74		103		86	
By Gender (Total Number)								
Female	450	33.5%	1,640	30.4%	1,167	29.2%	3,257	30.3%
Male	892	66.5%	3,764	69.6%	2,831	70.8%	7,486	69.7%
Total Number of Trespass Vehicles	577	100%	2,635	100%	1,822	100%	5,033	100%
Number of Trespass Vehicles per Day	82		88		59		74	
Number of Trespass Vehicles per 1,000 Vehicles	23		25		19		22	
By Vehicle Type (Total Number)								
Car	511	88.7%	2,289	86.9%	1,691	92.8%	4,491	81.8%
Bicycle	65	11.3%	285	10.8%	84	4.6%	434	7.9%
Truck	0	0.0%	42	1.6%	42	2.3%	84	1.5%
Bus	0	0.0%	14	0.5%	3	0.2%	17	0.3%
Motorcycle	0	0.0%	6	0.2%	2	0.1%	8	0.1%
Total Traffic Count of Pedestrians	12,804		73,100		38,792		124,695	
Total Traffic Count of Vehicles	25,233		105,811		95,676		226,720	

4.6.2 Distribution by daylight period

Assuming a 24-hour cycle, the majority of overall trespass events occurred during the daytime (62.3%). In particular, the percentages of trespassing events during the daytime are over 75% for both April and September. However, January data shows close trespassing frequency in daytime, as compared to dark time. These results are related to daylight period lengths and traffic volume in different seasons. Based upon the daylight periods and night periods of these months in the selected location, daylight lengths in April and September are around 13 hours, which is over one-and-a-half times the length of night periods in these two months (around 8 hours). However, January has a longer night period (11.20 hours) than daylight period (9.55 hours). Regarding traffic volume, around 80% of pedestrians and 74% of vehicles traveled through this grade crossing during the daylight period, while night periods accounted for only 10% of pedestrians and 15% of vehicles for April and September combined. However, in January, only around half of pedestrian and vehicle traffic occurred during daylight periods and nights involved 30% of traffic volumes. More detailed distributions are demonstrated in the following heat map.

4.6.3 Distribution before or after train passes

Table 4.5 shows that 68.9% of trespassing events at this grade crossing occurred after the train passed through the grade crossing, whereas only 31.1% of trespassing events occurred before the train passed. This shows that most trespassing incidents at this location occur while the gates are ascending. Prior study revealed that 50% of respondents believed it was safe to trespass (Silla and Luoma, 2012). This could indicate that people who trespass in a selected location may have a false sense of security, assuming that it is safe to trespass

after the train passes. However, the selected grade crossing has multiple tracks and several videos show the second train coming on the adjacent tracks right after the first one. Overall, the data shows that the main problem is the majority of people trespassing after the train passes. To ensure their own safety, trespassing violators should wait until the gates are fully open. This can also serve as one potential education material in safety improvement in New Jersey and other areas.

4.6.4 Distribution by gender

Out of 10,743 trespass pedestrians, 7,486 (69.7%) of them are deemed male, while only 30.3% of trespass pedestrians are female, per the manual identifications. Similar conclusions were also drawn in previous studies. In investigations of trespasses, George (2008) and Silla and Luoma (2012) pointed out that the vast majority of railroad-trespasser accident fatalities are males.

Meanwhile, the distribution of men and women walking through this grade crossing is also potentially one key factor. Although there is a lack of gender distribution in the grade crossing uses and the computational cost of automatic recognition of pedestrians' genders with AI is considerable, the population distribution by gender in this county is publicly available and there are more women than men in general. Based on the statistics from the U.S. Census Bureau (2019), this county has 452,201 males (48%) and 481,371 females (52%). Overall, men are more than twice as likely to trespass at this grade crossing as female pedestrians in general, while no clear evidence supports that gender difference significantly contributes to skewing the results towards more men trespassing.

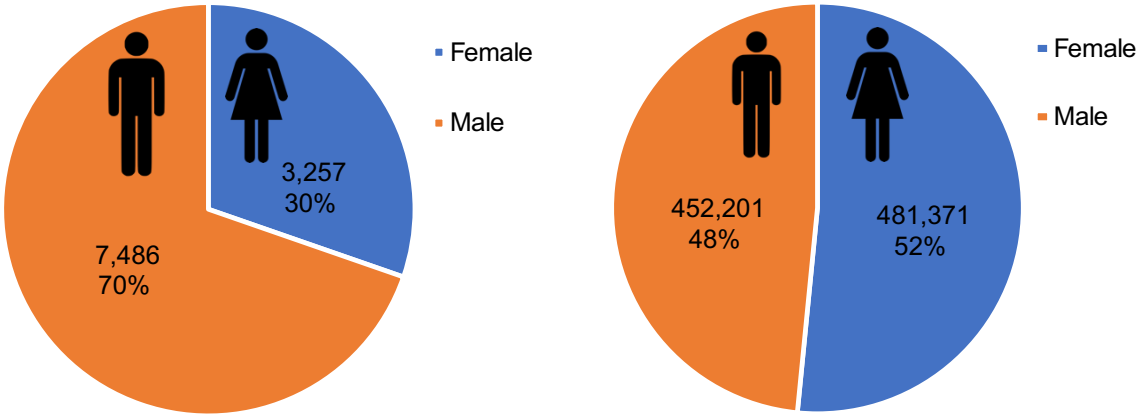

(a) Trespassers (b) Local County Population

Figure 4. 13. Distribution of Male vs. Female in (a) Trespassers and (b) Local County (U.S. Census Bureau, 2019)

4.6.5 Distribution by vehicle type

The distribution of trespass vehicles shows that cars are the most common vehicle type, accounting for over 80% of all trespassing vehicles. Bicycles are the second largest trespassing vehicle type in the recorded trespassing events. Although only 17 buses are detected and recorded in grade crossing violations, each trespassing bus represents a significant risk, particularly school buses providing services for three schools located around this grade crossing.

4.6.6 Distribution by gate angle and before/after train passes

Figure 4. 14 shows the angle of the gate as trespassing incidents occurred before the train crossed. From the value of the gate bar's "Open" angle, it is clear that many trespassers were already crossing when the warning lights activated. The graph also shows that a large portion of travelers were willing to trespass as the gates were closing, likely considering it safe at that point. Furthermore, 33 trespassers exhibited dangerous behavior

by crossing as the gate was closed before the train arrived. This population is particularly worrisome, as they are the most probable trespassers to be struck by a train.

This graph shows the angle of the gate as trespassing incidents occurred after the train crossed. Here, it is evident that trespassers are in a rush to cross the tracks after the train passes, as there is a clear jump in violations at 31-60 degrees. While trespassers may believe it safe, it is not. The Ramsey grade crossing contains two tracks. This means that while one train may have passed, another train may be arriving on the adjacent tracks. Trespassing violators should wait until the gates are fully open, to completely ensure their safety.

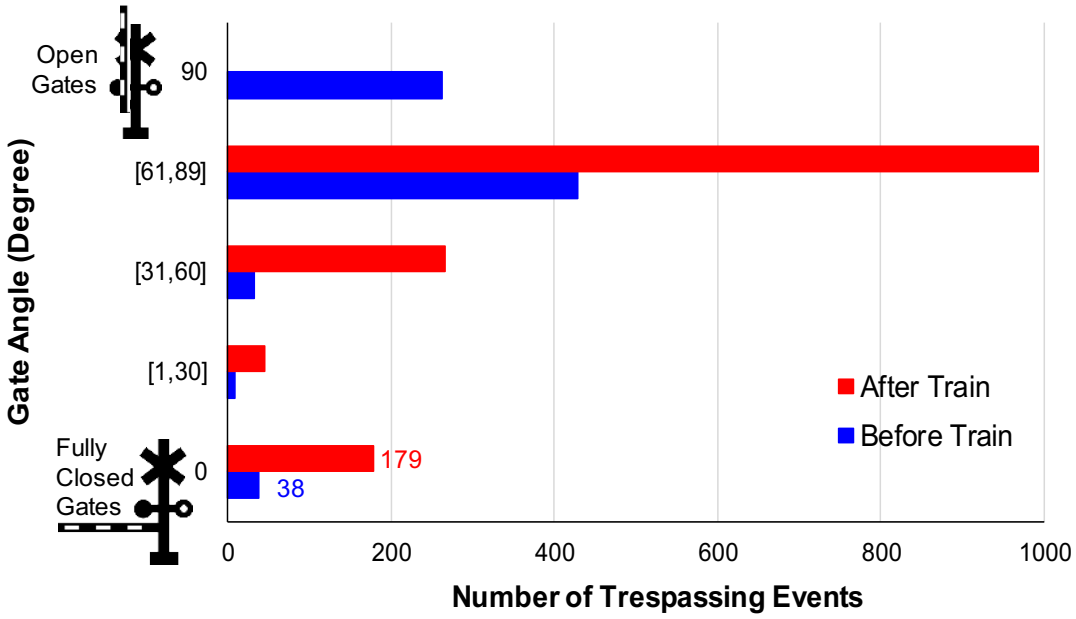

Figure 4. 14. Distribution of Trespassing Events by Gate Angles and Before/After Train Passes

The charts above exhibit violator behavior in differing weather conditions. When there was rain, fewer violators crossed the gate when it lowered to an angle below 60 degrees, compared to clearer weather patterns. This implies that people are more cautious about trespassing across the grade crossing during worse weather conditions. Rain understandably increases the risk of slipping on the tracks, cars skidding, and other unforeseeable consequences. Violators showed that they understood the riskier nature of trespassing in poor weather and chose to wait rather than take the risk.

4.6.7 Distribution by time of the day and day of the week

Frequencies of Trespass, Trespass Pedestrian, and Trespass Vehicle

An in-depth analysis of the distributions of trespasses by the time of the day and the day of the week is conducted. Three heatmaps in Figure 4. 15 show a breakdown of the number of trespassing events, the number of trespassing pedestrians, and the number of trespassing vehicles in a one-hour interval, respectively. Three main findings are concluded below:

- In terms of the hour of the day, 5 PM – 6 PM involves the largest proportion of trespassing events (12%), trespassing pedestrians (18%), and trespassing vehicles (13%). For a broader time period, a majority of trespassing events occurred between 3 PM and 7 PM, involving larger numbers of trespassing vehicles and pedestrians. This trend is consistent with a previous study, in which the FRA (2018d) investigated the percentage of trespass fatalities and concluded that the highest percentage of trespass fatalities occur in the evening commute hours, between 4:00 pm and 8:00 pm (23%). In this case study, one hypothesis is that in

the timeframe from 4 PM to 7 PM, many commuters are making their way back to their respective homes by train. Since two major parking lots are located on the west side of the rail track and New York-bound trains also move on the west track of this double-track line, most commuters can take the train from the same side in the morning rush hour and do not need to walk through intersections. On the other hand, during evening commute hours, most people arrive at the train station and need to walk through this grade crossing to get to the parking lots.

- In terms of day of the week, Saturday has the greatest number of trespassing events (21%), trespassing pedestrians (24%), and trespassing vehicles (21%). A similar conclusion was also drawn in previous studies regarding trespassing accidents resulting in fatalities. The FRA (2018) stated that Saturday accounts for the highest percentage of trespass fatalities (17%) and the trespass distribution may not strictly follow common work and commuting schedules.

Moreover, the overall trend of trespassing vehicles is identical to trends of trespassing events in general. It indicates that the number of trespassing vehicles per violation event has insignificant variations. In terms of trespassing pedestrians per event, each trespassing event from 5 PM to 7 PM would involve a larger group of violating pedestrians than any other timestamp. The Kolmogorov–Smirnov test (KS test) is used here to validate the similarity of these three continuous distributions. The P-value of trespassing events and trespassing pedestrians is much smaller than 0.05, which indicates that there is a significant difference between these two distributions, while the KS test for trespassing events and trespassing vehicles shows the two have close distributions (P-value = 0.06943).

Day/Time	0:00	1:00	2:00	3:00	4:00	5:00	6:00	7:00	8:00	9:00	10:00	11:00	12:00	13:00	14:00	15:00	16:00	17:00	18:00	19:00	20:00	21:00	22:00	23:00	Sum
Monday	2	1	2	0	0	1	1	3	16	9	15	8	24	25	37	7	16	11	9	3	6	2	9	3	207
Tuesday	1	1	0	0	0	5	8	30	22	14	26	25	34	30	31	52	42	47	19	22	28	9	5	6	454
Wednesday	3	7	1	0	2	1	11	25	30	18	31	17	31	30	31	43	36	55	35	18	24	14	9	7	475
Thursday	5	5	0	0	2	5	15	28	26	19	18	23	19	31	27	44	34	74	48	20	23	18	10	10	501
Friday	1	6	1	0	1	0	19	31	25	23	23	24	20	31	19	40	16	63	35	22	26	9	0	11	442
Saturday	3	12	6	2	2	1	9	32	42	26	19	33	37	36	22	55	53	100	49	51	19	10	6	5	628
Sunday	3	2	1	0	0	0	2	10	22	10	32	12	27	19	47	7	31	10	28	5	10	1	11	9	296
Sum	18	34	11	2	7	13	64	157	182	118	162	140	190	199	212	250	227	361	222	140	134	62	49	50	3004

(a) Trespassing Events

Day/Time	0:00	1:00	2:00	3:00	4:00	5:00	6:00	7:00	8:00	9:00	10:00	11:00	12:00	13:00	14:00	15:00	16:00	17:00	18:00	19:00	20:00	21:00	22:00	23:00	Sum
Monday	6	3	4	0	0	1	1	25	34	31	67	25	82	104	108	7	71	34	13	15	13	1	25	10	684
Tuesday	1	1	0	0	0	10	19	92	52	22	43	55	61	65	95	111	76	209	153	160	104	36	21	12	1398
Wednesday	6	13	1	0	0	3	21	98	76	49	70	33	47	46	96	116	85	310	283	110	110	49	21	15	1656
Thursday	4	7	0	0	6	7	30	77	58	52	27	43	27	59	55	126	83	317	350	219	101	95	27	24	1794
Friday	9	7	1	0	6	0	46	77	92	42	56	79	46	128	52	102	31	384	230	163	92	44	0	64	1751
Saturday	6	34	22	4	1	3	16	74	99	82	46	86	70	93	92	271	162	604	305	295	82	47	16	43	2555
Sunday	24	9	3	0	0	0	1	15	47	16	83	56	80	79	157	19	67	47	74	12	30	3	44	37	905
Sum	56	76	33	4	13	25	135	458	458	294	391	377	412	574	655	753	574	1905	1409	974	531	276	154	205	10743

(b) Trespassing Pedestrians

Day/Time	0:00	1:00	2:00	3:00	4:00	5:00	6:00	7:00	8:00	9:00	10:00	11:00	12:00	13:00	14:00	15:00	16:00	17:00	18:00	19:00	20:00	21:00	22:00	23:00	Sum
Monday	3	1	2	0	0	1	3	7	25	20	41	17	26	43	75	10	28	23	30	6	13	1	11	6	392
Tuesday	1	0	0	0	0	5	11	47	32	28	45	40	63	56	53	82	64	60	39	49	40	13	6	3	737
Wednesday	3	6	0	0	3	2	10	35	53	35	44	31	36	51	58	83	82	110	69	30	40	14	14	5	814
Thursday	5	5	0	0	1	3	15	42	52	38	34	30	20	52	44	85	77	127	91	36	39	16	15	11	838
Friday	1	5	1	0	2	0	25	39	39	30	31	32	30	49	26	82	28	133	66	33	25	13	0	11	701
Saturday	6	13	7	1	3	3	7	70	65	30	31	51	75	52	49	94	97	171	82	77	28	16	8	6	1042
Sunday	6	2	0	0	0	0	6	17	43	16	53	14	41	32	97	14	51	11	59	2	11	0	18	16	509
Sum	25	32	10	1	9	14	77	257	309	197	279	215	291	335	402	450	427	635	436	233	196	73	72	58	5033

(c) Trespassing Vehicles

Figure 4. 15. Trespass Distribution by Time and Day

Rates of Trespass Pedestrian and Trespass Vehicle

Figure 4. 16 illustrates the distribution of the trespassing pedestrian rate and trespassing vehicle rate by the hour of the day and day of the week. The trespassing pedestrian rate is defined as the number of trespassing pedestrians per 1,000 pedestrians in this location and similarly, the trespassing vehicle rate is defined as the number of trespassing vehicles per 1,000 vehicles. For the time of day, each hour within daylight

periods (e.g., 7 AM-8 PM) has a similar trespassing rate for pedestrians and vehicles. This indicates that although evening time has rush traffic and greater trespassing frequency, the trespassing pedestrian rate and trespassing vehicle rate per unit traffic volume (1,000 pedestrians and vehicles, respectively) mostly do not have significant variations. However, 1 AM-2 AM on Saturday has an extremely large trespassing pedestrian rate (344 per 1,000 pedestrians). This may result from relatively small population sizes in both trespassing events and pedestrian traffic volume during this time slot. Meanwhile, it is also noted that there is a pub adjacent to the grade crossing which closes at 2 AM on Saturdays. This may be a potential reference for trespassing prevention education.

Day/Time	0:00	1:00	2:00	3:00	4:00	5:00	6:00	7:00	8:00	9:00	10:00	11:00	12:00	13:00	14:00	15:00	16:00	17:00	18:00	19:00	20:00	21:00	22:00	23:00	
Monday	51	10	10	0	0	5	9	95	58	31	42	14	43	59	59	5	57	12	7	10	19	5	127	41	44
Tuesday	11	5	0	0	0	30	30	90	60	27	40	43	47	53	45	55	53	76	77	137	152	63	66	85	94
Wednesday	67	46	10	0	0	9	29	72	67	53	85	34	52	50	70	84	64	99	128	83	151	110	89	129	117
Thursday	5	10	0	0	17	11	39	45	42	50	28	39	24	55	31	58	46	77	111	117	125	161	84	111	91
Friday	37	30	6	0	55	0	37	41	49	23	31	48	36	113	26	39	16	96	81	99	118	98	0	114	85
Saturday	39	344	92	59	78	17	31	58	64	54	28	47	42	71	37	89	83	146	104	142	73	71	40	92	122
Sunday	104	32	9	0	0	0	3	24	60	17	82	40	43	42	64	9	42	11	21	7	34	6	142	100	48
	29	33	16	3	12	10	30	56	56	36	44	38	41	62	47	51	51	76	75	87	93	77	77	97	86

(a) Trespassing Pedestrian Rate per 1,000 Pedestrians

Day/Time	0:00	1:00	2:00	3:00	4:00	5:00	6:00	7:00	8:00	9:00	10:00	11:00	12:00	13:00	14:00	15:00	16:00	17:00	18:00	19:00	20:00	21:00	22:00	23:00	Sum
Monday	7	2	2	0	0	2	7	12	23	19	26	9	14	24	36	5	13	9	14	3	10	1	16	13	13
Tuesday	3	0	0	0	0	7	11	36	20	19	28	21	35	31	28	32	25	19	16	26	32	12	10	9	23
Wednesday	9	15	0	0	6	3	13	36	44	26	31	20	23	31	35	37	34	37	30	17	31	12	21	14	27
Thursday	8	12	0	0	4	4	14	28	29	24	22	18	11	30	25	41	35	37	33	17	28	11	17	20	25
Friday	2	10	3	0	14	0	20	27	24	20	21	21	18	32	16	34	11	41	26	16	18	10	0	19	21
Saturday	10	20	10	3	10	4	5	41	34	17	17	28	42	29	25	32	35	50	30	33	17	10	8	8	27
Sunday	8	3	0	0	0	0	7	11	28	9	32	7	20	16	41	6	21	4	22	1	8	0	19	23	14
Sum	7	9	3	0	4	3	11	28	29	19	25	18	23	27	30	27	25	29	25	16	20	8	13	16	21

(b) Trespassing Vehicle Rate per 1,000 Vehicles

Figure 4. 16. Trespass Rate Distribution by Time and Day in (a) Pedestrians and (b) Vehicles

4.7 Trespassing Safety Risk Mitigation Countermeasures

For a case study of one grade crossing in New Jersey, the developed AI-aided automated trespassing detection technology has processed two months and one week of raw video data efficiently and with an acceptable level of accuracy. On average, there are around 45 unsafe trespassing acts occurring in this location, which sees over 100 train passes every day. The analysis of these 3,004 trespassing events presents the distribution of key factors, such as gender, hour of the day, day of the week, violation type, before or after train passes, as well as their correlations. The results presented in this research are consistent with previous studies, and with newly identified trends in this location-specific case. In addition to highway-rail grade crossing trespassing detection, the developed AI-aided tool can also detect trespasses at rights-of-way without red signal identification as a prerequisite.

While there are a limited number of false positives in the application of the developed AI-aided tool, the collected trespassing events and preliminary analysis can be informative for proactive safety actions in engineering, education, and law enforcement (3 E's) and could even save lives. The statistical valuing of a life at over $9 million, a value employed by the railroad industry (FRA, 2016b), justifies the significance of such safety practices. Below are three trespassing mitigation strategies per the analysis of the collected trespassing events.

4.7.1 Law enforcement at peak trespassing hours

To reduce the number of trespassers in this location through law enforcement, it is recommended to post police officers at the railroad crossing during peak trespassing hours.

Having police officers at the crossing can deter pedestrians and vehicles from trespassing. According to previous explanatory analyses, most trespasses occurred from 3 PM to 7 PM on Thursday and Saturday (24% of trespassing pedestrians and 17% of trespassing vehicles for the whole week). Specifically, these 8-hours of police officer duty per week could put 177 pedestrians and 89 vehicles expected to be trespassers within view of law enforcement, and a majority of them would be anticipated to behave compliantly under these conditions. Considering that more trespasses occur during warm and clear weather, more law enforcement could be placed at the grade crossing during summer and/or clear days. With an increased budget, law enforcement could be present from 3 PM - 7 PM for the whole week, which would account for and possibly prevent around half of all trespassing pedestrians and vehicles.

4.7.2 Engineering with pedestrian channelization

At this location, some pedestrians can go around or under the gates and 217 trespasses were also observed with fully closed gates (horizontal gates). This population is particularly worrisome as they are the most probable trespassers to be struck by a train. The usage of a swing gate at the four corners would prohibit pedestrians from crossing in an unsafe way and provide a set route for them to follow (Figure 4. 17). When the red signal comes on, the gates will lock from the outside of the tracks so that people cannot enter. The gates will also have a push-bar on the inside (track side) that will allow pedestrians who are already on the tracks when the red signal activates to exit at all times. This will also force pedestrians to look at the tracks before they cross to ensure it is safe. An example of a swing gate is shown below. The FRA (2008) concluded that the use of

swing gates in Salt Lake City's light rail system has reduced incidents related to passenger inattention to trains around transit stations. However, swing gates are more beneficial in pedestrian-only crossings, while in this selected crossing, they cannot absolutely prevent all trespassing pedestrians. Instead, swing gates may result in more trespassing pedestrian violations via the gaps between or under vehicle gates. Thus, the installation of longer automatic gate arms and vehicle gate skirts can serve as supplementary solutions. A previous study (Chase et al., 2013) has proven that pedestrian gate skirts can reduce the number of pedestrian violations while the gates are descending and horizontal. Similarly, vehicle gate skirts are expected to prevent pedestrians who avoid existing pedestrian gate skirts and choose to violate by going under vehicle gates. These additional engineering actions can also contribute to the prevention of trespassing pedestrians and even trespassing vehicles.

(a) (b) (c)

Notes: Images: (b) California Public Utilities Commission, Pedestrian-Rail Crossings in California (c) Chase et al., 2013.

Figure 4. 17. Gate Options (a) Prototype Gate at the Selected Location; (b) Swing Gate in California; and (c) Gate Arm and Skirt at Knoxville, TN

4.7.3 Target-specific education

The analysis of collected trespassing events provides a clear reference for education among school bus drivers and local authorities, as well as education actions during winter and at the adjacent pub. In the studied period, there were several school buses violating red signals at the grade crossing (Figure 4. 18. a). This is a serious issue since two schools are located near the grade crossing and school buses regularly travel through it. These noncompliant actions put young students at high risk. Besides, the violations might have a potentially adverse impact on school students, in particular the ones riding regularly trespassing buses.

The trespassing data included a total of thirteen police car violations and one ambulance violation (Figure 4. 18. b and c). It is important to emphasize that incoming trains cannot make positive stops for local authorities, even in the case of local emergencies. It is the police's responsibility to protect the people; however, they should not be doing it in a way that puts their own lives at risk. One recent minor accident occurred when a Texas deputy's vehicle was hit by a train while responding to a call (FOX NEWS, 2019). With basic education regarding grade crossing safety, officers are able to strictly follow the rules, which can help prevent unnecessary accidents and save lives. The higher trespassing pedestrian rate in January discloses that on average, pedestrians walking through this location have a greater likelihood of trespassing in colder seasons, despite the traffic volume being lower. Thus, more safety education can be delivered in winter to reduce the possibility of individual violations. Moreover, the previous analysis also acknowledged that 1 AM-2 AM on Saturday has the greatest trespassing pedestrian rate, which is potentially related to an adjacent pub which closes at 2AM. Specialized education can be

provided in cooperation with this pub via educational flyers, warning information on the front-door board, and verbal reminders from waiters, addressed particularly to drunk people at closing time.

(a)

(b)

(c)

Notes: Low authority vehicles (e.g., police cars and ambulance) are manually masked.

Figure 4. 18. Trespassing with (a) School Bus; (b) Police Cars; and (c) Ambulance

4.8 Discussions and Conclusions

This research presents a state-of-the-art AI-aided methodology with high-accuracy fast-processing railroad trespassing detection capabilities for both highway-rail grade crossings and rights-of-way. The applications of YOLO and computer vision in trespassing detection have been validated in around 1,632 hours of video with reasonable accuracy. Around 3,000 trespassing violations are detected and recorded during the analyzed period. In the location-specific case study, the collected trespassing database discloses that a majority of trespassing events occurred from 4 PM-7 PM, on Saturday out of all days of the week, and after train passing. In particular, 1 AM-2 AM on Saturday has the largest trespass pedestrian rate. Although the number of males and females are identical in the local area, male trespassers are twice as likely to trespass as their female counterparts. Accordingly, potential mitigation solutions are proposed from engineering, enforcement, and education perspectives. Although the evaluations of proposed countermeasures are limited to accessible data and ongoing collaboration, the number of trespass vehicles per day can support the follow-up evaluation of one engineering action conducted in November 2018. Compared to September 2018, the number of trespass vehicles per day decreased 33% ($=\frac{59-88}{88}$) in January 2019. Based on the collected traffic information, the total number of vehicles at this location in January (95,676) is almost identical to the number in September (105,811). One potential justification for the majority declining trend in the number of trespass vehicles is a safety action taken by the New Jersey Department of Transportation (NJDOT). In November 2018, the anti-gridlock box design, a road marking meaning DO NOT BLOCK, was painted at the intersection between the highway and roadway. This is also consistent with results showing that the number of trespass vehicles per 1,000 vehicle

traffic counts in January (19) was significantly smaller than that in April (23) or September (25), as represented in Table 4. 5 **错误!未找到引用源。**. Meanwhile, it is acknowledged that additional factors may have potential impact on these differences but cannot be investigated due to data limitation. More follow-up quantitative assessments of proposed countermeasures can be conducted in future research with sufficient data.

Overall, this AI-based trespassing detection can contribute to harnessing the potential of big video data to obtain a better understanding of real-world trespassing behaviors and characteristics with the collection of near-miss events. The development of informed risk-mitigation strategies can enhance the safety of rail passengers and road users and aid in the relief of congestion by reducing the number of accidents and incidents.

Firstly, future work would focus on accuracy promotion by mitigating noise from sunlight on signal faces and extreme weather conditions. For example, the identification of closing grade crossings can involve decreasing gates as one additional trigger. Secondly, in addition to the use of a fixed camera at a grade crossing or along right-of-way, a forward-facing camera in the locomotive can also be employed for trespassing prevention. With the camera mounted in the locomotive, trespassing events along the rail line can be detected via the developed AI-aided tool and recorded in a database that would potentially advance understanding of human factors in railroad safety research.

CHAPTER 5

FUTURE RESEARCH AND INSIGHTS

This chapter highlights several directions for future work and research activities that are related to the subjects covered in this dissertation.

5.1 Accident Prevention in Obstacle and Intrusion Detections

A key part of YOLO performance is the training dataset which allows it to recognize objects. The developed AI algorithm focuses on the detection of pedestrians and vehicles (e.g., cars, trains, trucks, buses) at a grade crossing or right-of-way. The object classes are pre-defined in the AI algorithm with the COCO dataset, which consists of many labeled images of everyday scenes, built for use in object recognition research. It was selected because of its depth (330,000 Images), diversity (80 object categories) and timeliness due to its continual growth and refinement.

In addition to trespassing behaviors, there are also other intrusion behaviors (e.g., livestock) and obstacles (e.g., fallen cargo from trucks, fallen trees). Per the FRA REA database, there were 1,106 FRA-reportable obstruction accidents from 2000 to 2017 in the United States. There are three major types of obstructions and their frequencies are summarized below.

Table 5. 1. FRA-Reportable Obstruction Accidents from 2000 to 2017

FRA Cause Code	Frequency	Descriptions
M402	279	Object or equipment on or fouling track (motor vehicle – other than highway-rail crossing)
M403	5	Object or equipment on or fouling track (livestock)
M404	310	Object or equipment on or fouling track- other than above

5.2 Trespassing Risk Mitigation Research Integrated with Intelligent Transportation Systems

An increase in railroad freight shipments makes the rail network operate at continuously higher loads and increases the system's exposure factor. These developments emphasize the need for automatic continuous monitoring of the rail network with the capability of notifying the train operator and/or railroad dispatcher of any impending dangers and the ability of automatically controlling the locomotive. PTC systems are integrated with the command, control, communications, and information systems for controlling train movements with safety, security, precision, and efficiency. PTC has the potential to be deployed across the rail industry, which uses about 21,000 locomotives throughout the country. However, it would not prevent incidents due to trespassing on railroads' right-of-way or at highway-rail grade crossings.

Although preventing grade-crossing incidents is not specifically addressed in the PTC mandate of RSIA08, CRS (2018) pointed out that this could be achieved technically within the PTC framework by installing sensors at crossings that would engage the brakes of an oncoming train if a crossing gate is not working properly or if a vehicle is detected on the tracks. While this may require further investment and costs on the part of the railroads, it may also offer more significant gains in terms of safety than just train collision

prevention. Therefore, Congress has requested that the FRA study the effectiveness of PTC technology in preventing grade-crossing incidents once PTC is implemented (FAST Act, 2015). A similar introduction of this potential implementation was presented as one of the major critical issues and research opportunities in the age of PTC by Zhang et al. (2018b). Peters and Frittelli (2012) demonstrated that PTC can be integrated with highway Intelligent Transportation Systems (ITS) to reduce highway-rail grade crossing risks. In particular, PTC-connected vehicle technology, with which trains and cars would be able to share location information, movement information, and communicate with each other, could be one possible future direction for research. Additionally, the FRA (2017) worked with a variety of organizations to develop the standards for the deployment of grade crossing warnings in PTC systems. In summary, more research is needed to develop and implement ITS technology for grade-crossing safety improvement in the age of PTC systems and ITS.

REFERENCES

Ahmad, S.S., Mandal, N.K., Chattopadhyay, G. & Powell, J. (2013). Development of a unified railway track stability management tool to enhance track safety. Proceedings of the *Institution of Mechanical Engineers, Part F: Journal of Rail and Rapid Transit*, 227(5), 493-516.

Alsalam, B.H.Y., Morton, K., Campbell, D. & Gonzalez, F. (2017, March). Autonomous UAV with vision based on-board decision making for remote sensing and precision agriculture. In *2017 IEEE Aerospace Conference* (1-12). IEEE.

Al-Shanini, A., Ahmad, A., & Khan, F. (2014). Accident modelling and analysis in process industries. *Journal of Loss Prevention in the Process Industries*, 32, 319-334.

Amtrak (2012). Standard signal plan braking distance curves. Office of the Deputy Chief Engineer C&S, February 1, 2012.

Amtrak (2017). Amtrak fact sheet, fiscal year 2017, Amtrak Government Affairs, November 2017.

Amtrak (2018). Amtrak FY17 ridership. https://media.amtrak.com/wp-content/uploads/2015/10/FY17-Ridership-Fact-Sheet-Final.pdf. Accessed in June 2018.

Amtrak (2019). The Northeast Corridor. https://nec.amtrak.com/. Accessed in July 2019.

American Public Transportation Association (APTA) (2015). Positive Train Control: an assessment of PTC implementation by commuter railroads. Washington, DC.

Anderson, D. (1995). Study of the sensitivity of predicted stopping distances to changes to input parameters. Transportation Technology Center, Association of American Railroads, Pueblo, Colorado.

Anderson, R. & Barkan, C. (2004). Railroad accident rates for use in transportation risk analysis. Transportation Research Record: *Journal of the Transportation Research Board*, (1863), 88-98.

Association of American Railroads (AAR) (2014). PTC implementation: The railroad industry cannot install PTC on the entire nationwide network by the 2015 deadline.

Association of American Railroads (AAR) (2017). Positive Train Control. Washington, DC.

Aven, T. & Renn, O. (2009). On risk defined as an event where the outcome is uncertain. *Journal of Risk Research*, 12(1), 1-11.

Austin, R.D. & Carson, J.L. (2002). An alternative accident prediction model for highway-rail interfaces. *Accident Analysis & Prevention*, 34(1), 31-42.

Australian Transport Safety Bureau (2008). Analysis, causality and proof in safety investigations. Aviation Research and Analysis Report AR-2007-053. Australian Transport Safety Bureau, Canberra City.

Bagheri, M., Saccomanno, F., Chenouri, S. & Fu, L. (2011). Reducing the threat of in-transit derailments involving dangerous goods through effective placement along the train consist. *Accident Analysis & Prevention*, 43(3), 613-620.

Barkan, C., Tyler Dick, C. & Anderson, R., 2003. Railroad derailment factors affecting hazardous materials transportation risk. Transportation Research Record: *Journal of the Transportation Research Board*, (1825), 64-74.

Beck, A., Bente, H., & Schilling, M. (2013). Railway Efficiency. Railway efficiency. *International Transport Forum*, No. 2013-12.

Boston Region Metropolitan Planning Organization (2012). MBTA Commuter Rail Passenger Count Results. Boston, MA.

Brand, D., Kiefer, M. R., Parody, T. E., & Mehndiratta, S. R. (2001). Application of benefit-cost analysis to the proposed California high-speed rail system. *Transportation Research Record,* 1742(1), 9-16.

Branford, K., Hopkins, A., & Naikar, N. (2009). Guidelines for AcciMap analysis. *In Learning from High Reliability Organisations.* CCH Australia Ltd.

Caird, J.K. (2002). Transportation Development Centre (Canada), University of Calgary, Cognitive Ergonomics Research Laboratory. A Human Factors Analysis of Highway-Railway Grade Crossing Accidents in Canada. Transportation Development Centre, Montreal.

Catalano, A., Bruno, F.A., Pisco, M., Cutolo, A. & Cusano, A. (2014), May. Intrusion detection system for the protection of railway assets by using fiber Bragg grating sensors: a case study. In *2014 Third Mediterranean Photonics Conference* (1-3). IEEE.

Chase, S.G., Gabree S. H., & DaSilva, M. (2013). Effect of Gate Skirts on Pedestrian Behavior at Highway-Rail Grade Crossings. DOT/FRA/ORD-13/51, Washington DC.

Congressional Research Service (CRS), 2018. Positive Train Control (PTC): overview and policy issues. R42637, Washington DC.

Chadwick, S.G., Zhou, N. & Saat, M.R. (2014). Highway-rail grade crossing safety challenges for shared operations of high-speed passenger and heavy freight rail in the US. Safety Science, 68, 128-137.

Chauvin, C., Lardjane, S., Morel, G., Clostermann, J. P., & Langard, B. (2013). Human and organisational factors in maritime accidents: Analysis of collisions at sea using the HFACS. *Accident Analysis & Prevention*, 59, 26-37.

Checkland, P. (1981) Systems Thinking, Systems Practice. John Wiley & Sons, New York, 1981.

Code of Federal Regulations (CFR) (2010). Transportation. Title 49 Code of Federal Regulations, Part 229, 234, 235, 236.

Congress of the United States of America (2008). Rail Safety Improvement Act. Washington DC, Public Law, 110-432.

Congress of the United States of America (2015a). Fixing America's Surface Transportation Act (FAST Act). Washington DC, H.R. 22.

Congress of the United States of America (2015b). Positive Train Control Enforcement and Implementation Act of 2015. Washington DC. H.R. 3651.

Congressional Research Service (CRS) (2018). Positive Train Control (PTC): overview and policy issues. R42637, Washington DC.

Coplen, M.K. (1999). Compliance with railroad operating rules and corporate culture influences: results of a focus group and structured interviews (No. DOT/FRA/ORD-99/09). United States. Federal Railroad Administration.

Cortez, J. (2016). Modern bumper might have mitigated September train crash. http://www.daily-chronicle.com/2016/12/23/modern-bumper-might-have-mitigated-september-train-crash/a10fu6l/.

Cotter, J., & Dowd, K. (2006). Extreme spectral risk measures: an application to futures clearinghouse margin requirements. *Journal of Banking & Finance*, 30(12), 3469-3485.

DaSilva, M. P., Baron, W., & Carroll, A. A. (2012). Highway rail-grade crossing safety research: Railroad infrastructure trespassing detection systems research in Pittsford, New York (No. DOT-VNTSC-FRA-05-07).

Davidson, B. R. (1982). A benefit cost analysis of the New South Wales railway system. *Australian Economic History Review*, 22(2), 127-150.

Dong, Y., Hu, Z., Uchimura, K., & Murayama, N. (2010). Driver inattention monitoring system for intelligent vehicles: A review. *IEEE Transactions on Intelligent Transportation Systems*, 12(2), 596-614.

Dingler, M.H., Lai, Y-C., & Barkan, C.P.L. (2010). Effects of communications-based train control and electronically controlled pneumatic brakes on railroad capacity. Transportation Research Record: *Journal of the Transportation Research Board*. 2159: 77-84.

Dee H. M. & S.A. Velastin (2008). How Close Are We to Solving the Problem of Automated Visual Surveillance? *Machine Vision & Application*, Vol. 19.

Elias, B., Peterman, D.R. & Frittelli, J. (2016). Transportation security: issues for the 114th congress. Library of Congress, *Congressional Research Service*, 7-5700. May 9, 2016.

Epstein, L. J., Kristo, D., Strollo, P. J., Friedman, N., Malhotra, A., Patil, S. P., ... & Weinstein, M. D. (2009). Clinical guideline for the evaluation, management and long-term care of obstructive sleep apnea in adults. *Journal of Clinical Sleep Medicine*, 5(03), 263-276.

Evans, A. W., (2003) Accidental Fatalities in Transport. Journal of the Royal Statistical Society. Series A (Statistics in Society), Vol. 166, No. 2, 253-260.

Federal Railroad Administration (FRA) (2008). Rail Trespasser Fatalities - Developing Demographic Profiles. Washington DC.

Federal Railroad Administration (FRA) (2009). Positive train control systems economic analysis, U.S. Department of Transportation, Washington, DC.

Federal Railroad Administration (FRA) (2011a). 49 Code of Federal Regulations Part 236 - Rules, Standards, And Instructions Governing the Installation, Inspection, Maintenance, and Repair of Signal and Train Control Systems, Devices, and Appliances. Washington, DC.

Federal Railroad Administration (FRA) (2011b). FRA Guide for Preparing Accident/Incident Report, 2011. Washington, D.C.

Federal Railroad Administration (FRA) (2012). Safety Advisory 2012-02: Restricted Speed. Washington, DC.

Federal Railroad Administration (FRA) (2013). Rail Trespasser Fatalities. June 2013. Washington DC.

Federal Railroad Administration (FRA) (2014). BNSF San Bernardino Case Study: Positive Train Control Risk Assessment. DOT/FRA/ORD-14/31, September 2014.

Federal Railroad Administration (FRA) (2015). Office of Safety Analysis 3.01 –Accident Trends – Summary Statistics. http://safetydata.fra.dot.gov/officeofsafety/publicsite/summary.aspx.

Federal Railroad Administration (FRA) (2016a). Passenger Equipment Safety Standards; Standards for Alternative Compliance and High-Speed Trainsets. Washington, DC.

Federal Railroad Administration (FRA) (2016b). Benefit-cost analysis guidance for rail projects, U.S. Dept. of Transportation, Washington, DC.

Federal Railroad Administration (FRA) (2016c). Highway-Rail Crossing & Trespassing Fact Sheet. October 2016. Washington DC.

Federal Railroad Administration (FRA), 2017. Intelligent grade crossing. Retrieved from: https://www.fra.dot.gov/Page/P0309.

Federal Railroad Administration (FRA) (2018a). FRA Rail Equipment Accident (6180.54) database. https://safetydata.fra.dot.gov/OfficeofSafety/publicsite/on_the_fly_download.aspx. (Accessed in March 2018).

Federal Railroad Administration (FRA) (2018b). Track safety standards; improving rail integrity: Final rule, U.S. Dept. of Transportation, Washington, DC.

Federal Railroad Administration (FRA) (2018c). PTC Testing. Positive Train Control (PTC) Symposium #2, Washington, DC.

Federal Railroad Administration (FRA) (2018d). Characteristics of Trespassing Incidents in the United States (2012-2014). Washington, DC.

Federal Railroad Administration (FRA) (2019a). Welcome to the NASA Confidential Close Call Reporting System! https://c3rs.arc.nasa.gov/. Accessed by April 1, 2019.

Federal Railroad Administration (FRA) (2019b). A Literature Review of Rail Trespassing and Suicide Prevention Research. TRB's Transportation Research Circular E-C242.

Federal Transit Administration (FTA) (2018). Improving Public Transportation for America's Communities. https://www.transit.dot.gov/about-fta (Accessed in March 2018).

Ferjencik, M. (2011). An integrated approach to the analysis of incident causes. *Safety Science*, 49(6), 886-905.

Fixing America's Surface Transportation Act (FAST Act). 2016. 114th Congress. Washington DC, Section 11404.

FOX NEWS (2019). Texas deputy's vehicle hit by train as he rushed to save baby in distress, officials say. https://www.foxnews.com/us/texas-deputy-vehicle-train-baby-distress.

Gabree, S., Chase, S., Doucette, A., & Coplen, M. (2014). Potential countermeasures to mitigate suicides on the railroad right-of-way. In: 2014 Global Level Crossing Safety and Trespass Prevention Symposium, University of Illinois at Urbana-Champaign, August 2014.

Gali, J., & Gertler, M. (1999). Inflation dynamics: A structural econometric analysis. *Journal of Monetary Economics*, 44(2), 195-222.

George, B.F. (2008). Rail Trespasser Fatalities Demographic and Behavioral Profiles. Federal Railroad Administration, Washington, DC.

General Code of Operating Rules Committee (2010). General Code of Operating Rules (GCOR). Sixth Edition.

Government Accountability Office (GAO). (2013). Positive train control: Additions authorities could benefit implementation. Washington, DC, GAO-13-720.

Government Accountability Office (GAO). (2015). Positive train control: Additional oversight needed as most railroads do not expect to meet 2015 implementation deadline. Washington, DC, GAO-15-739.

Government Accountability Office (GAO) (2018). Positive Train Control: Most Passenger Railroads Expect to request an Extension, and Substantial Work Remains Beyond 2018.

Hallowell, M. R. (2008). A formal model of construction safety and health risk management.

Hartong, M., Goel, R., & Wijesekera, D. (2011). Positive Train Control (PTC) failure modes. *Journal of King Saud University-Science*, 23(3), 311-321.

Hilbe, J.M. (2007). Negative Binomial Regression. Cambridge University Press, Cambridge, United Kingdom.

Hosmer Jr, D.W., Lemeshow, S. & Sturdivant, R.X. (2013). Applied logistic regression (Vol. 398). John Wiley & Sons.

Hosseini, S. D., & Verma, M. (2017). A Value-at-Risk (VAR) approach to routing rail hazmat shipments. *Transportation Research Part D: Transport and Environment*, 54, 191-211.

Hollnagel, E. (1998). Cream-cognitive reliability and error analysis method. Elsevier Science Ltd, Oxford.

Hollnagel, E. (2012). FRAM—The Functional Resonance Analysis Method. Ashgate, Farnham.

Horton, S., Carroll, A., Chaudhary, M., Ngamdung, T., Mozenter, J. & Skinner, D., (2009). Success factors in the reduction of highway-rail grade crossing incidents from 1994 to 2003 (No. DOT-VNTSC-FRA-09-01). United States. Federal Railroad Administration.

Hu, S.R., Li, C.S. & Lee, C.K. (2010). Investigation of key factors for accident severity at railroad grade crossings by using a logit model. *Safety Science*, 48(2), 186-194.

Ishimatsu, T., Leveson, N. G., Thomas, J. P., Fleming, C. H., Katahira, M., Miyamoto, Y. & Hoshino, N. (2014). Hazard analysis of complex spacecraft using systems-theoretic process analysis. *Journal of Spacecraft and Rockets*, 51(2), 509-522.

Kalman, R.E. (1960). A new approach to linear filtering and prediction problems. *Journal of Basic Engineering,* 82(1), 35-45.

Koyama, R. G., Esteves, A. M., e Silva, L. O., Lira, F. S., Bittencourt, L. R., Tufik, S., & de Mello, M. T. (2012). Prevalence of and risk factors for obstructive sleep apnea syndrome in Brazilian railroad workers. *Sleep Medicine*, 13(8), 1028-1032.

Lee, W. K. (2006). Risk assessment modeling in aviation safety management. *Journal of Air Transport Management*, 12(5), 267-273.

Lee, H. H. & Mahony, I. G. (2017). Positive train control: roadblocks to interoperability. Holland & Knight LLP, New York City.

Leveson, N. (2004). A new accident model for engineering safer systems. *Safety Science*, 42(4), 237-270.

Le, N., Heili, A. & Odobez, J.M. (2016), October. Long-term time-sensitive costs for CRF-based tracking by detection. In *European Conference on Computer Vision* (43-51). Springer, Cham.

Li, Y. & Fernie, G. (2010). Pedestrian behavior and safety on a two-stage crossing with a center refuge island and the effect of winter weather on pedestrian compliance rate. *Accident Analysis & Prevention*, 42(4), 1156-1163.

Lin, C.Y., Saat, M.R., Barkan, C.P. & Lin, C.Y. (2014). Causal Analysis of Passenger Train Accident on Shared-Use Rail Corridor. Proceedings of *93rd Transportation Research Board*, Washington, DC.

Lin, T. Y. (2014). Microsoft COCO: Common Objects in Context. Computer Vision--ECCV 2014. ECCV 2014. Lecture Notes in Computer Science, 8693.

Liu, X., Saat, M. R., & Barkan, C. P. (2010). Benefit-cost analysis of infrastructure improvement for derailment prevention. In 2010 *Joint Rail Conference* (399-405). American Society of Mechanical Engineers Digital Collection.

Liu, X., Saat, M. R., & Barkan, C. P. L. (2011). Benefit-cost analysis of heavy haul railway track upgrade for safety and efficiency. In *Proc., International Heavy Haul Association Conference*. Alberta, Canada: Calgary.

Liu, X., Lovett, A., Dick, T., Rapik Saat, M., & Barkan, C. P. (2014). Optimization of ultrasonic rail-defect inspection for improving railway transportation safety and efficiency. *Journal of Transportation Engineering*, 140(10), 04014048.

Liu, X. (2016). Analysis of collision risk for freight trains in the United States." *Transportation Research Record: Journal of the Transportation Research Boar*d 2546 (2016): 121-128.

Lobb, B., Harre, N. & Terry, N. (2003). An evaluation of four types of railway pedestrian crossing safety intervention. *Accident Analysis & Prevention*, 35(4), 487-494.

Long Island Rail Road (LIRR) (2017). 2016 Ridership Book, http://web.mta.info/mta/news/books/docs/2016%20LIRR%20Ridership%20Book.pdf.

Madigan, R., Golightly, D., & Madders, R. (2016). Application of Human Factors Analysis and Classification System (HFACS) to UK rail safety of the line incidents. *Accident Analysis & Prevention*, 97, 122-131.

Metropolitan Transportation Authority (MTA) (2018). The MTA Network, http://web.mta.info/mta/network.htm#statslirr (Accessed in March, 2018).

Mitra, S. & Washington, S. (2007). On the nature of over-dispersion in motor vehicle crash prediction models. *Accident Analysis & Prevention*, 39(3), 459-468.

Moturu, S., & Utterback, J. (2018). Safe Approach of Trains into Terminal Stations. In 2018 *Joint Rail Conference*. American Society of Mechanical Engineers Digital Collection.

Mokkapati, C., Pascoe, R. D., & Ansaldo, S. (2011, September). A Simple and Efficient Train Braking Algorithm for PTC Systems. *In AREMA Annual Conference*.

Nena, E., Tsara, V., Steiropoulos, P., Constantinidis, T., Katsarou, Z., Christaki, P., & Bouros, D. (2008). Sleep-disordered breathing and quality of life of railway drivers in Greece. *Chest,* 134(1), 79-86.

NJ TRANSIT (NJT) (2018). NJ Transit Facts at A Glance, Fiscal Year 2017.

Nast, T., Baker, J., & Ramos, A. (2016). Positive train control desense mitigation test: research phase 1 (No. DOT/FRA/ORD-16/15). United States. Federal Railroad Administration. Office of Research, Development, and Technology.

National Transportation Safety Board (NSTB) (2012). Collision of BNSF coal train with the rear end of standing BNSF maintenance-of-way equipment train, Red Oak, Iowa, April 17, 2011. Railroad Accident Report RAR-12/02. Washington, DC.

National Transportation Safety Board (NSTB) (2013). Head-on collision of two Union Pacific Railroad freight trains near Goodwell, Oklahoma, June 24, 2012. Railroad Accident Report RAR-13/02. Washington, DC.

National Transportation Safety Board (NSTB) (2016). Collision of two Union Pacific Railroad freight trains, Hoxie, Arkansas, August 17, 2014. Railroad Accident Report RAR-16/03. Washington, DC.

National Transportation Safety Board (NSTB) (2018a). End-of-Track Collisions at Terminal Stations Hoboken, New Jersey, September 29, 2016 and Atlantic Terminal, Brooklyn, New York, January 4, 2017, SIR1801. Washington, DC.

National Transportation Safety Board (NSTB) (2018b). Railroad Accident Brief: New Jersey Transit Train Strikes Wall in Hoboken Terminal, RAB1801. Washington, DC.

National Transportation Safety Board (NSTB) (2018c). Long Island Rail Road Passenger Train Strikes Platform in Atlantic Terminal, RAB1802. Washington, DC.

Nayak, P.R., Rosenfield, D.B. & Hagopian, J.H (1983). Event probabilities and impact zones for hazardous materials accidents on railroads, in: Report DOT/FRA/ORD-83/20, FRA, U.S. Department of Transportation, Federal Railroad Administration.

Ngamdung, T. (2019). Effect of Grade Separation on Pedestrian Railroad Trespass Activity at Shuttlesworth Drive in Collegeville, AL. Federal Railroad Administration, DOT/FRA/ORD-19/11. May 2019.

Northeast Operating Rules Advisory Committee (2018). NORAC Operating Rules. Eleventh Edition.

Palo Alto Online (2018). Palo Alto to install cameras along Caltrain tracks. https://www.paloaltoonline.com/news/2018/03/20/palo-alto-to-install-cameras-along-caltrain-tracks Accessed by July 1st 2018.

Park, Y. T., & Lee, D. H. (2010). 3D vision-based security monitoring for railroad stations. *Journal of the Optical Society of Korea*, 14(4), 451-457.

Pascoe, R. D. & Eichorn, T. N. (2009). What is communication-based train control. IEEE Vehicular Technology Magazine. December 2009. 1556-6072, 16-21.

Peters, J. C. & Frittelli, J. (2012). Positive train control: overview and policy issues. *Congressional Research Service*.

Port Authority Trans-Hudson (PATH) (2018). PATH Ridership Report. https://www.panynj.gov/path/statistics.html (Accessed in March 2018)

Patriarca, R., Di Gravio, G., & Costantino, F. (2017). A Monte Carlo evolution of the Functional Resonance Analysis Method (FRAM) to assess performance variability in complex systems. Safety Science, 91, 49-60.

Qian, Q., & Lin, P. (2016). Safety risk management of underground engineering in China: Progress, challenges and strategies. *Journal of Rock Mechanics and Geotechnical Engineering*, 8(4), 423-442.

Radbo, H., Svedung, I., & Andersson, R. (2005). Suicides and other fatalities from train-person collisions on Swedish railroads: A descriptive epidemiologic analysis as a basis for systems- oriented prevention. *Journal of Safety Research*, 36(5), 423-428.

Railroad Safety Advisory Committee (RSAC) (1999). Report of the Railroad Safety Advisor Committee to the Federal Railroad Administrator: Implementation of positive train control, Washington, DC.

Raslear, T.G. (2015). Using Signal Detection Theory to Understand Grade Crossing Warning Time and Motorist Stopping Behavior (No. DOT/FRA/ORD-15/02), Washington DC.

Raub, R.A. (2009). Examination of highway-rail grade crossing collisions nationally from 1998 to 2007. *Transportation Research Record*, 2122(1), 63-71.

Reason, J. (1990). The contribution of latent human failures to the breakdown of complex systems. *Philosophical Transactions of the Royal Society of London. B, Biological Sciences*, 327(1241), 475-484.

Redmon, J., Divvala, S., Girshick, R. & Farhadi, A. (2016). You Only Look Once: Unified, real-time object detection. In *Proceedings of the IEEE conference on computer vision and pattern recognition* (779-788).

Redmon, J. & Farhadi, A. (2018). Yolov3: An incremental improvement. arXiv preprint arXiv:1804.02767.

Reason, J., Hollnagel, E., & Paries, J. (2006). Revisiting the Swiss cheese model of accidents. *Journal of Clinical Engineering*, 27(4), 110-115.

Resor, R. R., Smith, M. E., & Patel, P. K. (2005). Positive train control (PTC): Calculating benefits and costs of a new railroad control technology. In *Journal of the Transportation Research Forum* (Vol. 44, No. 1424-2016-117774, p. 98).

Rockafellar, R.T. & Uryasev, S. (2000). Optimization of conditional value-at-risk. *Journal of Risk*, 2, 21-42.

Roelen, A. L. C., Lin, P. H., & Hale, A. R. (2011). Accident models and organisational factors in air transport: The need for multi-method models. *Safety Science*, 49(1), 5-10.

Roskind, F. D. (2009). Positive Train Control Economic Analysis. Federal Railroad Administration, RIN 2130-AC03.

Rosenbloom, T., Haviv, M., Peleg, A. & Nemrodov, D. (2008). The effectiveness of road-safety crossing guards: Knowledge and behavioral intentions. *Safety Science*, 46(10), 1450-1458.

Salmon, P. M., Read, G. J., Stanton, N. A., & Lenné, M. G. (2013). The crash at Kerang: Investigating systemic and psychological factors leading to unintentional non-compliance at rail level crossings. *Accident Analysis & Prevention*, 50, 1278-1288.

Savage, I. (2007). Trespassing on the railroad. Res. *Transp. Econ*. 20, 199–224.

Savage, I. (2016). Analysis of fatal train-pedestrian collisions in metropolitan Chicago 2004–2012. *Accident Analysis & Prevention*, 86, 217-228.

Schafer, D. & Barkan, C. (2008). Relationship between train length and accident causes and rates. Transportation Research Record: *Journal of the Transportation Research Board*, (2043), 73-82.

Silla, A. & Luoma, J. (2012). Main characteristics of train-pedestrian fatalities on Finnish railroads. *Accident Analysis & Prevention*, 45, 61-66.

Soleimani, H., Seyyed-Esfahani, M., & Kannan, G. (2014). Incorporating risk measures in closed-loop supply chain network design. *International Journal of Production Research*, 52(6), 1843-1867.

Stanchak, K. & DaSilva, M. (2014). Trespass event risk factors (No. DOT-VNTSC-FRA-14-03). United States. Federal Railroad Administration. Office of Research and Development.

Stefanova, T., Burkhardt, J.M., Filtness, A., Wullems, C., Rakotonirainy, A. & Delhomme, P. (2015). Systems-based approach to investigate unsafe pedestrian behaviour at level crossings. *Accident Analysis & Prevention*, 81, 167-186.

Topel, K. (2019). A Literature Review of Rail Trespassing and Suicide Prevention Research. *Transportation Research Circular*, (E-C242).

Transportation Economics & Management Systems, Inc. (2017). The path to vital PTC and to operational impacts for the railroad industry, presented at Transportation Research Board, Washington, DC.

Thurston, D.F. (2004). Signaling and capacity through computer modeling, In: *Proceedings of International Conference on Computer Modeling for Rail Operations*, Delray Beach.

Toumazis, I., & Kwon, C. (2016). Worst-case conditional value-at-risk minimization for hazardous materials transportation. *Transportation Science*, 50(4), 1174-1187.

U.S. Department of Transportation (2016). Revised Departmental Guidance 2016: Treatment of the Value of Preventing Fatalities and Injuries in Preparing Economic Analyses, August 8, 2016. Washington, DC.

U.S. Census Bureau (2019). Bergen County, New Jersey Gender Ratios. Accessed by May 13, 2019.

Van Dyke, C. & Case R. (2010). Commercial benefits of Positive Train Control. New York City, NY.

Van Gulijk, C., Hughes, P., Figueres-Esteban, M., Dacre, M., & Harrison, C. (2015). Big Data Risk Analysis for Rail Safety. In *Proceedings of ESREL 2015*. CRC/Balkema.

Volpe The National Transportation Systems Center (Volpe Center) (2015). Trespassing Detection and Warning Research, Brunswick, ME. 2015 ROW fatality & Trespass Prevention Workshop, Charlotte, NC.

Volpe National Transportation Systems Center (Volpe Center) (2017). Opportunities to Reduce Crossing Fatalities: Gaps in the Current Safety Trends. Boston, MA.

Wali, B., Khattak, A. J., & Zhang, M. (2018). Injury Severity Analysis of Pedestrian and Bicyclist Trespassing Crashes at Non-Crossings: Application of Predictive Text Analytics (No. 18-00209).

Wang, X., Liu, J., Khattak, A.J. & Clarke, D. (2016). Non-crossing rail-trespassing crashes in the past decade: A spatial approach to analyzing injury severity. *Safety Science*, 82, 44-55.

Wright, L. & Van der Schaaf, T. (2004). Accident versus near miss causation: a critical review of the literature, an empirical test in the UK railway domain, and their implications for other sectors. *Journal of Hazardous Materials*, 111(1-3), 105-110.

Warner, H. W., & Sandin, J. (2010). The intercoder agreement when using the Driving Reliability and Error Analysis Method in road traffic accident investigations. *Safety Science*, 48(5), 527-536.

Weiss, N.A. (2006). A course in probability. Addison-Wesley.

Wickens, C. D (1992). Virtual reality and education. *IEEE International Conference on Systems, Man, and Cybernetics*. DOI: 10.1109/ICSMC.1992.271688

Woodburn, A. (2017). The impacts on freight train operational performance of new rail infrastructure to segregate passenger and freight traffic. *Journal of Transport Geography*, 58, 176-185.

World Bank. (2018) https://data.worldbank.org/indicator/ NY.GDP.DEFL.ZS?end=2016&locations=US&start=2000&view=chart. (Accessed in June 2018).

Xi, Y. T., Chen, W. J., Fang, Q. G., & Hu, S. P. (2010, December). HFACS model based data mining of human factors-a marine study. In *2010 IEEE International Conference on Industrial Engineering and Engineering Management* (1499-1504). IEEE.

Young, T., Peppard, P. E., & Gottlieb, D. J. (2002). Epidemiology of obstructive sleep apnea: a population health perspective. *American Journal of Respiratory and Critical Care Medicine,* 165(9), 1217-1239.

Zaman, A., Liu, X., & Zhang, Z. (2018). Video analytics for railroad safety research: an artificial intelligence approach. *Transportation Research Record*, 2672(10), 269-277.

Zaman, A., Ren, B. & Liu, X. (2019). Artificial Intelligence-aided automated detection of railroad trespassing. *Transportation Research Record*, 0361198119846468.

Zeng, S. X., Tam, C. M., & Tam, V. W. (2010). Integrating safety, environmental and quality risks for project management using a FMEA method. *Engineering Economics*, 66(1).

Zhang, Z., Liu, X., & Holt, K. (2018a). Positive Train Control (PTC) for railway safety in the United States: Policy developments and critical issues. *Utilities Policy*, 51, 33-40.

Zhang, Z., Liu, X., & Bian, Z. (2018b). Analysis of restricted-speed accidents using Fault Tree Analysis. In *2018 Joint Rail Conference*. American Society of Mechanical Engineers Digital Collection.

Zhang, Z., Trivedi, C. & Liu, X. (2018c). Automated detection of grade-crossing-trespassing near misses based on computer vision analysis of surveillance video data. *Safety Science*, 110, 276-285.

Zhang, Z., Turla, T., & Liu, X. (2019a). Analysis of human-factor-caused freight train accidents in the United States. *Journal of Transportation Safety & Security*, 1-29.

Zhang, Z., & Liu, X. (2019b). Safety risk analysis of restricted-speed train accidents in the United States. *Journal of Risk Research*, 1-19.

Zhang, Z., Liu, X., & Holt, K. (2019c). Prevention of end-of-track collisions at passenger terminals via positive train control. *Transportation Research Record*, 2673(9), 471-479.

Zhao, Y. & Ioannou, P. (2015). Positive train control with dynamic headway based on an active communication system. *IEEE Transactions on Intelligent Transportation Systems*. 16(6), 3095-3103.

APPENDIX A

SELECTED RESTRICTED-SPEED ACCIDENTS

Table A. 1. Selected High-Consequence Restricted-Speed Accidents, 2000-2016 [1]

Date	State	Railroad [2]	Speed (mph)	Fatality	Injury	Damage Cost	Number of Cars Derailed
09/30/2000	New York	ATK	10	0	10	$183,574	2
10/31/2000	Arizona	BNSF	1	1	3	$3,708,100	7
07/18/2003	California	UP	10	0	8	$558,168	1
08/15/2003	New York	MNCW	12	0	10	$135,572	1
04/19/2004	New York	ATK	10	0	31	$80,000	1
08/30/2004	New Jersey	NJTR	14	0	4	$24,000	1
11/29/2004	Florida	CSX	33	1	2	$817,777	15
10/15/2005	Arizona	UP	17	1	46	$2,379,170	0
01/18/2006	Alabama	NS	53	0	3	$2,534,100	10
10/13/2007	Indiana	NICD	14	0	4	$2,100,000	0
11/30/2007	Illinois	ATK	33	0	136	$1,719,000	1
02/07/2008	Washington DC	MACZ	12	0	8	$183,000	0
06/27/2008	California	ACEX	9	0	7	$18,872	1
11/14/2008	California	BNSF	11	0	5	$71,300	0
01/27/2009	Pennsylvania	SEPA	30	0	20	$700,000	0
04/17/2011	Iowa	BNSF	22	2	2	$2,276,952	4
05/24/2011	North Carolina	CSX	48	2	2	$1,457,301	11
01/06/2012	Indiana	CSX	44	0	2	$2,549,805	6
06/24/2012	Oklahoma	UP	63	3	1	$11,729,623	27
05/25/2013	Missouri	BNSF	23	0	7	$8,686,769	13
06/27/2013	New York	CSX	20	0	2	$2,406,203	21
09/25/2013	Texas	BNSF	46	0	6	$3,744,754	11
04/06/2014	Texas	UP	18	0	2	$2,301,504	1
09/29/2016	New Jersey	NJTR	21	1	110	$6,012,000	1
10/08/2016	New York	LI	50	0	0	$3,200,000	2

Notes: [1] Data sources: FRA REA database and NTSB railroad accident reports.

[2] Railroad Codes: ATK: Amtrak; BNSF: BNSF Railway Co.; UP: Union Pacific RR Co.; MNCW: Metro-North Commuter RR Co.; NJTR: New Jersey Transit Rail Operations; CSX: CSX Transportation; NS: Norfolk Southern Corp.; NICD: Northern Indiana Commuter Transportation District; MACZ: MARC Train Service; ACEX: Altamont Commuter Express Authority; SEPA: Southeastern Pennsylvania Transportation Authority; LI: Long Island Rail Road. For updates, please refer to http://safetydata.fra.dot.gov/OfficeofSafety/publicsite/downloads/auxrr.aspx.

Table A. 2 presents a sample of recent end-of-track collisions at U.S. terminals from 2011 to 2017. The train accident information summarized here is drawn from two data sources, the FRA Rail Equipment Accident (REA) database (FRA, 2018a) and railroad accident reports by the NTSB. In addition to the basic accident information listed in Table A. 2, more comprehensive information can be found in the FRA REA database, including operational factors, environmental factors, train characteristics, damage costs, and narratives. Additionally, NTSB railroad accident reports describe the major findings of NTSB investigations including accident details, factual data analysis, the (probable) cause of the accident, and safety recommendations. Instead of covering all railroad accidents, only the accidents with a significant loss of life, physical damage, important issues to public safety, or particular public interest are involved in the NTSB investigations (NTSB, 2018b) and then compiled into NTSB accident reports.

As shown in Table A. 2, from 2011 to 2017, eleven end-of-track collisions are collected from the FRA REA database and NTSB investigation reports. In the United States, over 35 passenger terminals have multiple terminating tracks ending at bumping posts and/or platforms (NTSB, 2018a) and each of them has a large number of train stops every day. For example, the Chicago Union Station provides ridership for Amtrak and Metra. Per the publicly accessible train schedules, hundreds of trains enter Chicago Union Station and other major terminal hubs every day. This large traffic exposure poses the potential risk of end-of-track collisions, although the probability is (fortunately) low. Possible end-of-track collisions may bring hazards to the onboard passengers, train crews, and bystanders, and cause high-impact damage to rolling stock, wayside equipment, and terminal infrastructure. Specifically, the selected eleven end-of-track collisions occurring between 2011 and 2017

have led to 310 casualties (injuries and fatalities) and over $13,745,548 total in damage costs. In terms of either casualties or damage cost, the most severe accidents (the LIRR train accident at Atlantic Terminal and the NJT train accident at Hoboken Terminal) took place in the last two years and each led to over 100 casualties and over $5 million in damage costs to rolling stock and infrastructure. Both end-of-track collisions were caused by operational violations by the engineers, who both had Obstructive Sleep Apnea (OSA) (NTSB, 2018b). Furthermore, the NSTB (2018b) also stated that the safety issues presented by the NJT accident and the LIRR accident could be pervasive in other commuter passenger train terminals and intercity passenger train terminals in the U.S.

Table A. 2. Selected End-of-Track Collisions in the United States, 2011-2017 [1]

Date	Location [2]	Railroad [3]	Speed (mph)	Injury	Fatality	Damage Cost
Jan. 4, 2017	Atlantic Terminal, NY	LIRR	12	112	0	$5,348,864
Sept. 29, 2016	Hoboken Terminal, NJ	NJT	21	156	1	$6,012,000
Mar. 7, 2016	Port Washington Station, NY	LIRR	2	0	0	$1,713,104
Jun. 2, 2015	Hoboken Terminal, NJ	NJT	3	1	0	$23,802
Jan. 6, 2014	LaSalle Street Station, IL	NIRC	7	0	0	$25,554
Sept. 23, 2012	Jamaica Station, NY	LIRR	2	2	0	$12,000
Feb. 21, 2012	Port Washington Station, NY	LIRR	3	0	0	$42,334
Jun. 8, 2011	Princeton Station, NY	NJT	16	1	0	$53,500
May 8, 2011	Hoboken Terminal, NJ	PATH	13	35	0	$352,617
Mar. 21, 2011	Port Jefferson Station, NY	LIRR	12	2	0	$110,283
Jan. 27, 2011	New Canaan Station, CT	MNCW	7	0	0	$51,500

Notes:

[1] Data sources: FRA REA database and NTSB railroad accident reports.

[2] Location: CT: Connecticut; IL: Illinois; NJ: New Jersey; NY: New York.

[3] Railroad: LIRR: Long Island Rail Road; NJT: New Jersey Transit; MNCW: Metro-North Commuter Railroad; NIRC: Northeast Illinois Regional Commuter Railroad; PATH: Port Authority Trans-Hudson.

APPENDIX B

RECORDED FIELDS IN TRESPASSING DATABASE

B.1. Through Terminal Area

In Figure B. 1, the station tracks are non-PTC tracks. With an I-ETMS system, these tracks could be mapped and the PTC system would enforce restricted speed as long as the train occupied either station track (Figure B. 1.b). With an ACSES system, transponders at each end of the main tracks would be used to cut in/out the ACSES system in almost all terminal areas. Then the ATC system will be active and enforce restricted speed within through terminal. Thus, no additional hardware equipment is needed here.

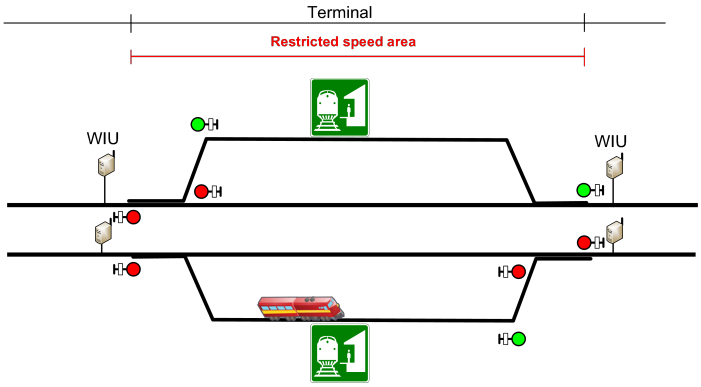

(a) Without modifications in I-ETMS

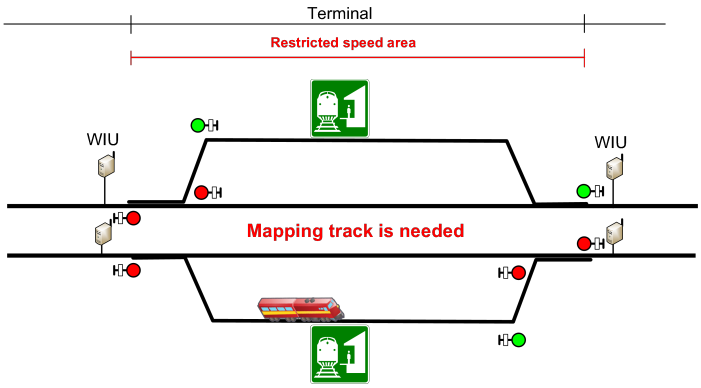

(b) With modifications in I-ETMS

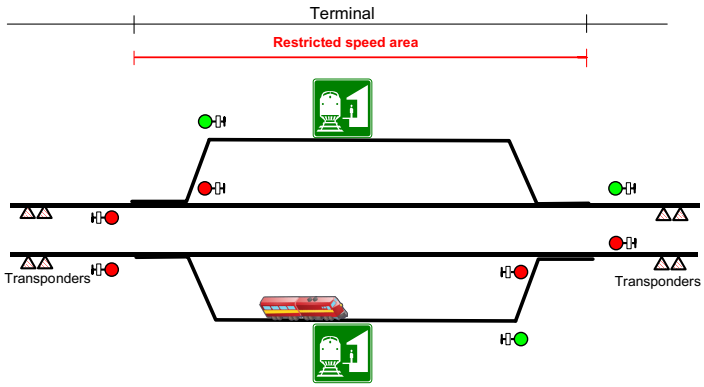

(c) Without modifications in ACSES

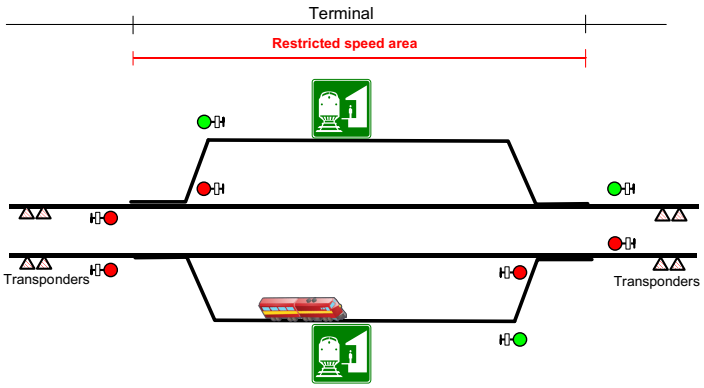

(d) With modifications in ACSES

Figure B. 1. Scenarios in Through Terminal (a) without I-ETMS; (b) with I-ETMS; (c) without ACSES; and (d) with ACSES

B.2. Non-Signaled Siding

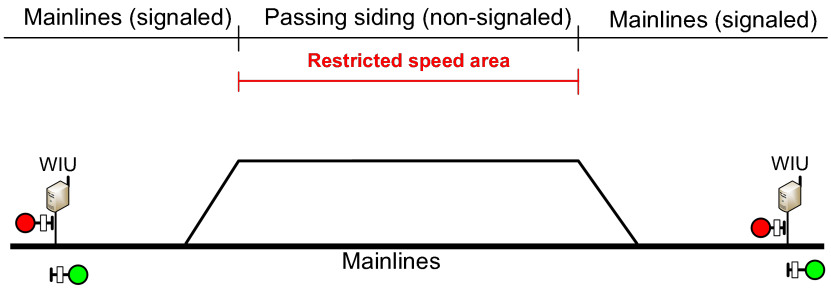

(a) Without modifications in I-ETMS

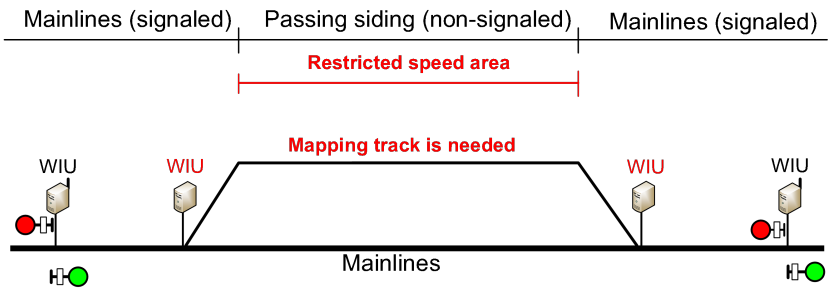

(b) With modifications in I-ETMS

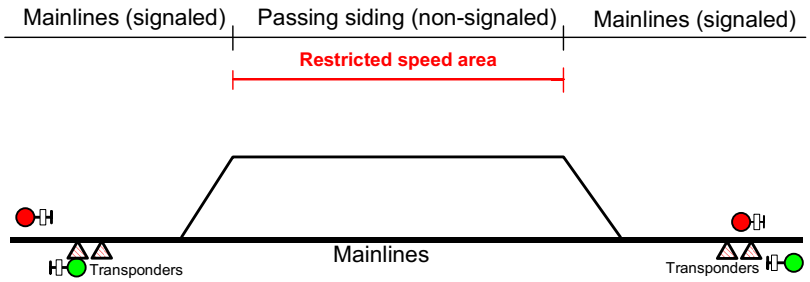

(c) Without modifications in ACSES

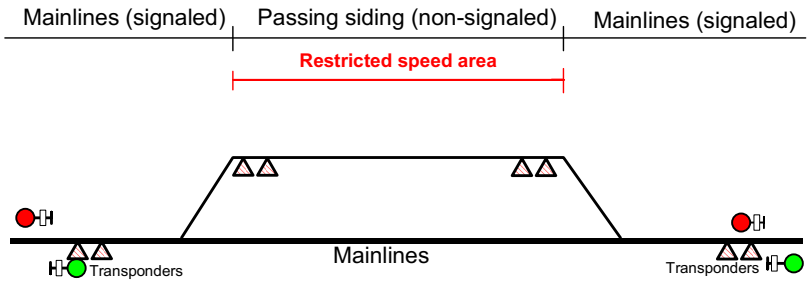

(d) With modifications in ACSES

Figure B. 2. Scenarios in Non-Signaled Siding with Hand-Operated Switch (a) without I-ETMS; (b) with I-ETMS; (c) without ACSES; and (d) with ACSES

In the case of a siding track with hand-operated switches, tracks could be mapped and the I-ETMS system would remain engaged. Restricted speed would be enforced while the train occupies the mapped track. A WIU would also be needed at a hand-operated switch location to monitor the switch conditions. (Figure B. 2.b). In the case of an ACSES system, transponders would be existing in PTC system. The ATC system would enforce the restricted speed and no additional hardware would be necessary for speed enforcement

(Figure B. 2. d). In addition, existing transponders are used to prevent the train from entering the main track without authorization.

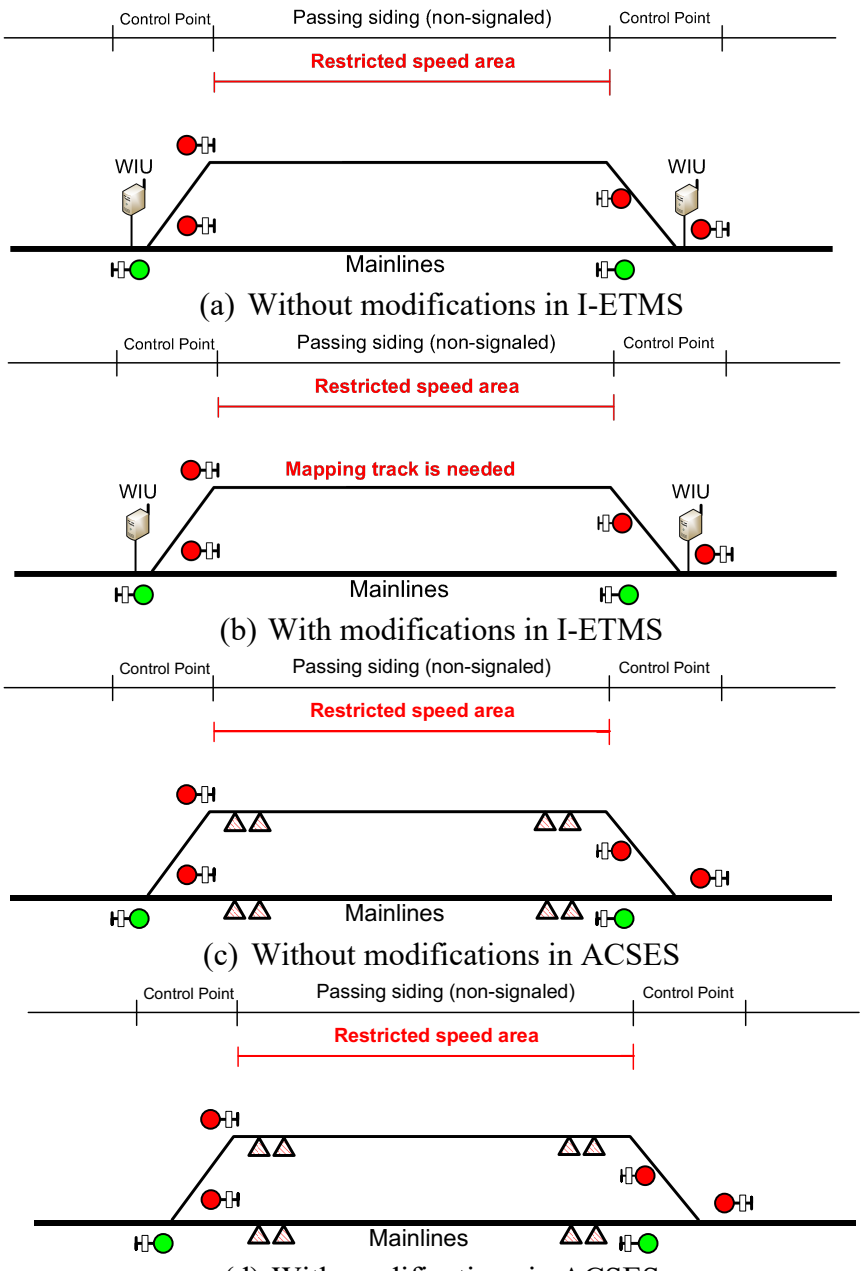

Figure B. 3. Scenarios in Non-Signaled Siding with Power-Operated Switch

(a) without I-ETMS; (b) with I-ETMS; (c) without ACSES; and (d) with ACSES

In the case of a siding track with power operated switches, it could also be mapped

and the PTC system would remain engaged. Restricted speed would be enforced while the train occupies the mapped track. A WIU would already be installed at a power-operated switch location and no need for additional WIUs at control points, in which absolute signals are controlled by a control operator. (Figure B. 3.b). In the case of an ACSES system, transponders would be existing in PTC system. The ATC system would enforce the restricted speed and no additional hardware would be necessary for speed enforcement (Figure B. 3. d).

B.3. Interlocking

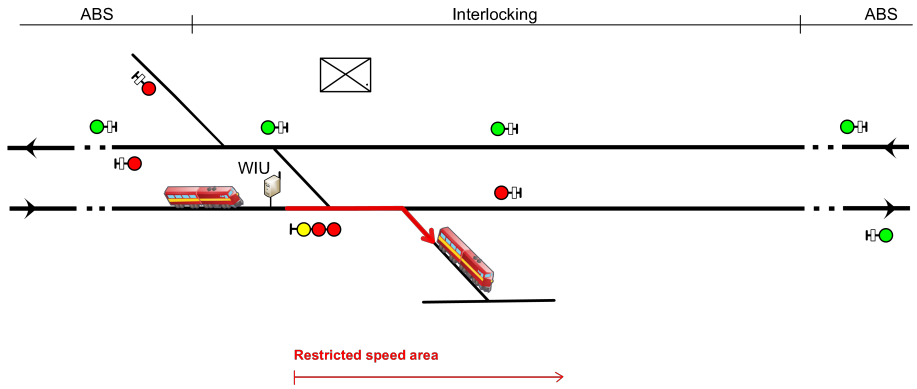

(a) I-ETMS (no modifications needed)

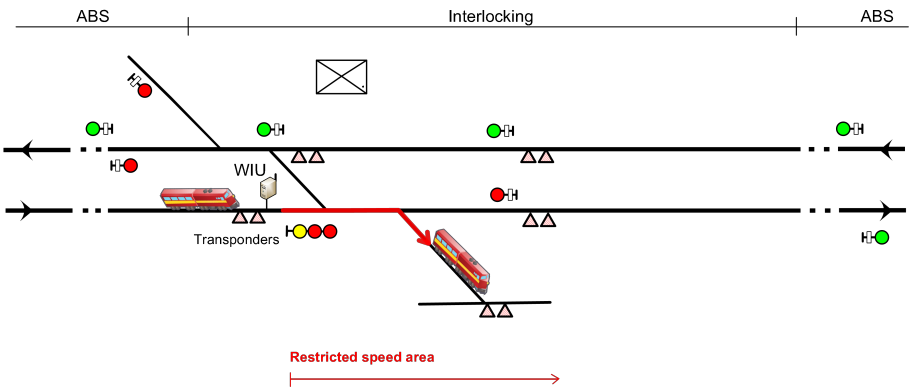

(b) ACSES (no modifications needed)

Figure B. 4. Interlocking with Occupied Yard in (a) I-ETMS and (b) ACSES

Interlocking is an interconnection of signals and signal appliances such that their movements must succeed each other in a predetermined sequence (NORAC, 2011). In the interlocking rules, signals cannot be displayed simultaneously on conflicting routes. Figure B. 4 shows a situation where both trains may have restricted speed enforcement and Call-On function enabled. In interlocking, power-operated switches are used and WIUs would already be installed. An I-ETMS system would require no additional hardware to enforce restricted speed into the yard tracks (Figure B. 4.a). An ACSES system with ATC would enforce restricted speed into the yard or non-PTC track due to restricted speed in the cab. WIUs and transponders that have been installed can provide necessary information ahead, such as cutting ACSES out/in. Thus, no additional equipment is needed in either I-ETMS or ACSES.

B.4. Automatic Block Signaling

Defect Detector Alarmed

(a) I-ETMS (no modifications needed)

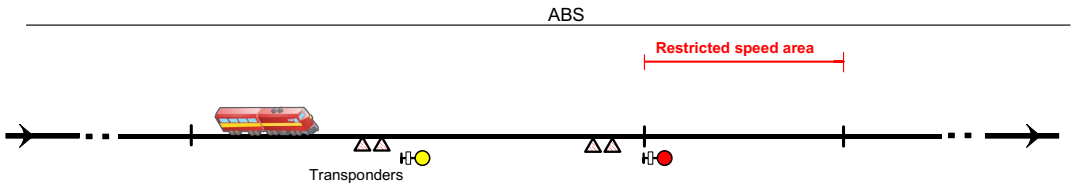

(b) ACSES (no modifications needed)

Figure B. 5. ABS with Alarmed Defect Detector in (a) I-ETMS and (b) ACSES

In this scenario, the train is slowed down by the signal system at the APPROACH signal (Figure B. 5). A STOP signal would be displayed at the entrance of the block where the defect was detected. The defect detector could be a slide fence detector, high-water detector, or fire detector for a wooden deck bridge or a broken rail. In such cases, the defect detector or broken rail would cause the signal governing the entrance to block to display STOP. The signal in approaching to the stop signal would display APPROACH and the PTC system would enforce a speed reduction that would allow the train to come to a safe stop at the stop signal. The PTC system should enforce the restricted speed as the train passes the red signal. The restricted speed would be enforced until the next signal. In an I-ETMS system, WIU is needed to get information about the status of the signal while approaching signal. 49 CFR 236 Subpart I require that defect detectors which are integrated into the signal or train control system be integrated into the PTC system. Thus, there would be a WIU at each signal already so that the signal indication could be enforced (Figure B. 5.a). In this case, the on-board computer would have to enforce the restricted speed until a more favorable signal is reached. In the case of the ACSES system equipped with ATC, the restricted speed would be enforced until the train was beyond the point where the defect occurred (Figure B. 5.b).

Occupied Block Ahead

(a) I-ETMS (no modifications needed)

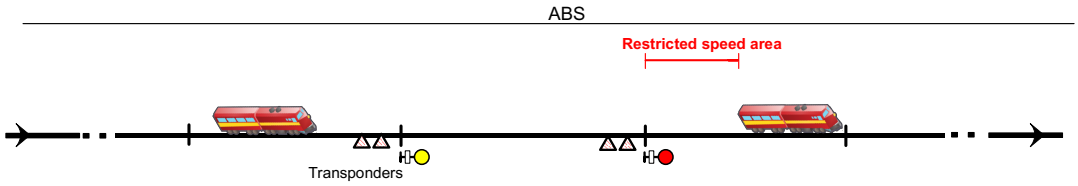

(b) ACSES (no modifications needed)

Figure B. 6. ABS with Occupied Block Ahead in (a) I-ETMS and (b) ACSES

In Figure B. 6, where there is a train in the block ahead, the signal system will react in the same manner as above. Most railroads allow a train to pass an ABS signal displaying STOP with the restricted speed. The second train could collide with the first train at the restricted speed. One of the alternatives to prevent this is to avoid restricted speed operations in the occupied block. A positive stop could be enforced at each ABS stop signal and permission would have to be received from the dispatcher to continue. This may prevent many rear-end collisions. To provide a positive prevention of a rear-end collision, an end of train device would be necessary to determine the location of the rear of the first train. The PTC system would have to have the capability to safely stop the second train before the collision with the first train.

Switch Improperly Lined

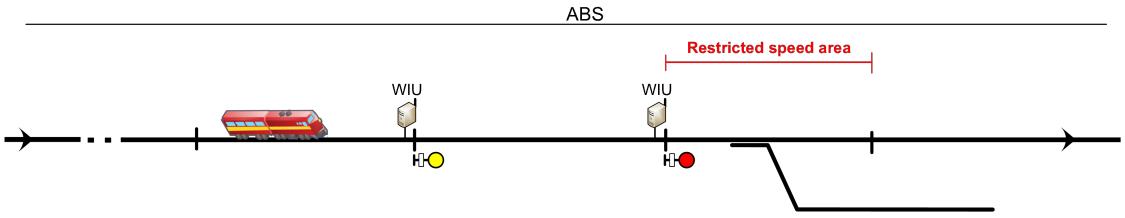

(a) I-ETMS (no modifications needed)

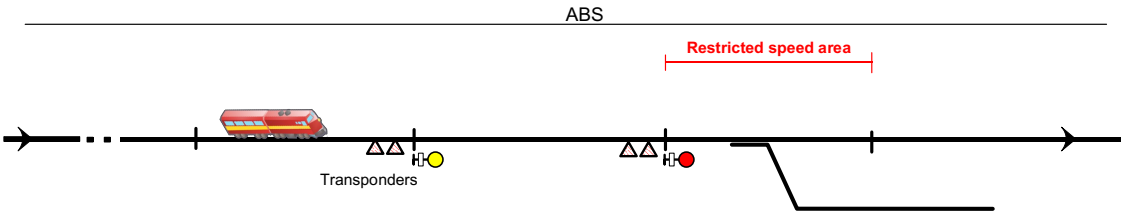

(b) ACSES (no modifications needed)

Figure B. 7. ABS with Improperly Switch (a) I-ETMS and (b) ACSES

In the last sub-case in ABS, an open hand-operated switch in the block would cause the signal governing entry into the block to display STOP. The PTC system would enforce restricted speed, but the engineer may not be paying attention or may not be able to determine the position of the switch. A WIU would already be placed at the signal location to provide information to the train (Figure B. 7.b). With the switch open or in an undetermined position, the PTC system could enforce STOP before the train passes the signal. Thus, no additional equipment is needed in either I-ETMS or ACSES to enforce restricted speed.

B.5. Centralized Traffic Control

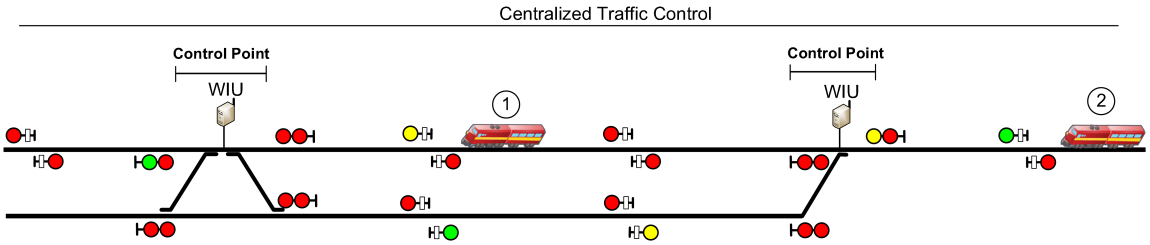

(a) I-ETMS (no modifications needed)

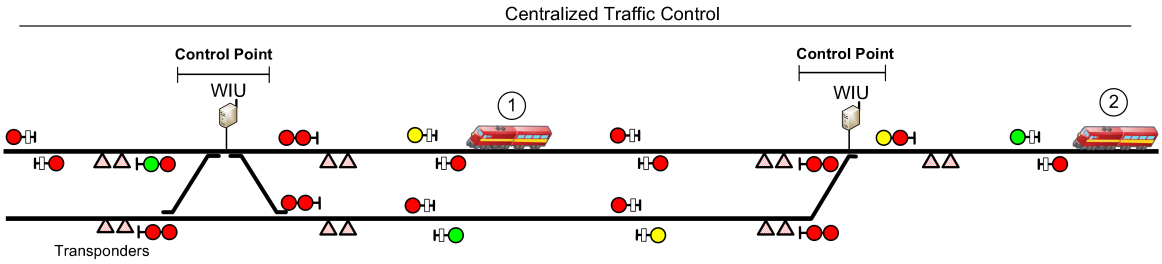

(b) ACSES (no modifications needed)

Figure B. 8. Restricted-Speed Scenarios in CTC (a) I-ETMS and (b) ACSES

Centralized Traffic Control (CTC) consists of interlocking and automatic blocks, thus aforementioned restricted speed scenarios and proposed modifications in the above two subsections are also feasible in CTC. In CTC territory (Figure B. 8), the PTC system will enforce absolute stop signals at the control points (refer to interlockings) or blocks. Most freight railroads allow trains to pass signals displaying Stop and proceed at the restricted speed. Most passenger railroads require a stop first and then the train may proceed at restricted speed. Others (especially freight railroads) allow trains to proceed at restricted speed without first bringing the train to a stop. This is commonly done where heavy freight trains are operating on upgrades where it may be hard to re-start the train after coming to a full stop. An ACSES system with ATC would enforce restricted speed in the cab.

B.6. Yard Limits

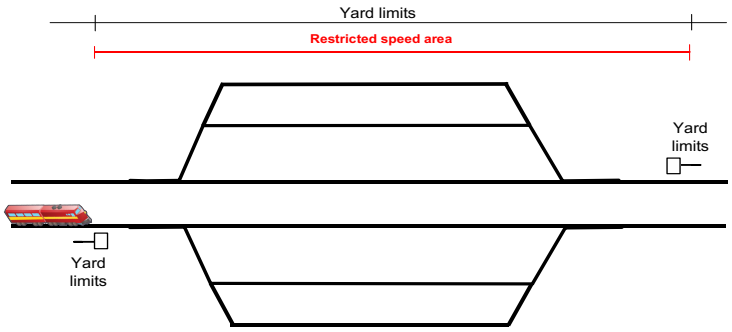

(a) Without modifications in I-ETMS

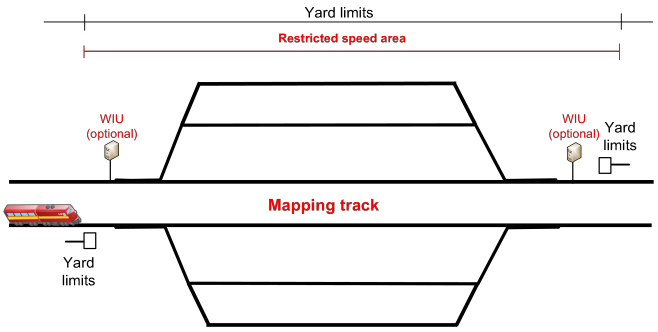

(b) With modifications in I-ETMS

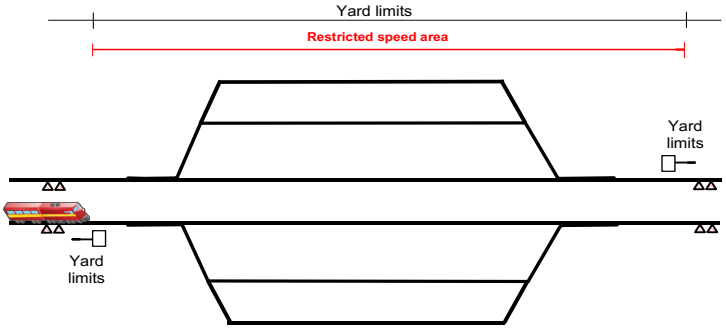

(c) ACSES (no modifications needed)

Figure B. 9. Yard Limits (a) without I-ETMS; (b) with I-ETMS; and (c) in ACSES

In Figure B. 9, a train is moving from PTC territory to yard limit which is defined by the yard limit signs at each end of the yard. When the train enters the yard limit area, the PTC system will disengage and will not enforce any speeds. By operating rule,

railroads require trains to move at restricted speed within yard limits.

To achieve the enforcement of restricted speed in I-ETMS system, the tracks must be mapped and designated as restricted speed tracks in the track database. With the tracks mapped, the I-ETMS system will remain engaged and will enforce restricted speed until the train leaves yard limits. Meanwhile, all the yard tracks do not have to be mapped. For example, the two main tracks in Figure B. 9 could be mapped and since the adjacent tracks are less than 50 ft. from the main tracks, the GPS system can't distinguish that the train might not be on the main track. In that case, the system would continue to enforce restricted speed of both main tracks and yard tracks within yard limits, once if main tracks are mapped. If the railroad only wanted to enforce restricted speed on the main tracks, then a WIU would have to be installed at each end of the yard to monitor the switch leaving the main track. The I-ETMS system would disengage when the train left the main track. Since ACSES is used mostly by passenger railroads, this situation would be rare. However, even if it occurs, the ATC system would enforce restricted speed through the yard limit area and no WIU would be required.

APPENDIX C

LOSS FUNCTION IN YOLO

YOLO predicts multiple bounding boxes per grid cell. To compute the loss for the true positive, it only wants one of them to be responsible for the object. For this purpose, the algorithm selects the one with the highest IOU (intersection over union) with the ground truth. This strategy leads to specialization among the bounding box predictions. Each prediction gets better at predicting certain sizes and aspect ratios.

YOLO uses a sum-squared error between the predictions and the ground truth to calculate loss. The loss function composes of the classification lost, the localization loss (errors between the predicted boundary box and the ground truth), and the confidence loss (the objectness of the box). The classification loss at each cell is the squared error of the class conditional probabilities for each class:

$$\sum_{i=0}^{S^2} \mathbb{I}_i^{obj} \sum_{c \in classes} (p_i(c) - \widehat{p}_i(c))^2 \tag{C-1}$$

$\mathbb{I}_i^{obj}$ = 1 if an object appears in cell i, otherwise 0.

$\widehat{p}_i(c)$ denotes the conditional class probability for class c in cell i.

The localization loss measures the errors in the predicted boundary box locations and sizes. It only counts the box responsible for detecting the object.

$$\lambda_{coord}\sum_{i=o}^{S^2}\sum_{j=0}^{B}\mathbb{I}_{ij}^{obj}[(x_i-\hat{x}_i)^2+(y_i-\hat{y}_i)^2]$$

$$+\lambda_{coord}\sum_{i=o}^{S^2}\sum_{j=0}^{B}\mathbb{I}_{ij}^{obj}[\left(\sqrt{w_i}-\sqrt{\hat{w}_i}\right)^2+(\sqrt{h_i}-\sqrt{\hat{h}_i})^2]$$

(C-2)

Where

$\mathbb{I}_{ij}^{obj}$ = 1 if the *j*th boundary box in cell i is responsible for detecting the object, otherwise 0.

λ_{coord} increases the weight for the loss in the boundary box coordinates

It does not want to weight absolute errors in large boxes and small boxes equally. i.e. a 2-pixel error in a large box is the same for a small box. To partially address this, YOLO predicts the square root of the bounding box width and height instead of the width and height. In addition, to put more emphasis on the boundary box accuracy, it multiplies the loss by λcoord (default: 5). If *an object* is detected in the box, the confidence loss (measuring the objectness of the box) is:

$$\sum_{i=o}^{S^2}\sum_{j=0}^{B}\mathbb{I}_{ij}^{obj}[\left(C_i-\hat{C}_i\right)^2]$$

(C-3)

Where

$\hat{C}_i$ is the box confidence score of the box j in cell i.

$\mathbb{I}_{ij}^{obj}$= 1 if the *j*th boundary box in cell i is responsible for detecting the object, otherwise 0.

If an object is not detected in the box, the confidence loss is:

$$\lambda_{noobj} \sum_{i=o}^{S^2} \sum_{j=0}^{B} \mathbb{I}_{ij}^{noobj} [(C_i - \hat{C}_i)^2]$$

(C-4)

Where

$\mathbb{I}_{ij}^{noobj}$ is the complement of $\mathbb{I}_{ij}^{obj}$

$\hat{C}_i$ is the box confidence score of the box j in cell i.

λ_{noobj} weights down the loss when detecting background.

Most boxes do not contain any objects. This causes a class imbalance problem, i.e. the algorithm trains the model to detect background more frequently than detecting objects. To remedy this, the algorithm weights this loss down by a factor λnoobj (default: 0.5). The final loss adds localization, confidence and classification losses together.

$$\lambda_{coord} \sum_{i=o}^{S^2} \sum_{j=0}^{B} \mathbb{I}_{ij}^{obj} [(x_i - \hat{x}_i)^2 + (y_i - \hat{y}_i)^2]$$

$$+ \lambda_{coord} \sum_{i=o}^{S^2} \sum_{j=0}^{B} \mathbb{I}_{ij}^{obj} [(\sqrt{w_i} - \sqrt{\hat{w}_i})^2 + (\sqrt{h_i} - \sqrt{\hat{h}_i})^2]$$

$$+ \sum_{i=o}^{S^2} \sum_{j=0}^{B} \mathbb{I}_{ij}^{obj} [(C_i - \hat{C}_i)^2] + \lambda_{noobj} \sum_{i=o}^{S^2} \sum_{j=0}^{B} \mathbb{I}_{ij}^{noobj} [(C_i - \hat{C}_i)^2]$$

$$+ \sum_{i=0}^{S^2} \mathbb{I}_{i}^{obj} \sum_{c \in classes} (p_i(c) - \hat{p}_i(c))^2$$

(C-5)